2-7-2017

Molecular polypyridine-based metal complexes as catalysts for the reduction of CO_2

Noémie Elgrishi
Chimie des Processus Biologiques

Matthew B. Chambers
Chimie des Processus Biologiques

Xia Wang
Chimie des Processus Biologiques

Marc Fontecave
Chimie des Processus Biologiques

Recommended Citation

Elgrishi, N., Chambers, M., Wang, X., & Fontecave, M. (2017). Molecular polypyridine-based metal complexes as catalysts for the reduction of CO_2. *Chemical Society Reviews, 46* (3), 761-796.
https://doi.org/10.1039/c5cs00391a

Molecular polypyridine-based metal complexes as catalysts for the reduction of CO 2

Noémie Elgrishi, Matthew B. Chambers, Xia Wang, Marc Fontecave

Molecular polypyridine-based metal complexes as catalysts for the reduction of CO_2

Noémie Elgrishi, Matthew B. Chambers, Xia Wang and Marc Fontecave*

Laboratoire de Chimie des Processus Biologiques, Collège de France,

Université Pierre et Marie Curie, CNRS UMR 8229, 11 place Marcelin Berthelot,

75005 Paris, France

*Correspondence to: marc.fontecave@college-de-france.fr

Abstract:

Polypyridyl transition metal complexes represent one of the more thoroughly studied class of molecular catalysts towards CO_2 reduction to date. Initial reports in the 1980's began with an emphasis on 2nd and 3rd row late transition metals, but more recently the focus has shifted towards earlier metals and base metals. Polypyridyl platforms have proven quite versatile and amendable to studying various parameters that govern product distribution for CO_2 reduction. However, open questions remain regarding the key mechanistic steps that govern product selectivity and efficiency. Polypyridyl complexes have also been shown to be amenable to a variety of immobilization methods to afford active catalytic materials for CO_2 reductions. While still an emerging field, materials incorporating molecular catalysts represent a promising strategy for electrochemical and photoelectrochemical devices capable of CO_2 reduction. In general, this class of compounds remains on the most promising for the continued development of molecular systems for CO_2 reduction and an inspiration for the design of related non-polypyridyl catalysts.

1. Introduction

In the context of global warming and the necessary substitution of renewable energies, solar and wind energy, for fossil fuels, efficient energy storage technologies need to be urgently developed.[1,2] Electrochemical storage, in the form of batteries, is one, extensively explored, option. Chemical storage, within chemical bonds of an energy-dense compound such as hydrogen from water splitting, offers

better gravimetric densities.[3] Recently energy storage via reduction of CO_2 has enjoyed renewed interest.[4,5] Although reduction of CO_2 into energy-dense liquid or gaseous fuels is a fascinating fundamental issue, its practical implementation into technological devices (electrolyzers coupled to photovoltaics or photoelectrochemical cells) is highly challenging due to the great stability of CO_2 and thus the endergonic nature of its transformation. Furthermore, the reactions involve multiple electrons and protons and thus require efficient catalysts to mediate these transformations. Finally, a recurring issue is the competition with proton reduction into dihydrogen which calls for the development of selective catalysts and appropriate tuning of the reaction conditions (temperature, pressure, solvent,…). Although not the focus of the following review, it ought to be noted that complete energy storage system would necessitate the coupling of CO_2 reduction with an anodic process, such as water or halide oxidation.

Regarding catalysts for CO_2 reduction current research focuses on two types of compounds, solid materials and homogeneous metal complexes (coordination and organometallic complexes). While appreciating the first approach, a particular focus will be placed in this review on the benefits of molecular catalysts, which are often ideal in finely tuning their reactivity via synthetic modifications of the ligands.

To mediate the multi-electron/multi proton transformations necessary for catalytic CO_2 reduction molecular catalysts require the ability of storing multiple reducing equivalents. This can either be achieved by reducing the metal centre, which then necessitates a ligand field capable of stabilizing reduced metal ions, or by reducing the ligand scaffold, with the metal serving as a mediator for electron relay. In this context, polypyridine ligands have been appropriate to support catalysts for CO_2 reduction, as they offer the ability to not only stabilize reduced metal centres but also accept reducing equivalents within the ligand π system, allowing for the storage of multiple reducing equivalents across the entire molecule.[6–9]

Polypyridine ligands have been used extensively in catalysis for the activation of small molecules, amongst other applications, and thus represent an extremely broad and diverse class of ligands.[10,11] Within the context of this review, we define polypyridyl ligands as possessing a minimum of two conjugated pyridine motifs, which might be more appropriately referred to as *oligopyridines*. Given nomenclature convention within organometallic catalysis, we have opted to continue the use of *polypyridines* to describe these ligands. The main classes of parent polypyridine ligands and their abbreviations are presented in **Figure 1**. These include bipyridine (bpy), terpyridine (tpy), quaterpyridine (qtpy), where 2, 3 or 4 pyridine groups are linked and conjugated, and also phenanthroline (phen) derivatives which offer a more rigid structure.

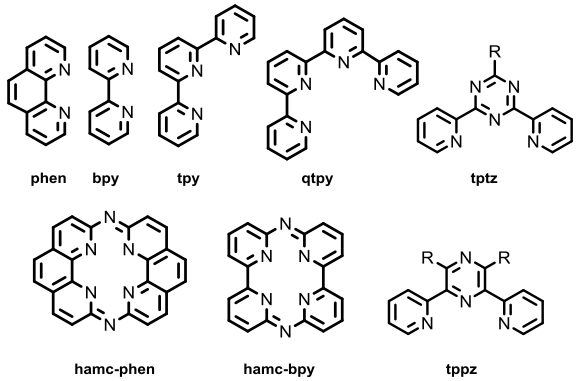

Figure 1. Structure and abbreviation of the most common polypyridyl ligands discussed herein (R = 2-pyridyl). Abbreviations: phen = 1,10-phenanthroline, bpy = 2,2'-bipyridine, tpy=2,2':6',2"-terpyridine, qtpy = 2,2':6',2":6", 2"' quaterpyridine, tptz = 2,4,6-tri(pyridine-2-yl)-1,3,5-triazine, hamc-phen = diaza-1,3(2,9)-diphenanthrolinacyclobutaphane, hamc-bpy = diaza-1,2,4,5(2,6)-tetrapyridinacyclo-hexaphane, tppz = 2,3,5,6-tetra(pyridine-2-yl)pyrazine.

Early developments of molecular CO_2 reduction catalysts have indeed involved polypyridine ligands, with the seminal work of Sauvage/Lehn using [Re(bpy)(X)$(CO)_3$] for photocatalytic and photo-assisted CO_2 reduction to CO.[12] Many more followed in the 1980's and 1990's, but the field was revitalized in the 2010s with a particular focus on first row transition metals. While no comprehensive review of the field exists to date, this review aims to cover the entirety of the field of molecular CO_2 reduction catalysed by polypyridyl complexes, focusing on mechanistic and selectivity aspects.[13] In each section molecular polypyridyl complexes will be reviewed both for their electrochemical and photosensitized catalytic activity towards the reduction of CO_2. Key advances and landmark papers will be discussed for Ru and Re-based catalyst, and comprehensive review will be given for all other metals. In the last section, advances towards applications with catalyst immobilization is presented providing a wider picture of the state-of-the-art in the field.

2. A note on comparing catalytic activity

Within this review, efforts are undertaken to allow for comparison of the reactivity of different catalysts. This is achieved through tables, to help compare the activity and product selectivity of the different catalysts assessed electrochemically and in photochemical systems. When systems were studied electrochemically, all potentials were converted to Fc^+/Fc whenever possible, and an emphasis is placed on product selectivity and faradic yields. For photochemical systems, turn-over-numbers (TON) are given, referring to the moles of product measured divided by the moles of catalyst. It is important to note that variations in experimental setups can render direct comparisons difficult. An important aspect of the value of this review is in providing these comparisons whenever possible. For this reason, "TON" reported after bulk electrolysis of homogeneous catalysts is not provided in this review. These numbers are too sensitive to the cell design to be meaningful to compare catalysts, unless exhaustive electrolyses were performed which is rarely the case in practice.

For photocatalytic systems, an important parameter to report is the wavelength or range of wavelengths that are being used to irradiate the catalysts. Within this review, the wavelength of irradiation will be reported in nm for photocatalytic results. While normalizations cannot be made across different wavelengths, it should be noted that *ranges of wavelengths* contain more energy than *single wavelengths*, and short wavelengths are more energetic than longer wavelengths. Additionally, photon flux is an important factor in photocatalytic systems and is often unreported. Direct comparisons across different photocatalytic systems are difficult and standards for normalizing the irradiation energy per unit time represents an area than needs improvement within the field of molecular photocatalytic CO_2 reduction.

Furthermore, the photocatalytic systems reported for CO_2 reduction are often multi-component requiring a photosensitizer and a sacrificial electron donor. As a consequence, the choice of photosensitizer and sacrificial electron donor can affect the rates and product distribution by changing the nature of the rate-limiting step and the thermodynamic driving force. A direct catalyst evaluation would ideally assess these aspects within such multi-component photocatalytic systems. As the effects of photosentizers and sacrificial electron donors are not always reported in detail, we encourage readers to be mindful of the complexities the photocatalytic systems discussed herein and the possible role of each component to the observed activity.

Electrocatalytic systems ought to be compared against a consistent reference potential. For aqueous systems, NHE (or SHE), is typically used as the reference potential. For organic solutions, the situation is more complex as various references exist and are used throughout the literature. For this review, we have recalculated all potentials to be with respect to the Fc^+/Fc potential in a given solvent. The Fc^+/Fc couple provides a practical reference that has been studied across a variety of solvents. For ease of comparison, we have also converted aqueous potentials to be reported versus Fc^+/Fc using well

documented estimated of the Fc^+/Fc potential versus NHE in aqueous conditions. Therefore, all potentials discussed within the review are directly comparable to one another. Few exceptions are present, due to some complex solvent mixtures or when the nature of the reference electrode used in the study is not fully specified. In some reports, the data was referenced internally using the ferrocenium/ferrocene couple but converted back to a different reference scale for publication. In such cases where the conversion used by the authors is explicitly stated, we have used this value for the conversion back to the Fc^+/Fc scale. The other conversions used are outlined below. When solvent mixtures were used, the conversion for the major solvent was selected to provide a best estimate. A combination of the reference paper by Astruc[14] and the Handbook of electrochemistry by Zoski[15] have proven useful to obtain the following conversions.

- The conversion factor for the SCE reference to Fc^+/Fc is −0.382 V in CH_3CN, −0.470 V in DMF and −0.435 V in DMSO.[14]
- The conversion from NHE to Fc^+/Fc is −0.720V in DMF, −0.690 V in CH_3CN and −0.400 V in H_2O.[15]
- The conversion used from SSCE to SCE is −0.005 V, and +0.241 V is used from SCE to NHE in H_2O.[15]
- The pseudo reference $Ag^+|Ag$ 10 mM in CH_3CN is converted to Fc^+/Fc using −0.089 V, and AgAgCl 3M KCl/NaCl is converted to SCE using −0.032 V.[15]
- Finally the conversion used from saturated Ag/AgCl to NHE is +0.197 V, and −0.044 V to SCE.[15]

An important component of catalytic activity is the distribution of carbon-containing products obtained from CO_2 reduction. From a thermodynamic perspective, the driving force for the formation of each product can vary significantly depending on solvent conditions.[16] Within this manuscript, catalysis in a variety of different solvents and conditions will be described, thereby inhibiting direct comparisons of product distributions with regard to overpotential. However, general trends to consider for the standard reduction potential for the most common products (CO, HCOOH, CH_2O, CH_3OH, and CH4) is that the standard reduction potential for the more reduced products is more positive than that required for less reduced products.

3. 4d and 5d transition metals

3.1. Polypyridyl complexes of Mo/W

Recently the [M(bpy)(CO)$_3$X] architecture was extended to Mo- and W- based catalysts. [M(L)(CO)$_4$] (M = Mo and W with L = bpy and ^{t}Bu-bpy) complexes were shown, by Kubiak and collaborators, to be catalysts for the reduction of CO_2 to CO in CH_3CN, even in the absence of a proton source.[17] The reported TOF, as determined by cyclic voltammetry (CV), appears modest (on average 2 s^{-1}) compared to the ones (> 300 s^{-1}) reported for rhenium-based systems (*vide infra*) in the presence of TFE (trifluoroethanol). Only one tungsten complex, in **Table 1**, was analysed through controlled potential electrolysis (CPE). The main product observed during bulk electrolysis was CO, although traces of H_2 were observed as well, usually < 3%. Nervi, Gobetto and co-workers investigated the effect of introducing phenyl ring substituents to extend the π-system and shift the reduction potential to less negative values.[18] The results of the CPE indicate a lower faradic yield of 35% for CO production. Hartl and co-workers reported the interaction of [Mo(CO)$_2$(η^3-allyl)(bpy)(NCS)] with CO_2 in THF solutions,[19] and explored the reactivity of the parent M(bpy)(CO)$_4$ (M = Mo or W) with CO_2 on gold electrodes.[20] Using a combination of cyclic voltammetry and IR-spectroscopy, they propose [M(CO)$_3$(bpy)]$_2^-$ as the active catalyst and explain the higher activity in N-methyl-2-pyrrolidone (NMP) versus THF by the easier dissociation of the CO ligand in NMP. These remain the only examples to date of Mo and W polypyridine-based homogeneous catalysts for CO_2 reduction.

Table 1. Tungsten polypyridyl complexes assessed for catalytic CO_2 reduction through CPE

Molecule	R	Solvent	Applied potential[a]	Proton source	Time	Products (faradic yields)	Ref.
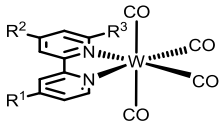	$R^1 = R^2 = {}^t$Bu R^3 = H	CH_3CN	−2.68 V	–	[b]	CO (109%) H_2 (<3%)	[17]
	R^1 = H; $R^2 = R^3 = C_6H_5$	CH_3CN	−2.58 V	–	1h	CO (35%) H_2 (<3%)	[18]

a: potentials in V *vs.* Fc^+/Fc. b: 24 min, 2h and 12h CPE were performed, it was not immediately apparent which one was used for product analysis.

3.2. Polypyridyl complexes of Re

Lehn, Ziessel and Hawecker,[12,21,22] in the early 1980s, reported that Re(bpy)(CO)$_3$Cl catalyses the reduction of CO_2 to CO (90% faradaic efficiency) electrochemically in a DMF/water mixture (90:10, v:v) with Et_4NCl as the supporting electrolyte (**Table 2**, entries 1-4). Catalysis occurred at −1.97 V *vs.* Fc^+/Fc, in the one-electron reduction wave, on a glassy carbon electrode, suggesting that [Re^0(bpy)(CO)$_3$Cl]$^-$ was the active catalytic species. Following these early observations, many bpy-derivatives of Re(CO)$_3$(L)Cl were assayed for CO_2 reduction and were generally shown to behave in similar fashions. Additional details regarding other derivatives can be found within more comprehensive

reviews of the field.[23,24] Within the context of this discussion, landmark studies and unique reports regarding the Re(bpy)(CO)$_3$X class of compounds will be emphasised.

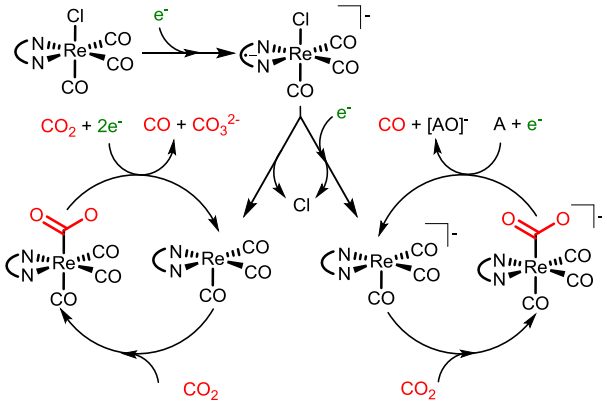

Scheme 1. One- and two-electron pathway mechanisms proposed by Meyer in 1985. "A" is an oxide ion acceptor. The bipyridine ligand is abbreviated to N⌒N.

In 1985, Meyer and collaborators studied by CV the electrochemical reduction of CO_2 catalysed by Re(bpy)(CO)$_3$Cl in MeCN and began proposing mechanistic models.[25] A first reversible feature at –1.68 V *vs.* $Fc^{+/}Fc$ was attributed to the one-electron reduction of the bpy ligand. The second, irreversible, feature, at around –1.98 V *vs.* $Fc^{+/}Fc$, was assigned to a $Re^{I/0}$ metal-centred reduction. Two pathways, depending on the applied potential, were proposed for the catalytic reduction of CO_2 to CO and formation of CO_3^{2-}, operating through either a one- or two-electron reduction of the catalyst (**Scheme 1**). Going down the two-electron reduction path **(Scheme 1**, right), transient formation of the two-electron reduced $[Re^0(bpy^{\bullet-})(CO)_3Cl]^-$ complex was claimed to be accompanied by fast loss of a Cl^- ligand and an intramolecular electron transfer from the ligand to the metal ion, to formally yield $[Re(bpy)(CO)_3]^-$ which is the active species for CO_2 binding and reduction to CO. In the one-electron pathway (**Scheme 1**, left), a slow intramolecular electron transfer in $[Re^I(bpy^{\bullet-})(CO)_3Cl]^-$ resulting in $[Re^0(bpy)(CO)_3Cl]^-$ is required before the slow loss of the Cl^- ligand. The Re^0 centre is presumably capable of interacting with CO_2 and reducing it into CO.

In 1996 Johnson and collaborators studied the electrochemical reduction of CO_2 to CO and formation of CO_3^{2-} catalysed by the Re(L)(CO)$_3$X class of complexes using IR spectroelectrochemistry.[26] They reported that the two-electron reduction yielding $[Re(bpy)(CO)_3]^-$ was necessary for interaction with CO_2 in MeCN. In weakly coordinating solvents such as THF, the one-electron pathway becomes operational as solvent exchange with the chloride ligand is more likely. In the case of Re(dmbpy)(CO)$_3$Cl, (dmbpy = 4,4'-dimethyl-2,2'-bipyridine) the five coordinate complex $[Re(dmbpy^{\bullet-})(CO)_3]^-$ can react with CO_2 directly, even in MeCN, via the one-electron pathway. These spectroscopic results demonstrated that both mechanistic pathways can be operational and are dependent upon solvent conditions, the nature of the bpy ligand as well as the applied potential.

More recently, in 2010, Kubiak and coll. reported a systematic study of ligand variations, using $Re(CO)_3(L)Cl$ complexes (L = bpy; dmbpy, dcbpy, 4,4'-dicarboxyl-2,2'-bipyridine; ^{t}Bubpy, 4,4'-di-*tert*-butyl-2,2'-bipyridine; MeObpy, or 4,4'-dimethoxy-2,2'-bipyridine) in MeCN.[27] They observed an increased catalytic current for more electron-donating substituents. The best activity, as defined by a calculated turnover frequency corresponding to a measured peak catalytic current, was obtained with the ^{t}Bu-substituted derivative (**Table 2** entry 5). It was proposed that the steric strain of the ^{t}Bu functionality served to inhibit the formation of an inactive dimer $[Re^I(L^{\bullet-})(CO)_3]_2$. This was in agreement with IR spectroelectrochemistry data which showed that, at potentials more positive than that for the second reduction event, formation of the Re dimer $[Re^I(bpy^{\bullet-})(CO)_3]_2$ was significant, while no $[Re^I(^tBubpy^{\bullet-})(CO)_3]_2$ could be detected. At potentials more negative than the second reduction potential ($Re^{I/0}$), the mononuclear $[Re^0(^tBu\text{-}bpy^{\bullet-})(CO)_3]^-$ complex was found to be the major species, while it was the inactive dimer $[Re^I(bpy^{\bullet-})(CO)_3]_2$ using the bpy-based complex. Therefore, in the absence of steric strain on the polypyridyl ligand, an inactive dimer forms of the type $[Re^I(L^{\bullet-})(CO)_3]_2$. This is strong evidence highlighting the potential importance of monomeric active catalysts for this family of Re complexes.

The steric and electronic effects on the bpy ligand were further investigated by Kubiak and coll. in 2014.[28] By studying $Re(CO)_3$(*n,n'*-dimethyl-bpy)Cl complexes (*n* = 3 and 5), they observed a higher catalytic current response with catalysts having methyl groups at 5- and 5'- positions as compared to unmodified bpy. In the contrary, catalysts with methyl groups at 3- and 3'- positions, bpy derivatives having similar Hammett parameters as 5,5'-methyl-bpy, showed a decreased catalytic current response as compared to bpy. Again the different behaviours could be explained by the larger steric hindrance created by methyl groups on 3- and 3'- positions of bpy.

The effect of adding weak Brönsted acids to related electrochemical Re-based systems has been first studied by Wong and collaborators in 1998.[29] The authors reported that the rate of electrocatalytic reduction of CO_2 by $[Re(bpy)(CO)_3(py)]^+$ in MeCN could be enhanced by increasing the pK_a of an external acid source (water, MeOH, trifluoroethanol and phenol). Under the optimised conditions, electrocatalytic reduction of CO_2 to CO occurs with nearly 100% faradaic efficiency, and with an apparent order in protons for the reaction of two. As a confirmation, in 2012, Kubiak and coll. proposed on the basis of a H/D kinetic isotope study that the transfer of protons to Re-CO_2 is the rate-determining step.[30]

The deactivation pathways of these catalysts were studied in more detail in 2012 by Kubiak and collaborators.[31] The inactive dimer $[Re(bpy)(CO)_3]_2$, supported by a Re–Re bond, was shown to be stable towards a one-electron reduction, but a second reduction event was required to break the metal–metal bond. Further studies on photochemical deactivation of $Re(dmbpy)(CO)_3Cl$ were undertaken recently by Rieger and collaborators, who confirmed that the two main photo-deactivation pathways

involve $[Re(dmbpy^{\bullet-})(CO)_3Cl]^-$, with monovalent Re and a radical anion on the ligand. This structure represents an electronic configuration required for catalysis yet is also susceptible to deactivation through dimerization.[32]

As these Re-based systems have extensive experimental data available as a guidepost, the mechanism of CO_2 reduction by $Re(bpy)CO_3(X)$ has been thoroughly studied computationally as well. Three major studies focus on explaining the selectivity between CO_2 and proton reduction,[33] the influence of weak Brönsted acids,[34] and the differences between the Re system and an analogous Mn-based system.[35] Specifically in regards to mechanistic considerations, DFT analysis indicated that, in the complex $[Re^0(bpy^{\bullet-})(CO)_3]^-$ obtained from a two-electron reduction, a portion of the electronic charge in the π^* orbital of bpy weakly overlaps the Re 5d orbitals and the HOMO involves thus both the metal center and the ligand. This electronic configuration drives the selectivity towards CO_2 reduction over H^+ reduction through an essentially barrier-less interaction with CO_2 as opposed to an approximately 21 kcal/mol unfavourable interaction with H^+ (**Scheme 2**).[30,33,36,37] The resulting $[Re(bpy)(CO)_3(CO_2)]^-$ intermediate is then computed to be susceptible to a barrier-less protonation to yield $Re(bpy)(CO)_3(CO_2H)$ as a second intermediate. Conversion of $Re(bpy)(CO)_3(CO_2H)$ into $[Re(bpy)(CO)_4]^{\bullet}$ requires an additional electron and proton. The protonation step is rate limiting, and DFT calculations show that whether proton transfer or electron transfer occurs first depends on the applied potential.[38,39]

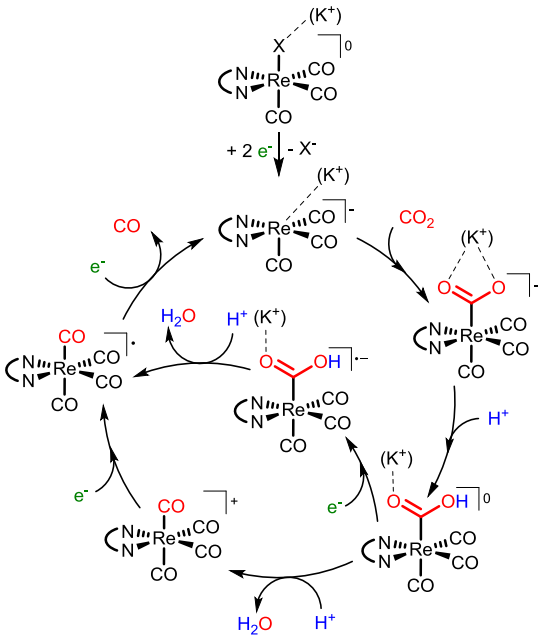

Scheme 2. Mechanism proposed by Kubiak and Carter (reference [33]). The bipyridine ligand is abbreviated to N^N.

Most computed reports so far target the reduction of CO_2 in the presence of excess H^+ to CO and H_2O. However, CO_2 reduction with these catalysts often results in the formation of CO and CO_3^{2-}

as a result of the disproportionation of two equivalents of the one-electron reduced form of CO_2. Since generation of $[CO_2]^{\bullet-}$ is thermodynamically unfavourable and cannot occur at the potentials used experimentally, it is assumed that the reaction involves a bimetallic disproportionation of two reduced Re-CO_2 complexes. In 2003, Fujita and coll. reported the presence of an important CO_2-bridged dimer intermediate, $(CO)_3$(dmb)Re-CO(O)-Re(dmb)$(CO)_3$.[40] Later, in 2012, Muckerman and coll. proposed a mechanism (**Scheme 3**) in dry DMF (no proton source) involving the intermediate formation of $(CO)_3$(bpy)Re-CO(O)-Re(bpy)$(CO)_3$, as proposed by Fujita.[41] Then a second CO_2 molecule inserts into the Re-O bond of the dimer, followed by an intramolecular rearrangement and a carbon-oxygen bond cleavage, finally yielding CO and carbonate.

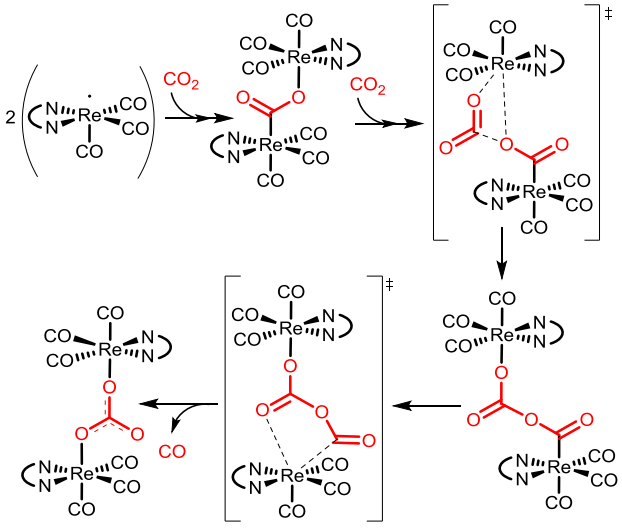

Scheme 3. Mechanism proposed by Muckerman[41] ([ ]‡ denotes a transition state). The bipyridine ligand is abbreviated to N⌒N.

In 2014, to evaluate further this bimetallic mechanism, Gilson, Kubiak and collaborators synthesised a modified version of the $[Re(bpy)(CO)_3]^+$ architecture by including substituents capable of hydrogen-bonding: 4,4′-bis(methyl acetamido-methyl)-2,2′-bipyridine (= dac).[42] The ligand was designed as to helping the assembly of two Re-centres in close proximity and promoting the electrocatalytic disproportionation of two molecules of CO_2 to CO and CO_3^{2-} as opposed to converting CO_2 and excess H^+ to CO and water.[42] This synthetic modification resulted in increased activity and supported the role of bimetallic constructs for the formation of CO and CO_3^{2-} from two equivalents of CO_2. (**Table 2**, entries 6-9)

Table 2. Rhenium polypyridyl complexes assessed for catalytic CO_2 reduction through CPE

Entry	Molecule	R	Solvent	Applied potential	Proton source[a]	Time (h)	Products (faradic yields in %)	Ref.
1		R = H	DMF	−1.97 V	–	5	CO (92)	22
2		R = H	DMF	−1.97 V	H_2O (5%)	4	CO (93)	22
3		R = H	DMF	−1.97 V	H_2O (10%)	14	CO (≥ 94)	22
4		R = H	DMF	−1.97 V	H_2O (20%)	3.5	CO (91)	22

5	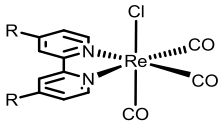	R = ^{t}Bu	CH_3CN	−2.38 V	–	2	CO (99)	27
6		R = dac[b]	CH_3CN	−2.01 V	–	[c]	CO (56)	42
7		R = dac[b]	CH_3CN	−2.01 V	TFE (0.5M)	[c]	CO (73)	42
8		R = dac[b]	CH_3CN	−2.61 V	–	[c]	CO (54)	42
9		R = dac[b]	DMF	−2.50 V	H_2O (10%)	[c]	CO (95)	42
10		R = CH_3	CH_3CN	−2.01 V	–	[c]	CO (46)	42
11		R = CH_3	CH_3CN	−2.01 V	TFE (0.5M)	[c]	CO (65)	42
12		R = CH_3	CH_3CN	−2.61 V	–	[c]	CO (90)	42
13		R = CH_3	DMF	−2.50 V	H_2O (10%)	[c]	CO (95)	42

a: %given by volume. b: dac = methyl acetamidomethyl. c: not specified.

Re-based catalysts have also been extensively studied for photochemical CO_2 reduction since 1983.[12] $Re(bpy)(CO)_3X$ is a photocatalyst. In a DMF-triethanolamine (TEOA) mixture (5:1, v:v), where TEOA served as both electron and proton donor, it converts CO_2 into CO (27 TON within 3 hours photolysis) **(Table 3)**. In this reaction Re catalysts are excited by light (λ> 400 nm) forming a triplet metal-to-ligand charge transfer (^{3}MLCT) excited state, which is quenched by TEOA to produce the one-electron reduced complex $[Re(bpy^{\bullet-})(CO)_3X]$.[43] In 1997, Ishitani and coll. demonstrated that the latter reacts with CO_2 in the dark.[44]

The effect of the ligand X on $Re(bpy)(CO)_3X$ (X = NCS^-, Cl^- and CN^-) activity was investigated in 2008 by Ishitani and collaborators.[45] The ligands NCS^- and Cl^- can be quickly released upon excitation and reduction, while this was not the case for CN^-. Thus $Re(bpy)(CO)_3CN$ is not a photocatalyst. It has been proposed that the reduced complex $[Re(bpy)(CO)_3NCS]^-$ was not only the source of the catalytically competent species $[Re(bpy)(CO)_3]^-$, but also an electron donor (**Scheme 4**).

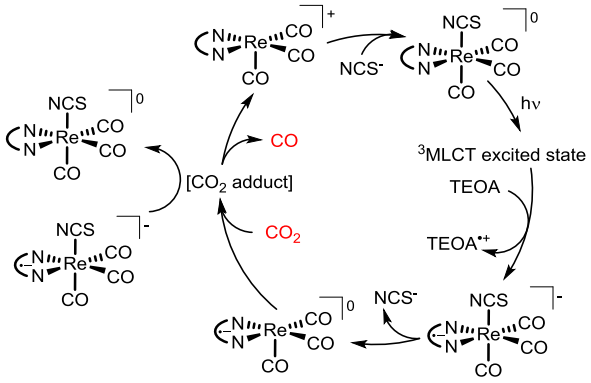

Scheme 4. Mechanism proposed by Ishitani in photochemistry.[45] The bipyridine ligand is abbreviated to N^N.

Recently the active catalyst in all these systems using $Re(bpy)(CO)_3(X)$ in DMF/TEOA solutions was identified as the $Re(bpy)(CO)_3(CO_2$-TEOA) species shown in **Figure 2**. This provided new insights into the role of TEOA which also contributes to capture CO_2. Formation of this intermediate was shown to be very effective, and to allow trapping low concentrations of CO_2, even in air.[46]

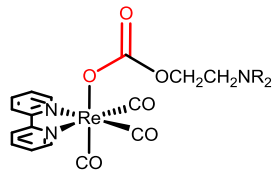

Figure 2. Structure proposed of Re-CO_2-TEOA complex.

Ishitani and collaborators also contributed to improve these systems by using different sacrificial electron donors: a NAD(P)H model compound 1-benzyl-*N*,*N*-diethylnicotinamide (BNAH)[47] as well as two benzoimidazole derivatives 1,3-dimetheyl-2-phenyl-2,3-dihydro-1*H*-benzo[d]imidazole (BIH)[48] and, more recently, 1,3-dimethyl-2-(o-hydroxyphenyl)-2,3-dihydro-1*H*-benzo[d]imidazole (BI(OH)H)[49] (**Figure 3**). With these compounds a base is nevertheless needed, such as TEA or TEOA. BIH and BI(OH)H can provide two electrons at once, and BI(OH)H can provide two protons as well.

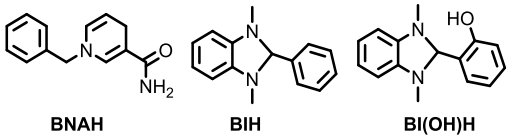

Figure 3. Structure of the electron donors BNAH, BIH and BI(OH)H proposed by Ishitani.

Ishitani and collaborators have also made great strides in extending these Re catalysts towards visible-light driven photosensitized systems. One of the major advances resides in the development of supramolecular photocatalysts combining a Re-based unit with Ru-based photosensitizing unit linked to each other, which proved more efficient than systems in which the two units are separated (**Table 3**, entries 3-7;9).[50] These studies nicely demonstrated that conjugated bridging linkers were not appropriate and that the best performances were obtained with systems having an aliphatic chain as the linker (**Table 3** entry 7). Variations were then brought to these systems via introduction of P-based[43,51] and pyridyl[52–54] ligands on the Re catalytic site, insertion of one O/S atom in the alkyl bridge,[55] and synthesis of Ru/Re tri-[56] and tetra-nuclear[50] supramolecular catalysts. Zn/Pd-based porphyrin photosensitizing units have also been coupled to a $[Re(bpy)(CO)_3L]^+$ (L = picoline) unit.[57–59]

Recently, Ishitani and collaborators reported a supramolecular Ru-Re complex that can photocatalytically reduce CO_2 to formic acid when photolysed in aqueous solution with ascorbate as the electron donor (**Table 3**, entry 8).[60] The system also produces a small amount of H_2 and CO (25 TON of HCOOH, 4.6 TON of H_2 and 1.2 of CO). Formation of formic acid and not CO is intriguing but a system working in water without producing H_2 as the major product is interesting. However, in aqueous conditions, ligand substitution is observed on the photoactive Ru centre, which is believed to lead to catalyst deactivation.

Ishitani and coll. also developed a supramolecular catalysts Ru/Os-$Re(CO)_2(PR_3)_2$,[54,61] with two CO and two P-based ligands to the Re center. With R = *p*-FPh, the catalyst was remarkably active with a high turnover frequency of CO formation (281 h^{-1}), allowed by a fast and exergonic electron transfer from the reduced Ru moiety to the Re center (**Table 3**).

Table 3. Rhenium polypyridyl complexes assessed for catalytic CO_2 reduction through Photolysis[a]

Entry	Molecule		λ[b]	Photosensitizer / Electron donor	Time (h)	Products (TON)	Ref.
1	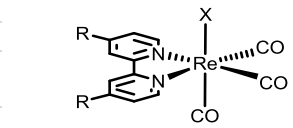	R = H, X = Cl	>400[a]	─ /TEOA	4	CO (27)	12
2		R = H, X = Br	>400[a]	─ /TEOA	4	CO (20)	12
3		R = CH_3, X = Cl	>500	$[Ru(dmb)_3]^{2+}$/ BNAH	16	CO (101)	50
4		R = CH_3, X = Cl	>500	─ / BNAH	16	CO (15)	50
5	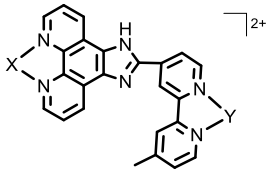	X = $(4dmbpy)_2Ru$, Y = $Re(CO)_3(Cl)$	>500[c]	─ / BNAH	16	CO (14)	50
6		X = $Re(CO)_3(Cl)$, Y = $(4dmbpy)_2Ru$	>500[c]	─ / BNAH	18.5	CO (28)	50
7	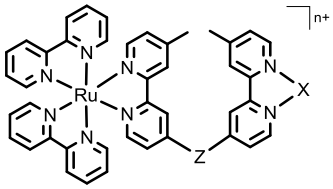	R = H, X = $Re(CO)_3(Cl)$; Z = $CH_2CH(OH)CH_2$	>500[c]	─ / BNAH	12.5	CO (50)	50
8		R = H, X = $Re(CO)_3(Cl)$; Z = CH_2CH_2	>500[c]	─ / Sodium ascorbate	24	HCOOH (25); CO (1); H_2 (5)	60
9	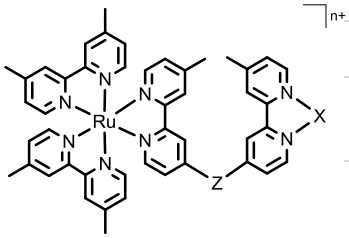	X = $Re(CO)_3(Cl)$; Z = $CH_2CH(OH)CH_2$	>500[c]	─ / BNAH	16	CO (170)	50
10		Z = CH_2CH_2; X = $Re(CO)_2(P(pF\text{-}Ph)_3)_2$	>500	─ / BNAH	20	CO (207) H_2 (9)	54
11		Z = CH_2CH_2; X = $Re(CO)_2(P(pF\text{-}Ph)_3)_2$	>500	─ / BIH	20	CO (3029)	48
12		X = $Re(CO)_2(PPh_3)_2$; Z = CH_2CH_2	>500	─ / BNAH	20	CO (144) H_2 (15)	54
13		X = $Re(CO)_2(P(OEt)_3)_2$; Z = CH_2CH_2	>500	─ / BNAH	20	CO (22) H_2 (10)	54
14		X = $Re(CO)_2(P(OEt)_3)_2$; Z = CH_2OCH_2	>500	─ / BNAH	20	CO (253)	55
15		X = $Re(CO)_2(P(OEt)_3)_2$; Z = $(CH_2)_3$	>500	─ / BNAH	20	CO (178)	55
16		X = $Re(CO)_2(P(OEt)_3)_2$; Z = CH_2SCH_2	>500	─ / BNAH	20	CO (73)	55
17	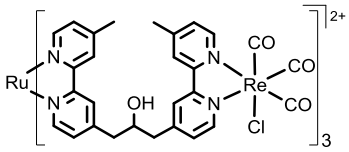		>500[c]	─ / BNAH	16	CO (240)	50
18	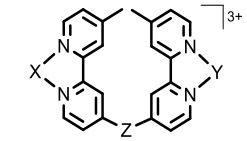	X = $Os(5dmbpy)_2$, Y = $Re(CO)_2(P(pCl\text{-}Ph)_3)_2$ Z = CH_2CH_2	>620[c]	─ / BIH	20	CO (1138) HCOOH (4)	61

a: all experiments were run in DMF/TEOA (1:5, v/v) except entry 8 which was run in H_2O at pH 5.5. b: irradiation wavelength.

In summary, reports on Re-polypyridyl complexes as CO_2 reduction catalysts are plentiful and primarily involve a family of complexes with a general structure of $Re(bpy)(CO)_3(X)$. These catalysts are stable and synthetically tuneable, which has afforded the opportunity to evaluate the mechanism of CO_2 reduction in detail. As these systems predominantly and selectively produce CO from CO_2 reduction, in depth mechanistic considerations regarding factors governing selectivity for CO over other carbon containing products as well as CO_2 reduction over H^+ reduction are unavailable. Since Re-polypyridyl catalysts have been demonstrated to be quite active in both electrocatalytic and photocatalytic systems, numerous ligand modifications have been reported. However, these modifications predominantly involve the electronic tuning of the parent bpy ancillary ligand, with significantly fewer reports towards the use of other polypyridyl structures of higher denticity or different coordination geometries.

3.3. Polypyridyl complexes of Ru/Os

Ru and Os complexes have afforded an interesting variety of mechanistic observations. A particular emphasis will be placed on the mechanisms proposed for the $Ru(bpy)_x$ and Ru(tpy)(bpy) family. Furthermore, as they generate a greater variety of products (as opposed to Re which almost exclusively yield CO as a CO_2 reduction product) the product selectivity issue has been specifically addressed. On the other hand, similar Ru and Os complexes have been reported to result in different catalytic behaviour. Given the common usage of $Ru(bpy)_3^{2+}$ as a photosensitizer during photocatalytic reduction of CO_2 and the propensity of this complex to decompose under irradiation, the behaviour of compounds derived from $Ru(bpy)_x$ is of particular interest.

3.3.1. Polypyridyl Ruthenium Complexes

The $[Ru(bpy)_2(CO)_n(X)_m]^{(2-m)+}$ family of compounds has received much attention over the past decades. Electrochemical CO_2 reduction catalysed by $[Ru(bpy)_2(CO)_2]^{2+}$ and $[Ru(bpy)_2(CO)Cl]^+$ was initially investigated by Ishida *et al*. using a H_2O/DMF (90:10, v:v) solvent mixture.[62,63] Bulk electrolyses at –2.14 V *vs.* Fc^+/Fc yielded different products depending on the pH of the solution. In slightly acidic conditions (pH = 6) a mixture CO and H_2 was produced, but under more basic conditions (pH = 9.5) formate was the major product (**Table 4**). $[Ru(bpy)_2(CO)(COOH)]^+$ was proposed to be the critical selectivity-determining intermediate (**Scheme 5**). Under acidic conditions, $[Ru(bpy)_2(CO)(COOH)]^+$, resulting from the protonation of the CO_2 adduct, $[Ru(bpy)_2(CO)(CO_2)]^0$, is protonated to yield an equivalent of H_2O and $[Ru(bpy)_2(CO)_2]^{2+}$. Subsequent two-electron reduction triggers the loss of CO and allows the complex $[Ru(bpy)_2(CO)]^0$ to coordinate a new molecule of CO_2. Formation of H_2 occurs via a different mechanism, initiated by the protonation of the $[Ru(bpy)_2(CO)_2]^{2+}$ intermediate. In basic conditions, $[Ru(bpy)_2(CO)(COOH)]^+$ is proposed to react with a proton and two electrons to yield HCO_2^- and regenerate $[Ru(bpy)_2(CO)]^0$. Of note, this process directly does not generate the

$[Ru(bpy)_2(CO)_2]^{2+}$ complex and thus much less H_2 is produced. These proposed mechanisms are supported by the changes in the observed product distribution as a function of the pK_a of the externally added acid source. At high pK_a production of formate is favoured whereas CO and H_2 are favoured in the presence of stronger acids (**Table 4**).[62]

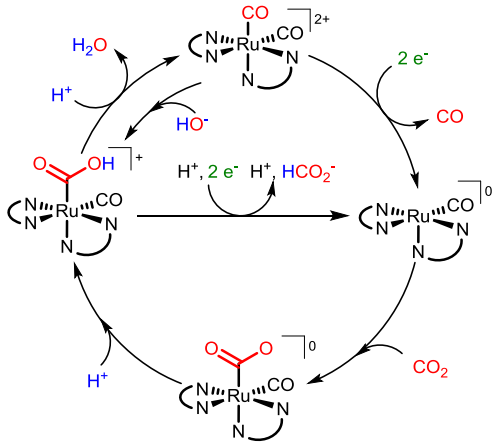

Scheme 5. Mechanism proposed by Ishida *et al*., see references [62] and [63]. The bipyridine ligands are abbreviated to N⌒N.

An alternative mechanism for the formation of formate by this class of compounds was proposed by Meyer and co-workers while studying the catalytic activity of *cis*-$[Ru(bpy)_2(CO)H]^+$ (**Table 4**).[64] Under preparative electrolyses of *cis*-$[Ru(bpy)_2(CO)H]^+$ under CO_2 reduction conditions, FTIR spectroscopy was used to identify *cis*-$[Ru(bpy)_2(CO)H]^+$ along with *cis*-$[Ru(bpy)_2(CO)(OC(O)H)]^+$ and *cis*-$[Ru(bpy)_2(CO)(NCCH_3)]^{2+}$ within the solution. They thus proposed a mechanism of formate production through the direct insertion of CO_2 into the Ru–H bond (**Scheme 6**).[64] This mechanism was unique in that it suggested (i) that a Ru–H bond was critical to the production of formate (ii) that no direct CO_2 adduct to a Ru centre was necessary for formate production and (iii) that redox equivalents were stored on the polypyridyl ligands.[64]

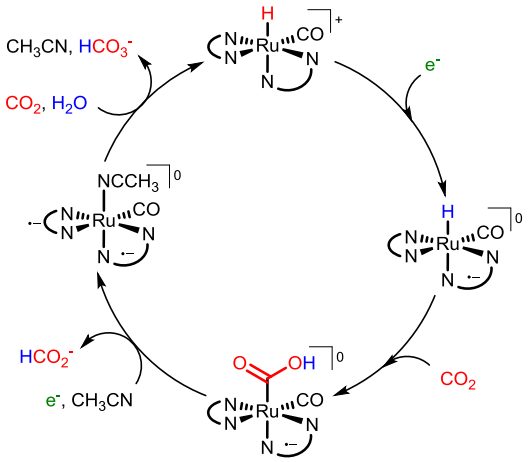

Scheme 6. Mechanism proposed by Meyer in 1991, see reference [64]. The bipyridine ligands are abbreviated to N^N.

Table 4. Ruthenium polypyridyl complexes assessed for catalytic CO_2 electroreduction through CPE

Entry	Molecule	Solvent	Applied potential[a]	Proton source[b]	Time (h)	Products (faradic yields in %)	Ref.
1	$[Ru(bpy)_2(CO)_2]^{2+}$	H_2O/DMF (1:1)	−1.5 V *vs.* SCE	—	[c]	CO (51); H_2 (—); HCO_2^- (35)	63
2		H_2O/DMF (9:1) pH 6	−1.66 V	—	[c]	CO (27); H_2 (35)	63
3		H_2O pH 6	−1.66 V	—	[c]	CO (17); H_2 (54)	63
4		H_2O/DMF (1:1) pH 6	−1.5 V *vs.* SCE	—	[c]	CO (42); H_2 (3)	63
5		H_2O/DMF (9:1) pH 9.5	−1.66 V	—	[c]	CO (26); H_2 (37); HCO_2^- (38)	63
6	$[Ru(bpy)_2(CO)Cl]^{2+}$	H_2O/DMF (1:1)	−1.5 V *vs.* SCE	—	[d]	CO (55); H_2 (5); HCO_2^- (17)	63
7		H_2O/DMF (9:1) pH 6	−1.66 V	—	[c]	CO (21); H_2 (42);	63
8		H_2O/DMF (9:1) pH 9.5	−1.66 V	—	[e]	CO (28); H_2 (44); HCO_2^- (26)	63
9		CH_3CN	−1.68 V	0.2 M $MeNH_2$•HCl	[c]	HCO_2^- (64); CO (20); H_2 (3)	62
10		CH_3CN	−1.68 V	0.2 M Me_2NH•HCl	[c]	HCO_2^- (84); CO (2); H_2 (7)	62
11		CH_3CN	−1.68 V	0.2 M Me_3N•HCl	[c]	HCO_2^- (56); CO (6); H_2 (31)	62
12		CH_3CN	−1.68 V	$PhCO_2H$	[c]	HCO_2^- (23); CO (10); H_2 (51)	62
13		CH_3CN	−1.68 V	PhOH	[c]	HCO_2^- (81); CO (16); H_2 (<1)	62
14	*cis*-$[Ru(bpy)_2(CO)H]^+$	CH_3CN	−1.68 to −1.98 V	H_2O 3 mM to 0.40 M	[f]	CO (57); H_2 (8); HCO_2^- (17)	64
15[g]	*trans*(Cl)-$Ru(Mesbpy)(CO)_2Cl_2$	CH_3CN	−1.7 V	Phenol 0.5 M	[h]	CO (63); H_2 (2); HCO_2^- ([h])	65
16[g]		CH_3CN	−2.2 V	Phenol 0.5 M	[h]	CO (95); H_2 (1)	65
17	$Ru(tpy)(CO)(Cl)_2$	CH_3CN	−1.64 V	H_2O 20%	[i]	CO (60); HCO_2^- (10)	66

18	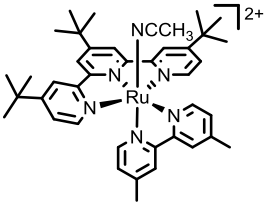	CH_3CN	−1.82 V	—	1	CO (95)	[67]
19[j]	$[Ru(tpy)(6DHBP)(S)]^{2+}$	CH_3CN	−2.3 V	—	1	CO (6); HCO_2^- (9)	[68]
20[k]	$[Ru(tpy)(4DHBP)(S)]^{2+}$	CH_3CN	−2.3 V	—	1	CO (14); HCO_2^- (18)	[68]
21	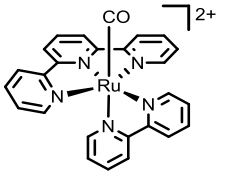	DMF/H_2O (2:8) pH 9	−1.70 V *vs.* Ag^+|Ag	—	[h]	CO (35); HCO_2H (30); H_2 (20); CH_3OH (0.4)	[69]
22		EtOH	−1.70 V *vs.* Ag^+|Ag	H_2O 20%	[h]	CO ([h]); HCO_2H ([h]); H_2 ([h]); CH_3OH (0.3)	[69]
23		EtOH	−1.70 V *vs.* Ag^+|Ag	H_2O 20%	[c]	HCHO ([h]); HCO_2H ([h]); H(O)COOH ([h]); $HOCH_2COOH$ ([h]); CH_3OH ([h]); CO ([h]);	[69]
24	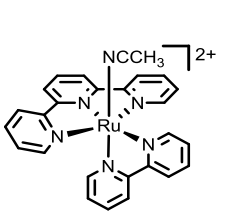	CH_3CN	−2.3 V	—	1	CO (30); HCO_2^- (8)	[68]
25		CH_3CN	−2.21 V	—	5	CO (76); HCO_2^- (< 20%); HCO_3^-([h]); CO_3^{2-}([h])	[70]
26		CH_3CN	−1.99 V	H_2O 10%	3	CO (90); H_2 (<2)	[71]
27		CH_3CN	−1.99 V	H_2O 10% H_2PO_4 50 mM	3	CO (43); H_2 (52)	[71]
28		CH_3CN	−1.99 V	H_2O 10% H_2PO_4 0.25 M	3	CO (35); H_2 (65)	[71]
29[l]	[Ru(tpy)(Mebim-py)(S)]$^{2+}$	CH_3CN	−2.15 V	—	5	HCO_3^-([h]); CO_3^{2-}([h]); CO (85); HCO_2^- (< 20)	[70]
30[l]		CH_3CN	−2.14 V	H_2O 5%	3	CO (85); H_2 (<2); CH_3OH (−); HCHO (−); HCO_2^- (−)	[72]
31[m]	$[(bpy)_2Ru(dmbbbpy)]^{2+}$	CH_3CN	−2.08 V	H_2O 2%	[d]	HCO_2^- (89); CO (2-3)	[73]
32[m]		CH_3CN	−2.08 V	—	[n]	$C_2O_4^{2-}$ (64); CO (—); HCO_2^- (—)	[73]
33[m]	$[(bpy)_2Ru(dmbbbpy)Ru(bpy)_2]^{4+}$	CH_3CN	−1.98 V	H_2O 2%	[h]	HCO_2^- (90)	[73]
34[m]		CH_3CN	−1.98 V	—	[h]	$C_2O_4^{2-}$ (70)	[73]

a: potentials in V *vs.* Fc^+/Fc except otherwise noted. b: % given by volume. c: after 100 C passed. d: after 90 C. e: after 75 C. f: after 4.8 to 28.2 C. g: Mesbpy = 6,6′- dimesityl-2,2′-bipyridine. h: not specified. i: after 68 C. j: 6DHBP = 6,6′-dihydroxy-2,2′-bipyridine. k: 4DHBP = 4,4′-dihydroxy-2,2′-bipyridine. l: Mebim-py = 3-methyl-1-pyridylbenzimidazol-2-ylidene. m: dmbbbpy = 2,2'-bis(1-methylbenzimidazol-2-yl)-4,4'-bipyridine, S = solvent. n: after 50 C.

One of the most commonly used photosensitizers is $[Ru(bpy)_3]^{2+}$. Lehn and Ziessel in 1990 studied the activity of $[Ru(bpy)_3]^{2+}$ and $[Ru(phen)_3]^{2+}$ as photocatalysts for CO_2 reduction.[74] In DMF/water mixtures, in the presence of TEOA, irradiation of solutions of $[Ru(bpy)_3]^{2+}$ at $\lambda > 400$ nm resulted in the conversion of CO_2 into formate. The amount of formate formed depended on the water content with the highest activity obtained with 15 % of water (**Table 5**, entries 1-6).[74] This activity was proposed to arise from the partial transformation of $[Ru(bpy)_3]^{2+}$ into $[Ru(bpy)_2]^{2+}$, which behaves as an active catalyst. The lack of reactivity of the $[Ru(phen)_3]^{2+}$ complex further supported this hypothesis since the latter is more stable under irradiating conditions (**Table 5** entry 10).[74]

Table 5. Ruthenium polypyridyl complexes assessed for photocatalytic CO_2 reduction

Entry	Molecule	Solvent[a]	Irradiation	Electron donor	Time (h)	Products (TON)	Ref.
1	$[Ru(bpy)_3]^{2+}$	DMF / H_2O 0%	>400nm	TEOA	2	HCO_2^- (—)	[74]
2		DMF / H_2O 5%	>400nm	TEOA	2	HCO_2^- (40)	[74]

3		DMF / H_2O 15%	>400nm	TEOA	2	HCO_2^- (69)	74
4		DMF / H_2O 30%	>400nm	TEOA	2	HCO_2^- (58)	74
5		DMF / H_2O 40%	>400nm	TEOA	2	HCO_2^- (41)	74
6		DMF / H_2O 50%	>400nm	TEOA	2	HCO_2^- (22)	74
7[b]		DMF / H_2O 30%	455 nm	BNAH[c]	2	HCO_2^- (0.4); CO (2)	75
8		DMF	> 320 nm	TEOA	20	HCO_2^- (7)	76
9		CH_3CN	> 320 nm	TEOA	20	HCO_2^- (0)	76
10	$[Ru(phen)_3]^{2+}$	DMF / H_2O 0-15 %	>400nm	TEOA	3	HCO_2^- (—)	74
11		DMF	> 320 nm	TEOA	20	HCO_2^- (7)	76
12	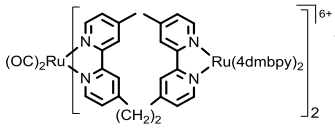	DMF / TEOA 20%	> 500 nm	BI(OH)H[d]	20	HCO_2^- (2766); CO (215); H_2 (212)	49
13		DMF / TEOA 20%	> 500 nm	BIH[e]	20	HCO_2^- (641); CO (237); H_2 (13)	49
14		DMF / TEOA 20%	> 500 nm	BNAH[f]	20	HCO_2^- (562); CO (69); H_2 (29)	49

a: % given by volume. b: performed in supercritical CO_2 at 150 bar.

With a better understanding of the reactivity of these photosensitizers, Ziessel and Lehn used $[Ru(bpy)_3]^{2+}$ and $[Ru(phen)_3]^{2+}$ to photosensitize a variety of ruthenium bis-bipyridine catalysts.[74] The conditions yielding the most productive systems are presented in **Table 6**. The general trend observed is that higher activities were obtained in the absence of water. Moreover, formate production was lower with $[Ru(phen)_3]^{2+}$ than with $[Ru(bpy)_3]^{2+}$ as the photosensitizer.[74] This general behaviour was confirmed by Tanaka and co-workers (**Table 6**).[76]

More recently the selectivity for CO or formate production was investigated as a function of CO_2 pressure. It was shown that CO production: (i) increases linearly with CO_2 pressure up to 150 bars, and (ii) is enhanced in a biphasic water/DMF supercritical CO_2 mixture. Formate production on the other hand is independent of CO_2 pressure in the 10-150 bar range in water/DMF solutions.[75] These observations support the Ishida-mechanism for CO production through a direct Ru–CO_2 interaction and the Meyer-mechanism for formate production through CO_2 insertion into a Ru–H bond.

In NMP instead of DMF, with an iridium-based photosensitizer, Beller and co-workers observed the production of mixtures of CO, formate and hydrogen using ruthenium bis-bipyridine catalysts (**Table 6**).[77] The iridium photosensitizer $[Ir(ppy)_2(bpy)]^+$ (ppy = 2-phenylpyridine) was selected to avoid potential formate production from the decomposition of $[Ru(bpy)_3]^{2+}$ and NMP was preferred to DMF as mixtures of DMF and TEA/TEOA have been shown to generate some formate .[78,79]

Ishitani and co-workers developed a supramolecular compound, with a $[Ru(bpy)_2(CO)_2]^{2+}$ unit tethered to two $[Ru(4dmbpy)_3]^{2+}$ (4dmbpy = 4,4'-dimethyl-2,2'-bipyridine) units, which generates formate as the major product, although the activity and selectivity were dependent on the electron donor

used (**Table 5** entry 12-14).[49] The activity of this photocatalyst is higher than the combination of the two separated units (**Table 6** entry 35).[49]

Table 6. Ruthenium polypyridyl complexes photosensitized for photocatalytic CO_2 reduction

Entry	Molecule	Solvent[a]	Irradiation	Photosensitizer / Electron donor	Time (h)	Products (TON)	Ref.
1	$[Ru(bpy)_2(CO)_2]^{2+}$	DMF	> 400 nm	$[Ru(phen)_3]^{2+}$ / TEOA	3	HCO_2^- (29)	74
2		DMF / H_2O 15%	> 400 nm	$[Ru(phen)_3]^{2+}$ / TEOA	3	HCO_2^- (13)	74
3		DMF	> 400 nm	$[Ru(bpy)_3]^{2+}$ / TEOA	2	HCO_2^- (54)	74
4		DMF / H_2O 15%	> 400 nm	$[Ru(bpy)_3]^{2+}$ / TEOA	4	HCO_2^- (19)	74
5		DMF	> 320 nm	$[Ru(bpy)_3]^{2+}$/ TEOA	20	HCO_2^- (394)	76
6		DMF	> 320 nm	$[Ru(phen)_3]^{2+}$/ TEOA	20	HCO_2^- (150)	76
7		CH_3CN	> 320 nm	$[Ru(bpy)_3]^{2+}$/ TEOA	20	HCO_2^- (93)	76
8		DMF	> 400 nm	$[Ru(bpy)_3]^{2+}$ / BNAH	10	HCO_2^- (<10); CO (<10)	76
9		DMF / H_2O 10%	> 400 nm	$[Ru(bpy)_3]^{2+}$ / BNAH	10	HCO_2^- (155); CO (125)	76
10		DMF / H_2O 30%	> 400 nm	$[Ru(bpy)_3]^{2+}$ / BNAH	10	HCO_2^- (50); CO (125)	76
11	$Ru(bpy)_2(Cl)_2$	DMF	> 320 nm	$[Ru(bpy)_3]^{2+}$/ TEOA	20	HCO_2^- (193)	76
12		NMP[b]	400-700 nm	$[Ir(ppy)_2(bpy)]^+$ / TEOA	[c]	HCO_2^- (13); CO (1); H_2 (2)	77
13	$[Ru(bpy)_2(CO)Cl]^+$	DMF	> 400 nm	$[Ru(bpy)_3]^{2+}$ / TEOA	2	HCO_2^- (163)	74
14		DMF	> 400 nm	$[Ru(phen)_3]^{2+}$ / TEOA	3	HCO_2^- (36)	74
15		DMF / H_2O 15%	> 400 nm	$[Ru(bpy)_3]^{2+}$ / TEOA	2	HCO_2^- (42)	74
16		DMF / H_2O 15%	> 400 nm	$[Ru(phen)_3]^{2+}$ / TEOA	3	HCO_2^- (17)	74
17		NMP[b]	400-700 nm	$[Ir(ppy)_2(bpy)]^+$ / TEOA	[c]	CO (40); HCO_2^- (419); H_2 (67)	77
18	$[Ru(bpy)_2(CO)H]^+$	DMF / H_2O 15%	> 400 nm	$[Ru(bpy)_3]^{2+}$ / TEOA	1	HCO_2^- (21)	74
19		DMF	> 400 nm	$[Ru(bpy)_3]^{2+}$ / TEOA	2	HCO_2^- (161)	74
20		DMF	> 400 nm	$[Ru(phen)_3]^{2+}$ / TEOA	3	HCO_2^- (43)	74
21		DMF / H_2O 15%	> 400 nm	$[Ru(phen)_3]^{2+}$ / TEOA	3	HCO_2^- (19)	74
22[d]		DMF / H_2O 30%	455 nm	$[Ru(bpy)_3]^{2+}$ / BNAH	2	CO (1020); HCO_2^- (100)	75
23		NMP[b]	400-700 nm	$[Ir(ppy)_2(bpy)]^+$ / TEOA	[c]	CO (25); HCO_2^- (225); H_2 (62)	77
24	$[Ru(bpy)_2(py)Cl]^+$	DMF	> 400 nm	$[Ru(bpy)_3]^{2+}$ / TEOA	2	HCO_2^- (60)	74
25		DMF H_2O 15%	> 400 nm	$[Ru(bpy)_3]^{2+}$ / TEOA	2	HCO_2^- (12)	74
26	$[Ru(bpy)_2(DMF)_2]^{2+}$	DMF	> 400 nm	$[Ru(bpy)_3]^{2+}$ / TEOA	2	HCO_2^- (66)	74
27	$Ru(bpy)_2(CO_3)$	NMP[b]	400-700 nm	$[Ir(ppy)_2(bpy)]^+$ / TEOA	[c]	HCO_2^- (21); CO (2); H_2 (4)	69
28	$[Ru(bpy)_2(acetone)_2]^{2+}$	NMP[b]	400-700 nm	$[Ir(ppy)_2(bpy)]^+$ / TEOA	[c]	CO (4); HCO_2^- (75); H_2 (44)	77

29	$[Ru(bpy)_2(CO)(H_2O)]^{2+}$	NMP[b]	400-700 nm	$[Ir(ppy)_2(bpy)]^+$ / TEOA	[c]	CO (45); HCO_2^- (335); H_2 (65)	77
30	$Ru(bpy)(CO)_2(Cl)_2$	DMF	> 400 nm	$[Ru(bpy)_3]^{2+}$ / TEOA	2	HCO_2^- (128)	74
31		DMF H_2O 15%	> 400 nm	$[Ru(bpy)_3]^{2+}$ / TEOA	2	HCO_2^- (24)	74
32	*trans*(Cl)-$Ru(bpy)(CO)_2(Cl)_2$	DMA[e] / H_2O 10%	> 400 nm	$[Ru(bpy)_3]^{2+}$ / BNAH	4	HCO_2^- (1000); CO (2800); H_2 (<5)	80
33		DMA[e] / H_2O 10%	> 400 nm	$[Ru(4dmbpy)_3]^{2+}$ / BNAH	4	CO (2800); HCO_2^- (750); H_2 (<5)	80
34[f]	*trans*(Cl)–$Ru(Mesbpy)(CO)_2(Cl)_2$	DMA[e] / H_2O 10%	> 400 nm	$[Ru(bpy)_3]^{2+}$ / BNAH	0.25	CO (38); HCO_2^- (<5); H_2 (<5)	80
35[g]	$[Ru(4dmbpy)_2(CO)_2]^{2+}$	DMF / TEOA 20%	> 500 nm	$[Ru(4dmbpy)_3]^{2+}$ / BI(OH)H	20	HCO_2^- (1969); CO ([c]); H_2 ([c])	49

a: % given by volume. b: NMP = N-Methyl-2-pyrrolidone. c: not specified. d: performed in supercritical CO_2 at 150 bar. e: DMA = Dimethylacetylamide. f: Mesbpy = 6,6′- dimesityl-2,2′-bipyridine. g: 4dmbpy = 4,4'-dimethyl-2,2'-bipyridine.

Chardon-Noblat *et al.* demonstrated that both *cis*(Cl)-$[Ru(bpy)(CO)_2Cl_2]$ and *cis*(CO)-$[Ru(bpy)(CO)_2(C(O)OMe)Cl]$ were pre-catalysts for the electroreduction of CO_2. They proposed that loss of Cl^- results in the formation of a Ru–Ru dimer which would catalyse CO_2 reduction to CO alongside traces of formate. Instead the *trans*(Cl)-$[Ru(bpy)(CO)_2Cl_2]$ complex led to the formation of a polymeric film, $[Ru(bpy)(CO)_2]_n$, on the electrode, thus showing that the homogeneous or heterogeneous nature of the catalyst can be controlled simply through the stereochemistry of the pre-catalyst in solution.[81]

Investigating the same system further, Ishida reported the photosensitization of *trans*(Cl)-$[Ru(bpy)(CO)_2Cl_2]$ with $[Ru(bpy)_3]^{2+}$ in DMA/water mixures.[80] CO and formate are formed (**Table 6** entries 32-33), with ratios depending on catalyst concentration. The authors explain this selectivity by invoking the formation of a Ru dimer which is responsible for the production of formate while a monomeric catalyst is proposed to generate CO. To test this hypothesis, the authors synthesized *trans*(Cl)–$Ru(Mesbpy)(CO)_2Cl_2$ in which the formation of a dimer is hindered by the mesityl groups on the bpy ligand. With this complex, photocatalytic CO_2 reduction led to the selective evolution of CO with only traces of formate (**Table 6** entry 34).[80] Kubiak in 2015 while studying the electrochemical CO_2 reduction by the same catalyst confirmed the inhibition of dimer formation.[65] CO was also the major product in CPE in the presence of phenol as a proton source (**Table 4** entries 15-16), although the selectivity was shown to be dependent on the applied potential.[65]

CPE of CO_2 at 20°C using $[Ru(tpy)(bpy)(CO)]^{2+}$ as a catalyst in DMF/H_2O (2:8) as well as EtOH/H_2O (8:2) resulted in the formation of CO, formate and H_2 along with trace amounts of methanol.[69] When the CPE was conducted at −20°C, however, a variety of products including CO, formate, formaldehyde, methanol, glyoxylic acid and glycolic acid were obtained (**Table 4** entries 21-23).[69] The study of the stoichiometric reactivity of $[Ru(bpy)_2(CO)(CHO)]^+$ as a mechanistic model led

to the proposal of the formyl complex $[Ru(tpy)(bpy)(CHO)]^+$ as an intermediate in the formation of HCO_2^- rather than the formato and hydroxycarbonyl intermediates proposed thus far.[82]

In 2006 while investigating this system further, Gibson and collaborators isolated a $[Ru(tpy)(bpy)CO]^+$ derivative in which one of the pyridine rings of the tpy ligand was de-coordinated and the carbonyl bridges the Ru and N atoms from this dangling ring.[83] This compound was proposed as a possible catalytic intermediate, however no supporting evidence beyond the existence of this structure has been reported.[83]

Recently, the activity of $[Ru(tpy)(bpy)(S)]^{2+}$ (S = solvent) was revisited, along with the related $[Ru(tpy)(Mebim\text{-}py)(S)]^{2+}$ (Mebim-py = 3-methyl-1-pyridylbenzimidazol-2-ylidene).[70] The catalysts displayed remarkable activity in MeCN at –2.21 V *vs.* Fc^+/Fc, CO being the major product (~80% faradaic efficiency after 5h) with detectable traces of CO_3^{2-}/HCO_3^- and $HCOO^-$ (< 20%).[70] Overtime during CPE, the solution turned purple and a precipitate formed, attributed to the insoluble combination of the catalyst with CO_3^{2-}. Upon addition of water, the catalytic current decreased, however CO remained the major product (**Table 4**).[71,72] The performances of $[Ru(tpy)(Mebim\text{-}py)(S)]^{2+}$ stimulated its integration in an electrochemical device to split CO_2 to CO and O_2 using a Nafion membrane to separate the cathodic and anodic compartments.[72] In this device, $[Ru(tpy)(Mebim\text{-}py)(S)]^{2+}$ was also used in the anodic compartment as a water oxidation catalyst. Electrolysis of a CO_2-saturated MeCN solution in the presence of $H_2PO_4^-$ and using complex $[Ru(tpy)(bpy)(S)]^{2+}$ as a catalyst resulted in the synthesis of syngas (mixtures of CO and H_2) (**Table 4**).[71] The proposed mechanism for CO_2 reduction to CO by this family of complexes, in **Scheme 7**, has similarities with the one proposed for the $[Ru(bpy)_2(CO)_2]^{2+}$ system in that the oxidation sate of the ruthenium centre remains constant while the ligands store reducing equivalents. The rate limiting step is proposed to be the reaction of the resting state $[Ru(tpy^{\bullet-})(bpy^{\bullet-})(S)]^{2+}$ with CO_2.

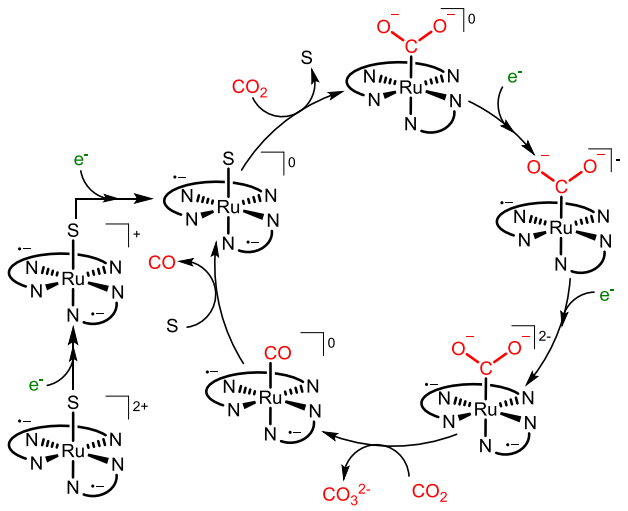

Scheme 7. Mechanism proposed by Meyer for the electrocatalytic CO_2 reduction to CO by $[Ru(tpy)(bpy)(S)]^{2+}$ (see reference [72]). The bipyridine ligand is abbreviated to N^N and N^N^N represents the terpyridine ligand.

Ott and collaborators have reported the synthesis of a library of $[Ru(tpy)(N^N)Cl]^+$ complexes (N^N = bipyridine-based ligand) with the goal of assigning all the features observed by cyclic voltammetry in the presence and absence of CO_2.[84] Based on their assignments, the authors now propose that the resting state of the catalyst involves a doubly reduced ancillary ligand sphere $[Ru(tpy^{\bullet-})(N^N^{\bullet-})(CO_2)]^0$. To enter the catalytic cycle, an electron transfer generates $[Ru(tpy^{\bullet-})(N^N)Cl]^0$. A second reduction and the loss of the Cl^- ligand (the ligand loss can precede the electron transfer depending on the potential) transiently generates $[Ru(tpy^{\bullet-})(N^N^{\bullet-})]^0$, which quickly binds CO_2 to afford $[Ru(tpy^{\bullet-})(N^N^{\bullet-})(CO_2)]^0$. From this intermediate, catalysis can proceed via two different pathways depending on the applied potential.[84] Regardless of the pathway, the mechanism proposed by Ott and co-workers is unique in that it implies that reduced ancillary ligand spheres exist in the catalytic resting state, facilitating the observed multi-electron transformations.[84] In a later report the authors were successful in changing the mechanism leading to the formation of $[Ru(tpy)(N^N)(CO_2)]^0$ from EEC to ECE (**Scheme 8**) by modifying the substituents on the bpy ligand while using an electron rich ^{t}Bu-tpy ligand.[67] An EEC pathway is favoured with electron enriched bpy ligands (4,4'-dimethyl-bipyridine) whereas the ECE pathway is accessed when 2-methyl-bipyridine is used instead. Subsequent catalytic steps are not described, but CPE confirmed CO as the only product (95% faradaic yield) (**Table 4**). The electrons in $[Ru(tpy)(N^N)(CO_2)]^0$ are proposed to be localized on CO_2 ligand in this study, while they were initially proposed to be localized on the polypyridine ligands.[67,84]

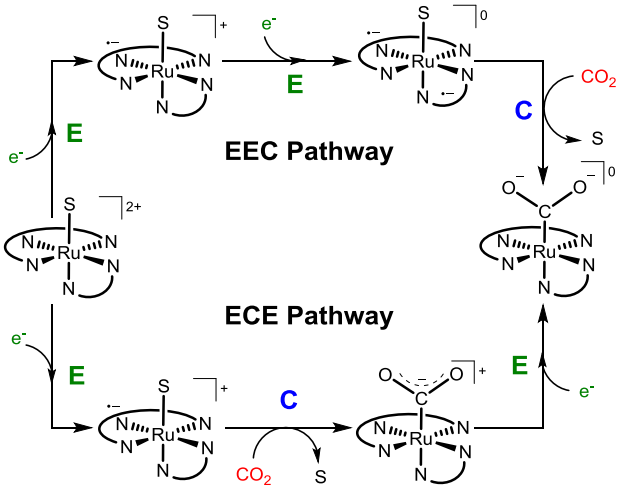

Scheme 8. Competing pathways accessed by Ott and collaborators by varying the electronic nature of the substituents where N^N^N is a tpy derivative and N^N a bpy derivative (reference [67]).

Fujita, Muckerman and co-workers examined the influence of proton-responsive ligands containing pendant bases on the catalytic activity of $[Ru(tpy)(bpy)(S)]^{2+}$ derivatives (**Table 4** entries 19-20).[68] Interestingly, CPE revealed the formation of formate as well as CO, suggesting that a new catalytic pathway was opened. The Faradaic yields were overall lower, and CO binding to the catalyst was proposed as a deactivation pathway.[68]

In 1998, Tanaka *et al.* investigated the effect of increasing further the presence of N atoms in the coordination environment by studying the mononuclear $[Ru(bpy)_2(dmbbbpy)]^{2+}$ and the binuclear $[(bpy)_2Ru(dmbbbpy)Ru(bpy)_2]^{4+}$ (dmbbbpy = 2,2'-bis(1-methylbenzimidazol-2-yl)-4,4'-bipyridine) complexes.[73] CPE of $[(bpy)_2Ru(dmbbbpy)]^{2+}$ in CO_2-saturated MeCN led to the formation of formate (89% faradaic yield) in the presence of 2.5% of water (**Table 4**). However, in the absence of a proton source (using anhydrous MeCN as the solvent) a faradaic efficiency of up to 64% for oxalate was observed. The bimetallic species $[(bpy)_2Ru(dmbbbpy)\text{-}Ru(bpy)_2](PF_6)_4$ was reported to have a similar behaviour. (**Table 4**). Intriguingly, the related $[Ru(bpy)_2(btpy)]^{2+}$ (btpy = 2-(2-pyridyl)benzothiazole) was also shown to exhibit catalytic CO_2 reduction activity whereas 1-methylbenzimidazole analogue did not.[85] It is noteworthy that these systems seemingly are competent catalysts despite the absence of an open coordination site for CO_2 coordination. Overall, this study nicely demonstrates the ability to drastically tune product selectivity on the Ru-polypyridyl platform with H_2O.

In summary, Ru-polypyridyl systems have been invaluable in the fundamental mechanistic study of CO_2 reduction catalysis to mostly formate and CO. The synthetic tunability, general stability and high activity towards the catalysis of CO_2 reduction of this class of compounds have resulted in a wealth of reports in the literature as well as continuing investigations into various aspects of the reactivity.

3.3.2. Polypyridyl complexes of osmium

Building on the successes of the Ru systems, polypyridyl Os complexes have also been studied for their potential as CO_2 reduction catalysts. In 1988, Meyer and collaborators reported the electrocatalytic reduction of CO_2 catalysed by *cis*-$[Os(bpy)_2(CO)H]^+$ in CH_3CN solutions using cyclic voltammetry.[86] CO was observed as the major product under anhydrous conditions, but up to 25% formate was produced in the presence of water in CH_3CN, as confirmed by a later study (**Table 7**, entries 1-3).[87] Reactivity of the *trans*- derivatives was also reported, and kinetic studies based on cyclic voltammetry led to a proposed mechanism in which, similar to the analogous Ru system, *cis*-$[Os(bpy)_2(CO)H]^-$ is a key intermediate.

Table 7. Osmium polypyridyl complexes assessed for catalytic CO_2 electroreduction through CPE

Entry	Molecule	R	Solvent	Applied potential[a]	Proton source	Time (h)	Products (faradic yields)	Ref.
1		R = H	CH_3CN	−1.78 V	0.15 M H_2O[b]	~1[c]	CO (80%) $HCOO^-$ (20%)	[87]

2	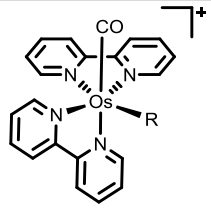	R = D	CH_3CN	−1.78 V	0.15 M H_2O[b]	~1[c]	CO (45%) $HCOO^-$ (20%)	[87]
3[d]		R = H	CH_3CN	−1.78 V	0.1 M H_2O[b]	~1[c]	CO (75%) $HCOO^-$ (5%)	[87]

a: potentials in V *vs.* Fc^+/Fc. b: estimated from the background current observed at the Pt electrode. c: after 40 C were passed. d: a cationic membrane was used to separate the working and auxiliary compartments.

Upon investigation of the behaviour of *trans*(Cl)-[Os(bpy)$(CO)_2Cl_2$], Deronzier, Hartl and Chardon-Noblat reported polymerization of the complex on carbon electrodes in a manner related to that of the Ru derivative, leading to an Os-polymer wire-type catalyst competent for the reduction of CO_2 in aqueous media to CO and formate in 60% and 10% faradic yields respectively.[88] Deronzier and Chauvin subsequently reported the photocatalytic reduction of CO_2 by *trans*(Cl)-[Os(bpy)$(CO)_2(Cl_2)$] and *trans*(Cl)-[Os(dmbpy)$(CO)_2(Cl_2)$] in DMF, with 0.1 M $TBAPF_6$ as a supporting electrolyte and with 1 M TEOA as the electron donor, yielding CO as the only product (**Table 8** entries 1-4).[89] The photocatalysts show remarkable stability over 4h, and addition of $[Ru(bpy)_3]^{2+}$ to create a photosensitised system is reported to increase the TON observed for CO by 30% after 4.5 h. With a 620 nm cut-off filter, however, Ishitani and collaborators recently reported no activity for the photocatalytic CO_2 reduction by $[Os(5\text{-dmbpy})_3]^{2+}$ (Table Y, entries 5-7) in DMF-TEOA solutions with 0.1M 1,3-dimethyl-2-phenyl-2,3-dihydro-1*H*-benzo[*d*]imidazole (BIH) as the electron donor.[61]

Table 8. Osmium polypyridyl complexes assessed for catalytic CO_2 photoreduction

Entry	Molecule	R	Solvent	Irradiation	Photosensitizer / Electron donor	Time (h)	Products (TON)	Ref.
1	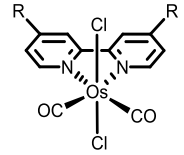	H	DMF	[a]	— / TEOA 1M	4.5	CO (12)	[89]
2		CH_3	DMF	[a]	— / TEOA 1M	4.5	CO (19)	[89]
3		H	DMF	[a]	— / TEA 1M	4.5	CO (4.3)	[89]
4		H	PrCN[b]	[a]	— / TEOA 1M	4.5	CO (3.5)	[89]
5	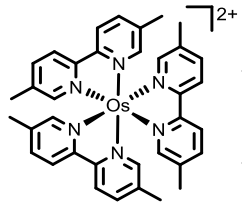		DMF / TEOA (5:1)	>650 nm	— / BIH[c] 0.1M	20	CO (—)	[61]
6			DMF TEOA (5:1)	>650 nm	$Re(CO)_3(P(p\text{-}Cl\text{-}C_6H_4)_3)_2$ / BIH[c] 0.1M	20	CO (363) HCOOH (3) H_2 (<1)	[61]
7			DMF	>650 nm	$Re(CO)_3(P(p\text{-}F\text{-}C_6H_4)_3)_2$ / BIH[c] 0.1M	20	CO (240) HCOOH (3) H_2 (<1)	[61]

a: 250 W Xe lamp, P = 1.8 W at 400 nm. b: PrCN = n-butyronitrile. c: 1,3-dimethyl-2-phenyl-2,3-dihydro-1*H*-benzo[*d*]imidazole.

Overall, while still in the active stages of development, the behaviour of Os-polypyridyl complexes towards CO_2 reduction closely mimics that of the more-studied Ru analogues. These

complexes, although promising, have not received more interest possibly because of osmium toxicity considerations.

3.4. Polypyridyl complexes of Rhodium and Iridium

Group 9 metal-polypyridyl complexes of second and third row transition metals were initially investigated as catalysts for the electrochemical reduction of CO_2 in a report by Meyer and co-workers in 1985[90] and 1988.[91] The activity of both rhodium and iridium complexes of 2,2'-bipyridine complexes, *cis*-$[M(bpy)_2X_2]^+$ (X = Cl^- or trifluoromethanesulfonate, $^-$OTf) were assessed using cyclic voltammetry (**Figure 4**). All cyclic voltammograms of the complexes presented in **Figure 4** under CO_2 were reported to give rise to increased cathodic current densities which the authors attribute to catalytic CO_2 reduction.

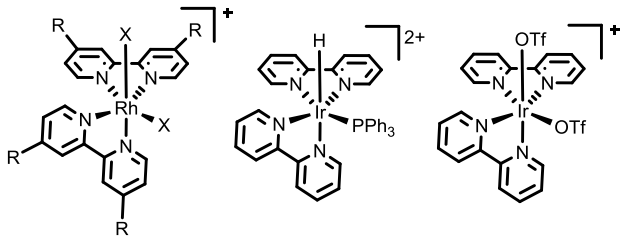

Figure 4. Scheme of compounds studied by Bolinger *et al.* in 1988 using cyclic voltammetry for R = H and X = Cl or OTf (OTf = trifluoromethanesulfonate) and for R = ^{t}Bu and X = Cl.

Table 9. Rhodium and Iridium polypyridyl complexes assessed for catalytic CO_2 electroreduction through CPE

Entry	Molecule	Solvent	Applied potential[a]	Proton source[b]	Time (h)	Products (faradic yields in %)	Ref.
1	*cis*-$[Rh(bpy)_2(Cl)_2]^+$	CH_3CN	−1.93 V	—	[c]	HCO_2^- (47); H_2 (15)	91
2		CH_3CN	−1.93 V	—	[d]	HCO_2^- (83); H_2 (17)	91
3		CH_3CN	−1.93 V	H_2O (5%)	[e]	HCO_2^- (23); H_2 (6)	91
4	*cis*-$[Rh(bpy)_2(OTf)]^{2+}$	CH_3CN	−1.94 V	—	1	HCO_2^- (64); H_2 (12)	90
5	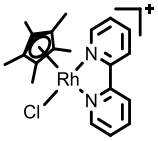	CH_3CN	−1.69 V	—	6.8	CO (—); H_2 (1); HCO_2^- (5)	92
6		CH_3CN	−1.79 V	—	5.8	CO (—); H_2 (6); HCO_2^- (24)	92
7		CH_3CN	−1.69 V	H_2O (5%)	4.4	CO (<1); H_2 (14); HCO_2^- (32)	92
8		CH_3CN	−1.79 V	H_2O (5%)	2.6	CO (<1); H_2 (19); HCO_2^- (34)	92
9		CH_3CN	−1.69 V	H_2O (20%)	3.6	CO (<1); H_2 (32); HCO_2^- (36)	92
10		CH_3CN	−1.79 V	H_2O (20%)	2.1	CO (<1); H_2 (16); HCO_2^- (49)	92
11	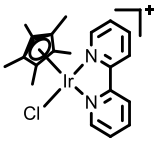	CH_3CN	−1.79 V	—	6.9	CO (<1); H_2 (2); HCO_2^- (16)	92
12		CH_3CN	−1.79 V	H_2O (5%)	4.2	CO (<1); H_2 ([f]); HCO_2^- (22)	92
13		CH_3CN	−1.79 V	H_2O (20%)	5.1	CO (2); H_2 (5); HCO_2^- (20)	92
14	$Rh(tpy)(Cl)_3$	DMF	−1.96 V	H_2O (2.5%)	5-6	HCO_2^- (83)	93
15	$Rh(tptz)(Cl)_3$	DMF	−1.84 V	H_2O (2.5%)	5-6	HCO_2^- (82)	93
16	$[Rh(tptz)_2]^{3+}$	DMF	−1.92 V	H_2O (2.5%)	5-6	HCO_2^- (71)	93
17	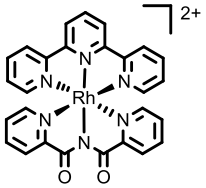	DMF	−2.00 V	H_2O (2.5%)	5-6h	HCO_2^- (78)	93

a: potentials in V *vs.* Fc^+/Fc. b: % given by volume. c: not specified, after 111 C passed. d: not specified, after 77 C passed. e: not specified, after 156 C passed. f: not measured.

The rhodium complexes were further studied by bulk electrolysis at −1.93 V *vs.* Fc^+/Fc in CH_3CN and mixtures of H_2 and formate were produced (**Table 9**, entries 1-3).[91] The faradaic yields varied depending on the total charge passed, starting close to 100% and dropping as more coulombs were passed. For example, the faradaic yield for formate dropped from 83% to 47 % as the charge passed increased from 77 C to 111 C, while the faradaic yield for H_2 diminished slightly, from 17% to 15%. Observations of the formation of a black precipitate during bulk electrolysis, coupled to the disappearance of the bpy-based reduction features by CV, have led the authors to propose a possible degradation by hydrogenation of the bpy ligands. No added proton source was reported in this study, which led to speculations regarding the source of the required proton for formate production.[91] A Hoffmann degradation of the electrolyte salt, $[(n\text{-}Bu)_4N](PF_4)$, was proposed as the source of protons, following the reactions:

$$[Rh(bpy)_2]^- + CO_2 \rightarrow [Rh(bpy)_2CO_2]^- \quad (1)$$

$$[Rh(bpy)_2CO_2]^- + (n\text{Bu})_4N^+ \rightarrow [Rh(bpy)_2CO_2H] + H_3CCH_2CH{=}CH_2 + (n\text{Bu})_3N \quad (2)$$

$$[Rh(bpy)_2CO_2H] \rightarrow [Rh^I(bpy)_2]^+ + HCOO^- \quad (3)$$

Similar general behaviour of Rh and Ir complexes of the form $[M(bpy)Cp^*]^+$ (**Table 9**, entries 5-13) were reported by Deronzier *et al.* in 1997 for the electrocatalytic reduction of CO_2 in H_2O/CH_3CN mixtures.[92] The major products observed were once again formate and H_2 with trace amounts of CO. The formate to H_2 ratio was observed to vary with the applied potential and the water content of the CH_3CN solution.

Table 10. Rhodium and Iridium polypyridyl complexes assessed for catalytic CO_2 photoreduction

Entry	Molecule		Solvent	λ[a]	Photosensitizer / Electron donor	Time (h)	Products (TON)	Ref.
1	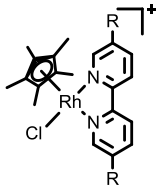	R = H	CH_3CN	> 415 nm	$[Ru(bpy)_3]^{2+}$ / TEOA	2.5	HCOOH (35) CO (—); H_2 (32)	94
2		R = H	CH_3CN	> 415 nm	$[Ru(bpy)_3]^{2+}$ / TEOA	24	HCOOH (110) CO (—); H_2 (54)	94
3		R = COOH	CH_3CN	> 415 nm	$[Ru(bpy)_3]^{2+}$ / TEOA	2.5	HCOOH (20) CO (—); H_2 (32)	94
4		R = COOH	CH_3CN	> 415 nm	$[Ru(bpy)_3]^{2+}$ / TEOA	24	HCOOH (49) CO (—); H_2 (46)	94
5	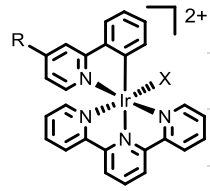	R = CH_3 X = Cl	CH_3CN	450 nm	— / TEOA	1	CO (33)	95
6		R = CH_3 X = I	CH_3CN	450 nm	— / TEOA	1	CO (54)	95
7		R = H X = Cl	CH_3CN	410 – 750 nm	— / TEOA	4.2	HCO_2H (—) CO (40); H_2 (—)	96
8		R = H X = Cl	CH_3CN H_2O (5%)[b]	410 – 750 nm	— / TEOA	4.2	HCO_2H (—) CO (28); H_2 (—)	96

a: irradiation wavelength. b: % given by volume.

Although seemingly forgotten for almost 20 years, these Rh(bpy)Cp*-based catalysts were recently revisited in a homogeneous photosensitised CO_2 reduction system. The results (**Table 10**, entries 1-4) confirmed the activity of the complex for CO_2 reduction to H_2 and formate. Furthermore, the complex proved also active and stable when incorporated into the metal organic framework UIO-67 (*vide infra*).[94]

Regarding polypyridyl ligands with greater denticity, $Rh(tptz)Cl_3$, $Rh(tpy)Cl_3$ and Rh(tpy)(bpca) (**Table 9** entries 14-17) were investigated by Paul *et al.* and were shown to catalyse the reduction of CO_2 to formate in DMF at potentials ranging from −1.84 V to −2.00 V *vs.* Fc^+/Fc.[93,97] Whereas a general observation can be made that Ir and Rh complexes are often more selective for formate production over other potential carbon-containing products, this needs not always be the case. Interestingly, related complexes of Ir with tpy and phenylpyridine-based ligands (**Table 10** entries 5-8) are reported as photocatalysts and electrocatalysts for the reduction of CO_2 to CO in CH_3CN solutions, even in the presence of water. [95,96] The proposed mechanism (eq. 4 to 8) for the production of CO highlights the redox active nature of the tpy backbone, which allows the storing of reducing equivalents (D = sacrificial electron donor, TEOA):[96]

$$[Ir(tpy)(ppy)Cl] + D + h\nu \rightarrow [Ir(tpy^{\bullet-})(ppy)Cl] + D^+ \quad (4)$$

$$[Ir(tpy^{\bullet-})(ppy)Cl] + H^+ + e^- \rightarrow [Ir(tpy)(ppy)H] + Cl^- \quad (5)$$

$$[Ir(tpy)(ppy)H] + D + h\nu + CO_2 \rightarrow [CO_2\ adduct] + D^+ \quad (6)$$

$$[CO_2\ adduct] + H^+ + e^- \rightarrow [Ir(tpy)(ppy)H] + CO \quad (7)$$

$$[CO_2\ adduct] + [Ir(tpy^{\bullet-})(ppy)H] \rightarrow Ir\ dimer \quad (8)$$

Details regarding the nature of the proposed electron transfers that do not involve light absorption are not clear, but it is speculated to involve disproportionation reactions. The authors propose a M–H bond to be an intermediate for CO_2 capture and reduction to CO as the product. This is in marked contrast to that which is generally proposed, wherein protonation of a metal-bound CO_2 yields CO while insertion of CO_2 into a M–H bond affords formate. Finally, this work identifies the formation of an inactive Ir dimer during the course of catalysis (eq. 8) which limits the overall system activity.

3.5. Polypyridyl complexes of Pd

Palladium complexes of derivatives of bipyridine and phenanthroline were assessed as CO_2 reduction catalysts by Ogura in 1997 (**Table 11**). In CPE, in dry CH_3CN, CO was the only product measured whereas formate was observed when H_2O was added to the solution. The activity and faradic efficiencies reported are on par with the homologous cobalt complexes also assessed in this report and presented in section 4.4.

Table 11. Palladium polypyridyl complexes assessed for catalytic CO_2 reduction through CPE

Entry	Molecule	Solvent	Applied potential[a]	Proton source[b]	Time	Products (faradic yields)	Ref.
1	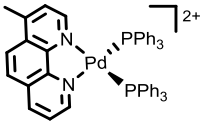	CH_3CN	−1.39 V	H_2O (8%)	1	CO (32); HCO_2^- (40)	98
2		CH_3CN	−1.39 V	—	1	CO (61); HCO_2^- (—)	98
3	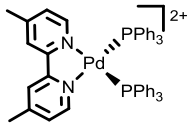	CH_3CN	−1.39 V	H_2O (8%)	1	CO (44); HCO_2^- (30)	98
4		CH_3CN	−1.39 V	—	1	CO (81); HCO_2^- (—)	98

a: potentials in V *vs.* Fc^+/Fc. b: % given by volume.

4. 3d transition metals

4.1. Polypyridyl complexes of Cr

To date, $[Cr(CO)_4(bpy)]$ is the only example of polypyridyl molecular homogeneous Cr complex reported to catalytically reduce CO_2.[20] In their 2015 report, Hartl and Dryfe use a combination of cyclic voltammetry, IR-spectroscopy and DFT to and propose $[Cr(CO)_3(bpy)]^{2-}$ as the active catalyst. The only other example of a Cr-polypyridyl system used as a CO_2 reduction catalyst involves a molecule grafted onto an electrode, this system will be presented in section 5.[99]

4.2. Polypyridyl complexes of Mn

The CO_2 reduction catalytic activity of manganese analogues to $[Re(bpy)(CO)_3]^+$ complexes were first reported in 2011 by Deronzier and collaborators. Electrocatalytic reduction of CO_2 to CO occurred at a potential of −1.789 V *vs.* Fc^+/Fc, using the precatalysts $Mn(bpy)(CO)_3Br$ and $Mn(dmbpy)(CO)_3Br$ (**Table 12**).[100] The catalytic activity was sustained for the 4h of the bulk electrolysis, with CO observed as the major product and trace H_2 measured. After longer bulk electrolysis, up to 22h, the faradic efficiency for CO_2 reduction to CO is 85% and the remaining 15% correspond to H_2 formation. This activity, observed in acetonitrile, only occurred in the presence of a proton source, in the form of 10% (v:v) water in the solvent. Building on this report, the group of Kubiak made strides to understand the influence of protons on the catalytic activity by studying the effect of weak Brönsted acids in solution.[101]

Table 12. Manganese polypyridyl complexes assessed for catalytic CO_2 electroreduction through CPE[a]

Entry	Molecule		Applied potential[b]	Proton source[c]	Time (h)	Products (faradic yields in %)	Ref.
1	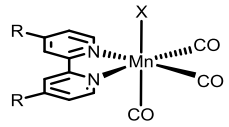	R = H X = Br	−1.789 V	H_2O (5%)	4	CO (100) H_2 (0)	100
2		R = H X = Br	−1.789 V	H_2O (5%)	22	CO (85) H_2 (15)	100
3		R = CH_3 X = Br	−1.789 V	H_2O (5%)	18	CO (100)	100
4		R = ^{t}Bu X = Br	−2.58 V	0.8 M TFE	3	CO (100)	101
5		R = H X = CN	−2.2 V	0.5 M Phenol	[d]	CO (98) H_2 (1)	102
6	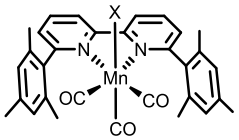	X = OTf	−2.2 V	0.3 M TFE	1.2	CO (98)	103
7		X = OTf	−1.6 V	1.3 M TFE	24	CO (96)	104
8		X = OTf	−1.6 V	— [e]	6	CO (98); H_2 (1)	104
9	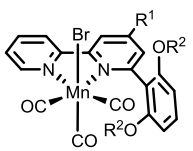	R^1 = Ph R^2 = H	−2.18 V	—	4	CO (70) HCOOH (22) H_2 (~1)	105
10		R^1 = Ph R^2 = CH_3	−2.18 V	—	4	CO (70) HCOOH (22) H_2 (~1)	105
11	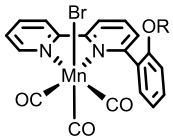	R = H	−1.88 V	H_2O (5%)	4	CO (86)	106
12		R = CH_3	−1.88 V	H_2O (5%)	4	CO (83)	106

a: all experiments were in CH_3CN. b: potentials in V *vs.* Fc^+/Fc. c: % given by volume. d: not specified. e: $Mg(OTf)_2$ is added to the solution and a sacrificial Mg counter electrode is used as well.

Studying the platform Mn(^{t}Bubpy)$(CO)_3$Br they reported increased TOF depending on the proton source and concentration, with the highest TOF of 340 s^{-1} obtained when using 1.6 M trifluoroethanol in CH_3CN in the presence of 0.27 M CO_2. In both reports, dimerization of the Mn^0 to form an inactive $[Mn(bpy)(CO_3)]_2$ is reported to occur after the 1-electron reduction of the starting Mn^I complex followed by loss of the halide counter anion. To minimize dimer formation, the strategy of increasing the steric strain around the metal center was first investigated, using the ligand 6,6'-dimesityl-2,2'-bipyridine (Mesbpy, entry 6 **Table 12**).[103] The resulting tremendous increase of the activity observed was attributed indeed to the inhibition of the formation of the inactive Mn-dimer during catalysis.[103] Two further strategies to minimize dimerization were investigated, either by immobilizing the complexes within metal organic frameworks[107] (discussed in **Section 5**) or by replacing the halide counter anions with a cyano group, which stabilizes the reduced Mn^0.[102]

Subsequently, the mechanism was probed by experimental[108,109] and computational[34,35] methods by several groups. The proposed mechanism, depicted in **Scheme 9**, supports the experimental observations and was obtained through a combination of DFT and microkinetics simulations. The mechanism involves the two-electron reduction of the pre-catalyst to reach $[Mn(bpy)(CO)_3]^-$ which can subsequently interact with H^+ or CO_2. The energy barrier for protonation of $[Mn(bpy)(CO)_3]^-$ is 10 kcal/mol higher than for reaction with CO_2 in these conditions,[35] explaining the observed selectivity for CO_2 reduction over H^+ reduction. Further reaction with a proton yields $[Mn(bpy)(CO)_3COOH]^0$. Two pathways are then opened, depending on the acid source and applied potential.[34,35] At high overpotentials, the mechanism proceeds through a reduction first followed by reaction with a proton and loss of water to yield $[Mn(bpy)(CO)_4]^0$. At lower overpotential, the reaction proceeds through protonation first and loss of H_2O, followed by reduction to yield $[Mn(bpy)(CO)_4]^0$. A further reduction and liberation of the product CO closes the cycle in both cases.

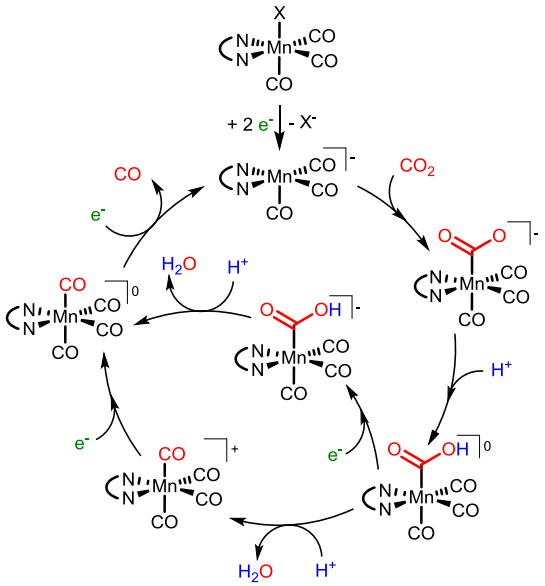

Scheme 9. Reaction mechanism proposed for the catalytic reduction of CO_2 to CO catalysed by $[Mn(bpy)(CO)_3]^-$ in the presence of weak Brønsted acids. The bpy ligand is abbreviated to N^N for clarity.

Recently a Mn-based system with a variation on the bpy ligand was tested. The ligands 4-phenyl-6-(1,3-dihydroxybenzen-2yl)-2,2'-bipyridine (dhbpy) with a local proton source, and the related 4-phenyl-6-(1,3-dimethoxybenzen-2yl)-2,2'-bipyridine (dmobpy), which acts as a control without the local proton source (entry 9 and 10 in **Table 12**).[105] The $Mn(dhbpy)(CO)_3Br$ complex was reported to catalyse the electrochemical reduction of CO_2, even in the absence of an external proton source, with only two equivalents of protons in the form of dihydroxybenenyl groups on the ligand. In contrast, the methoxy derivative showed no activity under the same conditions. These results confirmed the influence of the alcohol group as an effective local proton source. Interestingly, the inclusion of a local proton source afforded a more complicated mixture of products, with both CO and formate being detected with 70% and 22% faradaic efficiency respectively[105] compared to Deronzier catalyst which selectively produces CO as the only carbon-containing product.[100] No further comment has been reported regarding this change in selectivity. Bocarsly and co-workers further investigated the influence of a local proton source using MnBr(6-(2-hydroxyphenol)-2,2′-bipyridine)$(CO)_3$ as well as the corresponding 2-methoxyphenyl derivative (entry 11 and 12 in **Table 12**).[106] In the presence of 5% water as the proton source, they observe increased catalytic activity by the hydroxyphenol derivative in terms of current density and products formed as compared to the 2-methoxyphenyl derivative.

Taking a different approach to increasing the efficiency of the catalyst, Kubiak and co-workers recently explored the use of Mg^{2+} as a Lewis acid to both lift the requirement of a Brønsted acid and diminish the overpotential for catalysis by 600 mV using $[Mn(Mesbpy)(CO)_3](OTf)$.[104] Addition of Mg^{2+} has been employed in Fe-based systems[110] to favour the C-O bond cleavage as well as in Ni-based systems to sequester carbonate formed during the catalytic cycle.[111] Kubiak and co-workers observe a

catalytic current increase at −1.6 V vs Fc^+/Fc with addition of Mg^{2+} under CO_2 and confirmed catalytic CO formation through CPE in 98% faradaic efficiency in the absence of Brønsted acids (**Table 12**, entries 7-8).

Table 13. Manganese polypyridyl complexes assessed for catalytic CO_2 reduction through Photolysis

Entry	Molecule	R	Solvent[a]	λ[b]	Photosensitizer / Electron donor	Time (h)	Products (TON)	Ref.
1	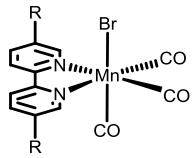	R = H	DMF / TEOA (25%)	480 nm	$[Ru(dmb)_3]^{2+}$ / BNAH	12	HCOOH (149) CO (12); H_2 (14)	112
2		R = H	DMA[c] / TEOA (25%)	480 nm	$[Ru(dmb)_3]^{2+}$ / BNAH	12	HCOOH (98) CO (9); H_2 (14)	112
3		R = H	CH_3CN / TEOA (25%)	480 nm	$[Ru(dmb)_3]^{2+}$ / BNAH	12	HCOOH (78) CO (40); H_2 (17)	112
4		R = H	DMF / TEOA (25%)	480 nm	$[Ru(bpy)_3]^{2+}$ / BNAH	12	HCOOH (157) CO (12); H_2 (8)	112
5		R = H	DMF / TEOA (25%)	470 nm	$[Ru(dmb)_3]^{2+}$ / BNAH	18	$HCOO^-$ (170) CO (5); H_2 (<1)	107
6		R = COOH	DMF / TEOA (25%)	470 nm	$[Ru(dmb)_3]^{2+}$ / BNAH	18	$HCOO^-$ (57) CO (5); H_2 (<1)	107
7	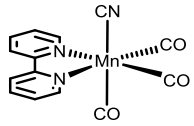		DMF / TEOA (25%)	470 nm	$[Ru(dmbpy)_3]^{2+}$ / BNAH	15	HCOOH (130) CO (9.1); H_2 (1.6)	113
8			CH_3CN / TEOA (25%)	470 nm	$[Ru(dmbpy)_3]^{2+}$ / BNAH	15	HCOOH (9.0) CO (21); H_2 (1.3)	113

a: % given by volume. b: irradiation wavelength. c: DMA = Dimethylacetylamide.

Whereas photosensitisation of the $Mn(bpy)(CO)_3Br$ catalyst with $[Ru(dmbpy)_3]^{2+}$ would be expected to yield CO as the only product (as observed electrocatalytically), it was shown that instead it leads to the formation of a mixture of CO and formate in DMF/TEOA solutions (4:1, v/v), with BNAH (1-benzyl-1,4-dihydronicotinamide) as a sacrificial electron donor (**Table 13**, entries 1-4).[112] This observation was independently confirmed in two reports by Kubiak in which the CO_2 reduction catalytic activity of $Mn(bpy)(CO)_3Br$ and $Mn(bpy)(CO)_3CN$ was assessed in the same photosensitized system (**Table 13**, entries 5-8).[107,113] The selectivity of the reaction towards CO and formate in the photosensitized system with $Mn(bpy)(CO)_3CN$ was shown to be dependent on the nature of the solvent, with formate production favoured in DMF and CO production favoured in CH_3CN.

As a conclusion, whereas the analogous Re systems give CO as the primary product of CO_2 reduction with very few counter-examples, the Mn-derivatives have already been shown to be capable of producing formate in addition to CO. Although there are currently fewer reports on Mn-bpy catalysts for CO_2 reduction, the studies to date suggest that Mn-bpy platforms are possibly more susceptible to product selectivity tuning via simple system modifications.

4.3. Polypyridyl complexes of Fe

Surprisingly, very few reports of Fe-polypyridyl catalysts for the reduction of CO_2 exist, even though the Fe-porphyrin family is among the most active homogeneous catalysts reported in the literature.[114–116]

Table 14. Iron polypyridyl complexes assessed for catalytic CO_2 electroreduction through CPE

Entry	Molecule	Solvent	Applied potential[a]	Proton source[c]	Time (h)	Products (faradic yields in %)	Ref.
1	$[Fe(phen)_3]^{2+}$	DMSO	[b]	[b]	[b]	CH_4 ([b])	117
2	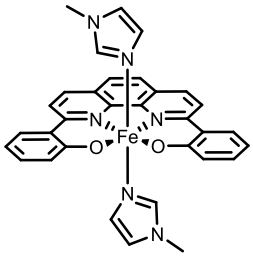	DMSO	−2.0 V	—	1	CO (19); $C_2O_4^{2-}$ (10); $HCOO^-$ (67); H_2 (—)	118
3		DMSO	−2.0 V	1.23 M TFE	1	CO (30); $C_2O_4^{2-}$ (3); $HCOO^-$ (65); H_2 (—)	118
4		DMSO	−2.0 V	1.23 M MeOH	1	CO (26); $C_2O_4^{2-}$ (6); $HCOO^-$ (66); H_2 (—)	118
5		DMSO	−2.0 V	0.16 M[c]	1	CO (10–11)[c]; $C_2O_4^{2-}$ (—)[c]; $HCOO^-$ (—)[c]; H_2 (70 – 79)[c]	118
6		DMF	−2.0 V	—	1	CO (23); $C_2O_4^{2-}$ (13); $HCOO^-$ (57); H_2 (—)	118
7		DMF	−2.0 V	1.23 M TFE	1	CO (30); $C_2O_4^{2-}$ (11); $HCOO^-$ (52); H_2 (—)	118
8		DMF	−2.0 V	1.23 M MeOH	1	CO (31); $C_2O_4^{2-}$ (9); $HCOO^-$ (53); H_2 (—)	118
9[d]	$[Fe(dophen)Cl]_2$	DMF	−2.0 V	—	1	CO (24); $C_2O_4^{2-}$ (11); $HCOO^-$ (59); H_2 (—)	118
10[d]		DMF	−2.0 V	1.23 M TFE	1	CO (42); $C_2O_4^{2-}$ (3); $HCOO^-$ (46); H_2 (—)	118
11[d]		DMSO	−2.0 V	—	1	CO (13); $C_2O_4^{2-}$ (7); $HCOO^-$ (74); H_2 (—)	118
12[d]		DMSO	−2.0 V	1.23 M TFE	1	CO (26); $C_2O_4^{2-}$ (5); $HCOO^-$ (64); H_2 (—)	118

a: Potentials given in V *vs.* Fc^+/Fc. b: Unspecified. c: Three ammonium acids tested: $(CH_3)_3NH^+Cl^-$, $(CH_3)_2NH_2^+Cl^-$ and $(C_2H_5)_3NH^+Cl^-$. d: H_2dophen = 2,9-bis(2-hydroxyphenyl)-1,10-phenanthroline.

Durand and collaborators in 1988 reported the electrocatalytic reduction of CO_2 by $[Fe(phen)_3]^{2+}$ in DMSO at −1.84 V *vs.* Fc^+/Fc with CH_4 as the only gaseous product observed (**Table 14** entry 1).[117] Iron complexes based on phenanthroline derivatives were later investigated for their possible electrocatalytic CO_2 reduction activity (**Table 14**, entries 2-12). $[Fe(dophen)(N\text{-}MeIm)_2]^+$ and the related [Fe(dophen)(Cl)] are reported to be electrocatalysts for the reduction of CO_2 into mixtures of CO, formate, and oxalate in DMF and DMSO. During bulk electrolyses in the absence of an acid source, at −2.0 V *vs.* Fc^+/Fc, formate is the major product. Addition of weak Brönsted acids is reported to increase overall catalytic activity but does not lead to a better selectivity, as formate remains the major product but upwards of 40% faradaic yield for either H_2 or CO is observed.[118]

Preliminary study of the electrocatalytic activity of $[Fe(bpy)(P(OET_3)_3)H]^+$ in CH_3CN showed current enhancement under CO_2 at an applied potential beyond two reduction features, at about −2.03 V *vs.* Fc^+/Fc, suggesting that the two-electron reduced species is a potential CO_2 reduction catalyst. However, no carbon-containing products were identified in this study.[119]

In 1992, Abruña and collaborators reported that the cyclic voltammograms of $[Fe(tppz)_2]^{2+}$, $[Fe(tpy)_2]^{2+}$ and $[Fe(tptz)_2]^{2+}$ in DMF (0.1M TBAP as a supporting electrolyte) exhibited current enhancement under CO_2 starting at −2.03, −1.62 and −1.85 V *vs.* Fc^+/Fc respectively. The authors ascribed this behaviour to catalytic activity for the electrochemical reduction of CO_2, however no bulk

electrolysis or product analysis was reported.[120] This behaviour was confirmed by the authors in 1994 for $[Fe(tpy)_2]^{2+}$ with an observed current enhancement of 100% at –1.6 V *vs.* Fc^+/Fc in DMF (0.1M TBAP as supporting electrolyte) and 500% at –1.74 V *vs.* Fc^+/Fc . Both electrochemical events are proposed to be ligand-based processes.[121] A later study of $[Fe(tpy)_2]^{2+}$ in DMF, in the presence of H_2O (95:5, v/v) however, reported no current enhancement under CO_2 up to −2.0 V *vs.* Fc^+/Fc.[122]

Iron complexes of phenanthroline were recently investigated as CO_2 reduction catalysts in a photosensitised system with copper-based photosensitisers (**T able 15**, entries 1-3). Remarkably, the products obtained are a mixture of H_2 and CO without any formate in contrast to what has been observed electrochemically for iron phenanthroline derivatives. This change in selectivity in photosensitized systems echoes the observations on the $Mn(bpy)(CO)_3Br$ where CO and H_2 were produced in electrocatalytic systems while formate was produced in photosensitised systems.

Table 15. Iron polypyridyl complexes assessed for catalytic CO_2 reduction through Photolysis

Entry	Molecule	Solvent[a]	Irradiation	Photosensitizer / Electron donor	Time (h)	Products (TON[b])	Ref.
1	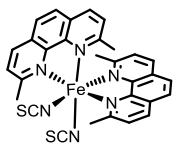	CH_3CN / TEOA (20%)	436 nm	$[Cu^I]$[c] / BIH[d]	1	CO (73); H_2 (45)	[123]
2		CH_3CN / TEOA (20%)	436 nm	$[Cu^I]$[c] / BIH[d]	5	CO (95); H_2 (56)	[123]
3		CH_3CN / TEOA (20%)	436 nm	— / BIH[d]	1	CO (56); H_2 (38)	[123]

a: % given by volume. b: calculated based on the concentration of iron catalyst. c: bimetallic Cu^I complex of the type $Cu^I(phenR)(P)_2^+$ with phenR a derivative of 1,10-phenanthroline and P a phosphine ligand. d: BIH = 1,3-dimethyl-2-phenyl-2,3-dihydro-1*H*-benzo[*d*]imidazole.

On the whole, the general class of Fe-polypyridyl complexes have offered promising preliminary results as potential catalysts of the electrochemical reduction of CO_2. However, much more effort is needed for understanding the trends in product selectivity as well as for increasing system stability.

4.4. Polypyridyl complexes of Co

The first Co-polypyridyl complex catalysing CO_2 reduction was reported by Lehn and Ziessel in 1982.[124] In this initial report, it was evaluated with $[Ru(bpy)_3]^{2+}$ as the photosensitiser in CO_2-saturated solutions of aqueous CH_3CN (20% H_2O) and TEOA as a sacrificial electron donor (**Table 16**, entries 1-5). As for the catalyst, no discrete molecular species was pre-synthesised and characterised, but rather variable concentrations of $CoCl_2$ and bpy were added to the mixture and assumed to form Co-bpy complexes *in situ* (presumed to have the chemical identity $[Co(bpy)_3]^{2+}$). Utilizing a 400 nm cut-off filter, photolysis of these systems resulted in the formation of mixtures of H_2 and CO. Upon varying the ratios of bpy:$CoCl_2$, the general trend was observed wherein larger amounts of additional bpy ligand in solution significantly decreased the amount of CO produced but increased production of H_2. Interestingly, under the same conditions, simply replacing the $CoCl_2$ salt with $RhCl_3$, $NiCl_2$, $CuCl_2$ or K_2PtCl_4 did not result in any observable reduced carbon products. This report was the first indication that Co-polypyridyl

complexes could be potentially used in catalytic systems for CO_2 reduction and possibly generated in straightforward in situ procedures.

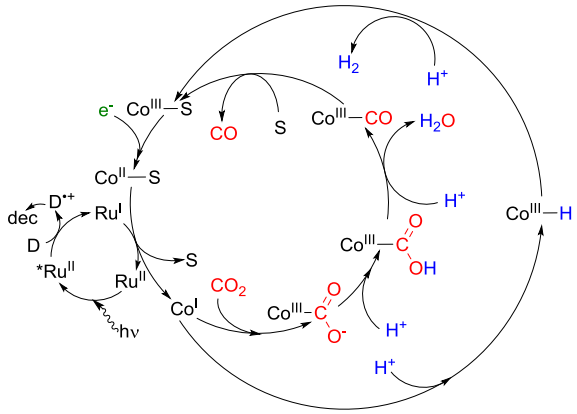

Scheme 10. General mechanism proposed by Lehn in 1986 to explain the two competitive pathways for CO_2 and proton reduction (reference [125]). "S" is a solvent molecule.

Soon after, Lehn and Ziessel extended their previous observations to other polypyridyl ligands.[125] Using similar conditions, by mixing cobalt salts with a variety of bidentate ligands in DMF, mixtures of CO and H_2 were again observed (**Table 16**, entries 6-15). Isotopic labelling experiments using $^{13}CO_2$ confirmed the source of CO to be CO_2. Subsequently, the mechanism depicted in **Scheme 10** was proposed to account for the production of H_2 and CO. Within the mechanism, the authors suggested that a Co^I-polypyridyl complex was the active catalyst, which could either react with a H^+ source or CO_2 in the selectivity determining step. By reaction with H^+, a Co^{III}–H would form and was proposed to be susceptible to further protonation to yield H_2 and a Co^{III}-polypyridyl complex. If the Co^I-polypyridine instead reacts with CO_2, CO was directly produced along with an equivalent of H_2O and a Co^{III}-polypyridyl compound. While not excessively detailed, this mechanistic proposal directed subsequent investigations of Co-polypyridyl systems. It suggested Co^I as being the likely identity of an active catalytic species, as well as the need for open coordination sites for interaction with H^+ or CO_2.

Table 16. Cobalt polypyridyl complexes assessed for catalytic CO_2 reduction through Photolysis

Entry	Complex[a]	Solvent[b]	Irradiation	Photosensitizer / Electron donor	Time (h)	Products (TON)	Ref.
1	$CoCl_2$:bpy (1:0)	CH_3CN / H_2O (20%)	> 400 nm	$[Ru(bpy)_3]^{2+}$ / NEt_3	22	CO (0.85); H_2 (1.23)	124
2	$CoCl_2$:bpy (1:0.3)	CH_3CN / H_2O (20%)	> 400 nm	$[Ru(bpy)_3]^{2+}$ / NEt_3	22	CO (0.50); H_2 (1.07)	124
3	$CoCl_2$:bpy (1:1)	CH_3CN / H_2O (20%)	> 400 nm	$[Ru(bpy)_3]^{2+}$ / NEt_3	22	CO (0.23); H_2 (1.02)	124
4	$CoCl_2$:bpy (1:3)	CH_3CN / H_2O (20%)	> 400 nm	$[Ru(bpy)_3]^{2+}$ / NEt_3	22	CO (0.23); H_2 (1.55)	124
5	$CoCl_2$:bpy (1:10)	CH_3CN / H_2O (20%)	> 400 nm	$[Ru(bpy)_3]^{2+}$ / NEt_3	22	CO (0.07); H_2 (2.57)	124
6	$CoCl_2$:bpy (1:3)	DMF	> 400 nm	$[Ru(bpy)_3]^{2+}$ / TEOA	15	CO (0.60); H_2 (1.08)	125
7	$CoCl_2$:phen (1:3)	DMF	> 400 nm	$[Ru(bpy)_3]^{2+}$ / TEOA	15	CO (0.19); H_2 (0.38)	125

8	$CoCl_2$:dm-phen (1:3)	DMF	> 400 nm	$[Ru(bpy)_3]^{2+}$ / TEOA	15	CO (1.85); H_2 (12.04)	125
9	$CoCl_2$:dph-phen (1:3)	DMF	> 400 nm	$[Ru(bpy)_3]^{2+}$ / TEOA	15	CO (0.37); H_2 (0)	125
10	$CoCl_2$:bathophen-S^2 (1:3)	DMF	> 400 nm	$[Ru(bpy)_3]^{2+}$ / TEOA	15	CO (0.32); H_2 (0.10)	125
11	$CoCl_2$:bathocup-S^2 (1:3)	DMF	> 400 nm	$[Ru(bpy)_3]^{2+}$ / TEOA	15	CO (0.65); H_2 (5.89)	125
12	$CoCl_2$:dmdph-phen (1:3)	DMF	> 400 nm	$[Ru(bpy)_3]^{2+}$ / TEOA	15	CO (0.05); H_2 (11.85)	125
13	$CoCl_2$:bpyR^2 (1:3)	DMF	> 400 nm	$[Ru(bpy)_3]^{2+}$ / TEOA	15	CO (0.68); H_2 (1.65)	125
14	$CoCl_2$:bpyR^4 (1:3)	DMF	> 400 nm	$[Ru(bpy)_3]^{2+}$ / TEOA	15	CO (1.67); H_2 (1.16)	125
15	$CoCl_2$:bpyR^3 (1:3)	DMF	> 400 nm	$[Ru(bpy)_3]^{2+}$ / TEOA	15	CO (0); H_2 (1.37)	125
16	$[Co(bpyF44)_3]^{2+}$	CO_2[c]	400-750 nm	$[Ru(bpyF44)_3]^{2+}$ / TEOA	48	CO (6); H_2 (1.2)	126
17		DMF-CO_2[d]	400-750 nm	$[Ru(bpyF44)_3]^{2+}$ / TEOA	48	CO (27.1); H_2 (3.3)	126
18	$[Co(bpyF62)_3]^{2+}$	CO_2[e]	400-750 nm	$[Ru(bpyF62)_3]^{2+}$ / TEOA	48	CO (17.7); H_2 (1.8)	126
19		DMF-CO_2[f]	400-750 nm	$[Ru(bpyF62)_3]^{2+}$ / TEOA	48	CO (15.6); H_2 (0.5)	126

a: dm-phen: 2,9-dimethyl-phen; dph-phen: 4,7-diphenyl-phen; dmdph-phen: 2,9-dimethyl-4,7-diphenyl-phen; bathophen-S_2: disodium, 4,7-diphenyl-phen-4',4''-disulfonate; bathocup-S_2: disodium, 2,9-dimethyl-4,7-diphenyl-phen-4',4''-disulfonate; bpy-R^2: 4,4'-dimethyl-bpy; bpy-R^4: 4,4',5,5'-tetramethyl-bpy; bpy-R^3: 3,3'-dimethyl-bpy; bpyF44: 4,4'-bis(*p*-(4-(perfluorobutyl)butoxy)phenyl)-2,2'-bipyridine; bpyF62: 4,4'-bis(2-(perfluorohexyl)ethoxy)-2,2'-bipyridine.
b: % given by volume. c: 35°C, 6.8 MPa. d: 50°C, 7.3 MPa. e: 35°C, 6.8 MPa. f: 50°C, 6.6 MPa.

The first pre-synthesised Co-polypyridyl system evaluated as a CO_2 reduction catalyst was $[Co(bpy)_3]Cl_2$ and the investigation was reported by Sutin and co-workers in 1985.[127] The study was conducted in aqueous solution with a bicarbonate buffer (pH = 8.5 - 10) instead of an organic solvent. The preparation of $[Co(bpy)_3]^+$ was reported and afforded the opportunity to monitor the behaviour of the Co(I)-polypyridyl complex towards CO_2 spectrophotometrically. In the dark and in the presence of CO_2, the pre-synthesised $[Co(bpy)_3]^+$ disappears, in parallel to the production of CO, alongside H_2 with trace amounts of formate. However, CO then further reacts with $[Co(bpy)_3]^+$ and yield the insoluble dimer $[Co(bpy)(CO)_2]_2$ (identified by diagnostic IR features) according to equations 9 and 10 (**Figure 5**).[127]

$$2\ [Co(bpy)_3]^+ + HCO_3^- + H_2O \rightarrow 2\ [Co(bpy)_3]^{2+} + CO + 3\ HO^- \quad (9)$$

$$[Co(bpy)_3]^+ + CO \rightarrow ¼\ [Co(bpy)(CO)_2]_2 + bpy + ½\ [Co(bpy)_3]^{2+} \quad (10)$$

$$[Co(bpy)(CO)_2]_2 + 6\ H^+ \rightarrow 4\ CO + 2\ H_2 + 2\ Co^{2+}(aq) + 2\ bpyH^+ \quad (11)$$

Of note, the production of CO could be quantified via the acidification of the solution (pH = 1), which decomposes the proposed dimeric species and liberates the trapped CO according to the reaction (11).

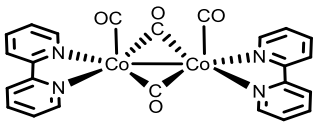

Figure 5 Structure of the proposed Co dimer studied by Sutin (reference [127]).

Despite these initial efforts towards incorporating Co-polypyridyl complexes into photochemical systems for CO_2 reduction catalysis, the electrochemistry of Co-polypyridyl complexes under CO_2 reduction conditions was not explored until 1988 by Durand and collaborators.[117] In this study, the authors reported cyclic voltammograms of $[Co(phen)_3]^{2+}$ in DMSO. Under an N_2 atmosphere, the complex exhibits a metal-based reduction wave at –1.28 V *vs.* Fc^+/Fc (Co^{II}/Co^{I}) and a two-electron feature at –1.97 V *vs.* Fc^+/Fc, described as Co^{I}/Co^{-I} redox event. Under an atmosphere of CO_2, the current increased in the region of the electrochemical feature at –1.97 V *vs.* Fc^+/Fc. This current enhancement was attributed to the reduction of CO_2 to formate, as no CO was detected. The only gaseous product detected was CH_4, but it is hypothesised to arise from decomposition of the solvent. As the primary catalytic wave occurs within an electrochemical feature containing significant ligand-reduction character, it was proposed that the loss of a phen ligand occurred at that potential, liberating a coordination site for interaction with CO_2.

Table 17. Cobalt polypyridyl complexes assessed for catalytic CO_2 reduction through CPE

Entry	Molecule	Solvent	Applied potential[a]	Proton source[b]	Time (h)	Products (faradic yields in %)	Ref.
1	$[Co(phen)_3]^{2+}$	DMSO	[c]	—	[c]	CH_4 (traces); H_2 (—); CO (—)	117
2	$[Co(tpy)_2]^{2+}$	DMF	−2.17 V	—	[d]	HCO_2^- ([c])	121
3		DMF	−1.93 V	H_2O (5%)	3	CO (20); H_2 (1)	122
4		DMF	−2.03 V	H_2O (5%)	3	CO (12); H_2 (5)	122
5		DMF	−2.08 V	H_2O (5%)	3	CO (9); H_2 (7)	122
6		DMF	−2.13 V	H_2O (5%)	3	CO (7); H_2 (11)	122
7		DMF	−2.23 V	H_2O (5%)	3	CO (3); H_2 (12)	122
8	$CoCl_2$:tpy (1:2)	DMF	−2.03 V	H_2O (5%)	2	CO (7)	122
9	$CoCl_2$:tpy (1:1)	DMF	−2.03 V	H_2O (5%)	1.5	CO (76)	122
10	$CoCl_2$:tpy (1:0.5)	DMF	−2.03 V	H_2O (5%)	2	CO (46)	122
11	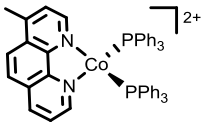	CH_3CN	−1.39 V	H_2O (8%)	1	CO (33); HCO_2^- (41)	98
12		CH_3CN	−1.39 V	—	1	CO (63); HCO_2^- (—)	98
13	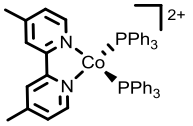	CH_3CN	−1.39 V	H_2O (8%)	1	CO (45); HCO_2^- (29)	98
14		CH_3CN	−1.39 V	—	1	CO (83); HCO_2^- (—)	98

a: potentials in V *vs.* Fc^+/Fc. b: % given by volume. c: not specified. d: after 4 equivalents of charge per cobalt center were passed.

Towards assessing Co-polypyridyl complexes with ligands having different denticities, Abruña reported in 1992 observations of current enhancement under CO_2 in the cyclic voltammograms of $[Co(tptz)_2]^{2+}$, $[Co(tppz)_2]^{2+}$ and $[Co(tpy)_2]^{2+}$. In DMF solutions, these complexes are reported to catalyse

the electrochemical reduction of CO_2 at potentials of –1.40, –1.67 and –2.00 V *vs.* Fc^+/Fc, respectively.[120] While the characterisation of the activity of these complexes is limited to the observation of current enhancement under an atmosphere of CO_2, this report indicates a strikingly high degree of versatility of Co-polypyridyl systems as CO_2 reduction catalysts. Taken with the previously described results, there is a general observation of activity for almost any variant of Co-polypyridyl systems. Abruña and collaborators elaborated further on the behaviour of $[Co(tpy)_2]^{2+}$ in solutions in DMF by cyclic voltammetry and controlled-potential electrolyses. In general agreement with previous systems, the cyclic voltammograms indicated that two ligand-based cathodic features could be observed past the $Co^{II/I}$ reduction event, and for both features a current enhancement under CO_2 could be observed of 95% at –2.03 V *vs.* Fc^+/Fc and 820% at –2.38 V *vs.* Fc^+/Fc. In contrast to the previous Co-polypyridyl catalysts however, bulk electrolysis at –2.17 V *vs.* Fc^+/Fc are reported to yield formate as the product of this catalytic process after four equivalents of charge per Co centre were passed (**Table 17** entry 2).[121]

Renewed interest in the $[Co(tpy)_2]^{2+}$ platform prompted further mechanistic studies. Using DMF/H_2O mixture as the solvent (95:5; v:v), the observation of reversible one-electron waves at −0.17 and −1.17 V *vs.* Fc^+/Fc corresponding to the $Co^{III/II}$, $Co^{II/I}$ as well as two ligand based reductions at −2.03 and −2.46 V *vs.* Fc^+/Fc was confirmed. Cathodic current enhancement in the −2.03 V *vs.* Fc^+/Fc wave in CO_2-saturated solutions was observed and CPE were performed to identify the nature of the CO_2 reduction products.[122] The only carbon-containing product reported is CO, alongside varying ratios of H_2. No CH_4, formaldehyde and more surprising, no formate was detected above background levels in these conditions. The ratios of CO and H_2 produced can be tuned with the applied potential during CPE, allowing for the production of syngas of specific composition (**Table 17**, entries 3-7). The overall low faradaic efficiency (15-21%) for this catalytic system was probed further. Mixing varying ratios of $CoCl_2$ and tpy ligand in a manner reminiscent to the previous study described by Lehn and Ziessel[124,125] and monitoring product evolution during CPE gave surprizing results. While a metal to ligand ratio of 1:2 exhibited similar activity and product selectivity as the pre-synthesized $[Co(tpy)_2]^{2+}$ complex, confirming the in-situ formation of the complex, lower ligand ratios, down to 1:0.5 showed higher faradaic efficiency for CO_2 reduction to CO (**Table 17**, entries 8-10). Up to 76% Faradic efficiency for CO production was measured in the 1:1 case after 60 min of CPE at −2.03 V vs Fc^+/Fc.[122] The identity of the active catalyst was theorized to contain only one tpy ligand per cobalt center, leaving open coordination sites for reaction with CO_2. The overall constant albeit slow activity for CO_2 reduction to CO was attributed to the formation of a resting state inactive cobalt species proposed to be dimeric following the observations by Sutin and co-workers on the related $[Co(bpy)_3]^{2+}$ system.[127]

Table 18. Cobalt polypyridyl complexes assessed for catalytic CO_2 reduction through chronopotentiometry

Entry	Molecule	R	Solvent	Applied Current[a]	Proton source[b]	Time (h)	Products (faradic yields in %)	Ref.

1	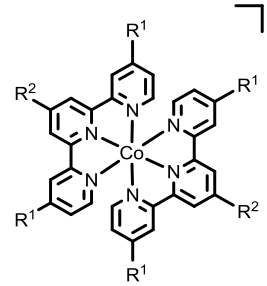	$R^1 = H$ $R^2 = PhCl$	DMF	−300 µA	H_2O (5%)	4	CO (31); H_2 (2)	128
2		$R^1 = H$ $R^2 = PhCH_3$	DMF	−300 µA	H_2O (5%)	4	CO (12); H_2 (5)	128
3		$R^1 = R^2 = H$	DMF	−300 µA	H_2O (5%)	4	CO (11); H_2 (18)	128
4		$R^1 = H$ $R^2 = OCH_3$	DMF	−300 µA	H_2O (5%)	4	CO (4); H_2 (23)	128
5		$R^1 = R^2 = {}^t$Bu	DMF	−300 µA	H_2O (5%)	4	CO (37); H_2 (4)	128

a: cathodic current applied at a 1.5 cm diameter pool of mercury working electrode. b: % given by volume.

Erreur ! Signet non défini.

Modifications to the H_2:CO ratio produced was also found to be attainable through tailoring of the electronic structure.[128] Ligand modifications to the positions para to the nitrogen with withdrawing or donating groups yielded complexes exhibiting minimal perturbation to the potential of the Co^{II}/Co^{I} reduction wave but a strong correlation was found between the first ligand based reduction and the Hammet parameter of the substituent para to the central nitrogen. Cathodic current enhancement in CO_2-saturated solutions were observed for all five complexes studied. The catalytic activity for CO_2 reduction was confirmed through chronopotentiometry, where a constant current was applied and the evolution of the potential was measured overtime. This set-up allowed for straightforward comparison of all 5 catalysts at a constant catalytic speed of reaction (**Table 18**). Interestingly, the selectivity for CO_2 reduction to CO over proton reduction to H_2 was dependent on ligand substituents, with the more donating groups yielding better proton reduction catalysts.[128]

The use of polypyridyl ligands on a Co centre as a component of a heteroleptic ancillary ligand field for CO_2 reduction electrocatalysts was initially reported by Ogura in 1997.[98] Using $[Co(dmbpy)(PPh_3)_2]^{2+}$ and $[Co(mphen)(PPh_3)_2]^{2+}$ as homogeneous catalysts in an anhydrous CO_2-saturated CH_3CN solution, CPE resulted in the production of CO in 60-80% faradic efficiency (**Table 17**, entries 11-14). However, when 8% water was added as a co-solvent to the system, the product selectivity shifted to 25-32% faradic yields for CO and 29-43% faradic yields for formate. These results nicely demonstrated the ability of Co-polypyridyl systems to be amenable to significant changes in product selectivity upon inclusion of alternative ligand types.

Several noteworthy examples of significantly modified Co-polypyridyl systems have also been reported. In 2010, Hirose modified the bpy ligand to include fluorinated alkyl chains in the 4,4’ positions which afforded complexes of the type $[Co(bpyR)_3]^{2+}$ (**Table 16**, entries 16-19) soluble in supercritical CO_2. In this solvent, under irradiation, at a pressure of 6.8 MPa and a temperature of 35°C, mixing $[Co(bpyR)_3]^{2+}$ with the photosensitiser $[Ru(bpyR)_3]^{2+}$ in the presence of an amine-based sacrificial electron donor resulted in the conversion of CO_2 to CO with H_2 as a side product.[126]

The last class of polypyridyl ligand assayed on a cobalt centre for CO_2 reduction catalysis was investigated by Costamagna and co-workers. They reported Co-polypyridyl systems wherein the polypyridyl ligand was fully conjugated and macrocyclic. Discrete Co complexes of hexaaza-macrocylic ligands derived from the condensation of bipyridines ($[Co(hamc\text{-}bpy)]^{2+}$) and phenanthrolines ($[Co(hamc\text{-}phen)]^{2+}$) were synthesised and characterised. Cyclic voltammetery under CO_2 resulted in cathodic current enhancement which the authors describe as evidence of catalytic CO_2 reduction.[129,130] Formation of CO and trace amounts of formaldehyde are detected in CPE in the presence of water, although it was not immediately clear which catalyst was being used in this experiment.[130]

In summary, while not exhaustively studied mechanistically, the Co-polypyridyl platform is reported to be a versatile and active catalytic system for CO_2 reduction resulting in primarily CO and H_2 production. While we better understand how to control the selectivity of the reaction via steric and electronic effects, the generally low faradaic yield values are still intriguing. Whether other products still not identified are produced and how to improve these numbers are issues which deserve further investigations. Furthermore, stability if often limited, possibly due to catalyst poisoning with CO, and here again appropriate modifications of the polypyridine ligands might improve the system if one understands the deactivation mechanism better.

4.5. Polypyridyl complexes of Ni

Investigations of Ni-polypyridyl platforms as CO_2 reduction catalysts date back to the late 1980s. The electrochemical reduction of CO_2 catalysed by $[Ni(bpy)_3]^{2+}$ was reported by Fiorani and collaborators in 1987.[131] Under an inert atmosphere, $[Ni(bpy)_3]^{2+}$ undergoes a two-electron reduction at –1.58 V *vs.* Fc^+/Fc. This reduction event was proposed to be accompanied by the loss of a bpy ligand to yield $[Ni(bpy)_2]^0$ as the active catalyst. When exposed to CO_2, cathodic current at potentials beyond –1.58 V *vs.* Fc^+/Fc increased and was assigned to catalytic CO_2 reduction. The major products detected are reported to be CO and CO_3^{2-}. Stability of this system is found to be limited and two deactivation pathways were identified, with an overall reaction mechanism presented in eq. 12-15:

$$[Ni(bpy)_3]^{2+} + 2\ e^- \leftrightarrow [Ni(bpy)_2] + bpy \quad (12)$$

$$[Ni(bpy)_2] + 2\ CO_2 + bpy \rightarrow [Ni(bpy)_3]^{2+} + CO + CO_3^{2-} \quad (13)$$

$$2\ CO + [Ni(bpy)_2] \rightarrow [Ni(bpy)(CO)_2] + bpy \quad (14)$$

$$m\ (CO_3^{2-}) + [Ni(bpy)_3]^{2+} \rightarrow [Ni(bpy)_{3-n}(CO_3^{2-})_m]^{(2-2m)+} + n\ (bpy) \quad (15)$$

The carbonyl and carbonate complexes of Ni-bpy are reported to be inert, and as such eqs. 14 and 15 represent deactivation pathways of the catalyst. Faradaic yields were around 30% for CO production. If bound CO molecules trapped in a Ni-carbonyl complex are taken into account, an extra 40-49% faradaic yield was found, thus resulting in upwards of 79% faradaic efficiency for total CO

production by this system. The faradaic yield for total CO_3^{2-} detected was found to be around 90%. Product inhibition and trapping was identified as a problem, and the authors proposed a bulk electrolysis setup with no separation between the working and counter electrode compartment to resolve this issue. In theory, the deactivated Ni/CO/CO_3^{2-} species could diffuse to the counter electrode where oxidation could occur, resulting in the continuous liberation of the bound equivalents of CO. Upon evaluating this reaction setup, no deactivation of the catalyst was observed and a constant stream of CO, as desired, was obtained. Although circumventing the deactivation pathways, it should be noted however that faradaic yields were significantly lower in this cell design. Furthermore, the need to oxidize the catalyst as part of a cycle to liberate the generated CO would hinder possible energy storage applications.

In 1989, Périchon and collaborators more deeply evaluated the behaviour $[Ni(bpy)_3]^{2+}$ using DMF or NMP (*N*-Methyl-2-pyrrolidone) as a solvent system for the electrochemical synthesis of symmetrical ketones from alkyl halides and CO_2.[111] Périchon and collaborators also proposed the initial formation of $[Ni(bpy)_2]^0$, at an applied potential of –1.67 V *vs.* Fc^+/Fc. However, they suggested the next steps in the catalytic cycle to be a reaction with four equivalents of CO_2 accompanied by a rapid six-electron reduction affording a free bpy ligand, two equivalents of CO_3^{2-} and a nickel complex with the stoichiometry $[Ni(bpy)(CO)_2]^0$. While no further comments were made regarding the nature of this complicated transformation, the authors state that $[Ni(bpy)(CO)_2]^0$ is further reduced by one-electron at –2.07 V *vs.* Fc^+/Fc to yield $[Ni(bpy)(CO)_2]^-$ which is claimed to be capable of performing an electron transfer to CO_2 yielding the radical species $CO_2^{\bullet-}$ transiently and regenerating $[Ni(bpy)(CO)_2]^0$. Two equivalents of the one-electron reduced radical $CO_2^{\bullet-}$ species are then proposed to undergo an electronic disproportionation to generate CO and CO_3^{2-}. An interesting experimental detail is that the authors utilised stoichiometric amounts of Mg^{2+} cations to sequester the carbonate generated as part of the reaction so as to avoid the deleterious side reactions observed by Fiorani and coworkers. In general, Périchon's mechanism for Ni-bpy electrocatalytic reduction of CO_2 is unique in that it proposes the active catalyst to be $[Ni(bpy)(CO)_2]^0$ and that reduction of CO_2 occurs through one-electron reduction and formation of a transient $CO_2^{\bullet-}$ species with minimal direct interaction with a Ni-centre.

As was the case for cobalt systems, Durand and co-workers extended the scope of polypyridyl ligands of Ni to phen (1,10-Phenanthroline) by reporting the electrochemical reduction of CO_2 catalysed by $[Ni(phen)_3]^{2+}$ at a potential of –1.63 V *vs.* Fc^+/Fc in DMSO (0.1M TBAP as the supporting electrolyte). The products are CO and a small amount of CH_4.[117] These results are in agreement with the observations for the related $[Ni(bpy)_3]^{2+}$ system. Of note, the cyclic voltammograms of $[Ni(phen)_3]^{2+}$ are qualitatively identical to that of $[Ni(bpy)_3]^{2+}$, with a two-electron cathodic feature under inert atmosphere that exhibits current enhancement in CO_2-staurated solutions. However, there is a significant difference in the assignment of this feature. Whereas the initial reports for $[Ni(bpy)_3]^{2+}$ identified the two-electron reduction as metal-based, accompanied by ligand loss, Durand and coworkers identify the two-electron

reduction feature for $[Ni(phen)_3]^{2+}$ as two coincidental one-electron reductions, one ligand-based and one metal-based, accompanied by loss of a ligand. The authors postulate that the reduction of the polypyridyl ligand could be instrumental to the observation of CO_2 reduction catalysis, but further mechanistic considerations are not given.

Table 19. Nickel polypyridyl complexes assessed for catalytic CO_2 reduction through CPE

Entry	Molecule	Solvent	Applied potential[a]	Proton source[b]	Time (h)	Products (faradic yields in %)	Ref.
1	$[Ni(bpy)_3]^{2+}$	CH_3CN	−1.63 V	—	[c]	CO (free:26, bound: 49) CO_3^{2-} (90)	131
2		CH_3CN	−1.88 V	—	[c]	CO (free: 39, bound: 40) CO_3^{2-} (92)	131
3	$[Ni(phen)_3]^{2+}$	DMSO	[d]	—	[d]	CH_4 ([d]) CO ([d])	117
4	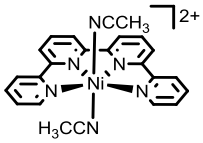	CH_3CN	−2.08 V[c]	—	[d]	CO (traces)	132
5	$[Ni(tpy)_2]^{2+}$	DMF	–1.72 V	H_2O 5%	3	CO (18); H_2 (0)	122
6		DMF	–1.76 V	H_2O 5%	3	CO (17); H_2 (0)	122
7		DMF	–1.89 V	H_2O 5%	3	CO (17); H_2 (0)	122
8		DMF	–2.14 V	H_2O 5%	3	CO (16); H_2 (0)	122

a: potentials in V *vs.* Fc^+/Fc. b: % given by volume. c: after 8 mol of electron per mol of nickel were passed. d: not specified.

In a report that ultimately combines the notion of the active species having the structural identity of $[Ni(L)(CO)_2]$ (L= polypyridine) as well as the importance of ligand reduction events for catalysis, Christensen *et al.* studied the behaviour of $[Ni(dmbpy)_3]^{2+}$ (dmbpy = 4,4′-dimethyl-2,2′-dipyridyl) and $[Ni(phen)_3]^{2+}$ under electrocatalytic CO_2 reduction conditions in CH_3CN using in-situ FTIR spectroscopy.[133] Using IR resonances, the authors directly identified the formation of $[Ni(dmbpy)_2]^0$ and $[Ni(phen)_2]^0$ upon the two-electron reduction of $[Ni(dmbpy)_3]^{2+}$ and $[Ni(phen)_3]^{2+}$ at –1.68 V *vs.* Fc^+/Fc. Complexes $[Ni(dmbpy)_2]^0$ and $[Ni(phen)_2]^0$ were further reported to react slowly with multiple equivalents of CO_2 to yield the corresponding $[Ni(L)(CO)_2]$ structures, presumably via a mechanism similar to that proposed by Périchon.[111] Using the carbonyl vibrational frequencies as a spectroscopic handle, the authors observed new frequencies under electrocatalytic conditions. They assigned these IR features to a catalytically competent $[Ni(L^{\bullet-})(CO)_2]^-$ state, with a ligand-localised radical anion, that is derived from one-electron reduction of the $[Ni(L)(CO)_2]$ complex. The authors proposed that decomposition of these species could occur in basic reducing conditions with $[Ni(dmbpy^{\bullet-})(CO)_2]^-$ and $[Ni(phen^{\bullet-})(CO)_2]^-$ reacting with trace water to yield inactive bimetallic clusters of the proposed structure $[Ni_2(\mu\text{-}H)(CO)_6]^-$.

In conjunction with reports on analogous Co- and Fe-polypyridyl systems, efforts were made towards assessing the activity of Ni-polypyridyl systems with ligands of higher denticity as catalysts of the reduction of CO_2. Abruña and collaborators published in 1992 that cyclic voltammograms in DMF of Ni complexes of tppz and tpy displayed cathodic current increase in the presence of CO_2, at –2.01

and –1.67 V *vs.* Fc^+/Fc respectively; however, no insights into mechanism or selectivity were reported.[120] Further probing of the $[Ni(tpy)_2]^{2+}$ system in DMF (0.1 M TBAP as a supporting electrolyte) under an atmosphere of N_2 by cyclic voltammetry revealed the presence of three reversible electrochemical features at +1.18, –1.85, and –1.67 V *vs.* Fc^+/Fc.[121] The features at +1.18 and –1.85 V *vs.* Fc^+/Fc are attributed respectively to $Ni^{III/II}$ and $Ni^{II/I}$ metal-centred reductions, however the feature at –1.85 V *vs.* Fc^+/Fc is reported to be ligand-centred. The onset of catalytic current under an atmosphere of CO_2 is shown to occur within the feature at –1.67 V *vs.* Fc^+/Fc. No further information is provided, but the assignments by the authors imply that, unlike the systems with bpy and phen ligands, no ligand reduction is required for catalysis in these examples and that generation of a Ni^I centre affords a catalytically active species towards CO_2 reduction.

The $[Ni(tpy)_2]^{2+}$ system was recently probed further in DMF both through cyclic voltammetry and controlled-potential eletrolysis.[122] Cyclic voltammograms confirmed the observations of two one-electron reduction waves close in potential, reported at −1.62 V and −1.88 V vs Fc^+/Fc. Interestingly, both waves are assigned to ligand based reduction events by comparison to cyclic voltammograms of $[Zn(tpy)_2]^{2+}$ which exhibit two one electron-reduction waves at −1.68 V and −1.81 V vs Fc^+/Fc.[122] CPE at potentials ranging from −1.72 V to −2.14 V vs Fc^+/Fc yielded CO as the only carbon-containing product detected in faradic yields of ~ 20% (**Table 19**, entries 5-8). Despite being performed in the presence of added water (95:5 in CH_3CN), no hydrogen was detected during CPE. The selectivity of $[Ni(tpy)_2]^{2+}$ towards CO_2 reduction to CO is all the more remarkable given the inactivity of related $Ni(bpy)_3$ complexes for CO_2 reduction in the presence of trace amount of water.[111,131] Overall the low faradic efficiency combined with the slow decrease of the catalytic current during CPE raised concerns over the long term stability of this catalytic platform.[122]

The qtpy (2,2′:6′,2″:6″,2‴-quaterpyridine) complexes of nickel were also investigated. In contrast to the analogous $[Co(qtpy)(OH_2)_2]^{2+}$ complexes, $[Ni(qtpy)(CH_3CN)_2]^{2+}$ (**Table 19**, entry 4) did not lead to the formation of an electroactive film on glassy carbon electrodes. Traces of CO were observed during controlled-potential electrolysis of $[Ni(qtpy)(CH_3CN)_2]^{2+}$ at –2.08 V *vs.* Fc^+/Fc under CO_2.[132] Thus, whereas nickel complexes supported by bidentate and tridentate polypyridyl ligands are found to be catalytically active for CO_2 reduction, tetradentate polypyridyl ligands seemingly behave differently and do not allow for the formation of an active species.

Ni complexes of bpy-based[134] and phen-based[129] hexa-aza-macrocycles $[Ni(hamc\text{-}bpy)]^{2+}$ and $[Ni(hamc\text{-}phen)]^{2+}$ have been reported to exhibit CO_2 reduction electrocatalytic activity in DMF.[130] However, no product detection was reported

In 1998, Fujita and coworkers published initial efforts towards evaluating Ni-bpy systems as photocatalysts.[135] In the absence of an external photosensitiser, the authors reported the results of photolysing solutions of $[Ni(bpy)_3]^{2+}$ in CO_2-saturated CH_3CN/TEA solutions using a 313 nm cut-off

filter. Via UV-Vis spectroscopy, the species $[Ni(bpy)_2]^+$ was identified as the product of the one-electron reduction of the excited state of $[Ni(bpy)_3]^{2+}$, which implies a rapid loss of a bpy ligand upon reduction. The authors further identified a second reduction event yielding $[Ni(bpy)_2]^0$. This formally Ni^0 species is proposed to react with CO_2 to yield CO as the only product. If water was added as a co-solvent, no CO production was observed. While no explanation was directly given for this behaviour, the observations are in agreement with those previously made by Christensen *et al.*[133] Also, in agreement with electrochemical investigations, Fujita and co-workers proposed that the CO produced from CO_2 reduction can lead to the formation of multimetallic and catalytically inactive adducts to $[Ni^I(bpy)_2]^+$ or $[Ni(bpy)_2]^0$. This inhibition explains the sub-stoichiometric amounts of CO produced during photocatalysis (0.5 mol of CO produced per mole of starting $[Ni(bpy)_3]^{2+}$).

Table 20. Nickel polypyridyl complexes assessed for catalytic CO_2 reduction through Photolysis

Entry	Molecule	Solvent	Irradiation	Photosensitizer / Electron donor	Time (h)	Products (TON)	Ref.
1	$[Ni(bpy)_3]^{2+}$	CH_3CN	313 nm	None / TEA 0.5M	1.7	CO (0.49[a])	135
2		CH_3CN	313 nm	None / TEA 0.5M	0.8	CO (0.38[a])	135
3[b]		CH_3CN	313 nm	None / TEA 0.5M	1.7	CO (0.46[a])	135
4		CH_3CN-EtOH (1:1)	313 nm	None / TEA 0.5M	0.7	CO (0.34[a])	135
5		CH_3CN-H_2O (1:1)	313 nm	None / TEA 0.5M	0.8	CO (0[a])	135

[a] Calculated based on catalyst concentration. Solutions were kept in the dark for 2h, then 0.1 mL air and 0.1 mL water were added just before GC analysis. [b] 1 mM bpy added to the catalytic run.

Upon considering precedent for Ni-polypyridyl systems as CO_2 reduction catalysts, a few general observations can be made. First, the major product is predominantly CO. Second, production of H_2 through H^+ reduction is exceedingly rare, which suggests that Ni-based systems might be ideal candidates for selective reduction of CO_2 over H^+ sources. Third, catalysts are often reported to be inhibited by CO and/or CO_3^{2-}. Finally, the active catalytic species might not necessarily require an entirely polypyridyl ancillary ligand field, but rather a combination of polypyridyl ligands and carbonyl ligands could be optimal. This heteroleptic ligand environment would have some similarities to those ligand fields found within active Re, Ru, Mn, W, and Mo systems.

4.6. Polypyridyl complexes of Cu

Reports on Cu-polypyridyl complexes as catalysts for CO_2 reduction are limited. From initial synthesis and activity studies by Haines and collaborators[136] and with further investigations by Kubiak and Haines,[137] the dinuclear $[Cu_2(\mu PPh_2bpy)_2(CH_3CN)_2]^{2+}$ (PPh_2bpy = 6-diphenylphosphino-2,2'-bipyridine) complex was found to catalyse the production of CO and CO_3^{2-} selectively under CO_2 electroreduction conditions, as assessed by IR spectroelectrochemistry. The proposed mechanism is depicted in **Scheme 11**. The polypyridyl framework was proposed to assist in storing multiple redox

equivalents, and to take an active role in catalysis. The authors point to comparable rate constants as well as redox behaviour and potentials to related Os catalysts as supporting evidence for mechanistic similarities.

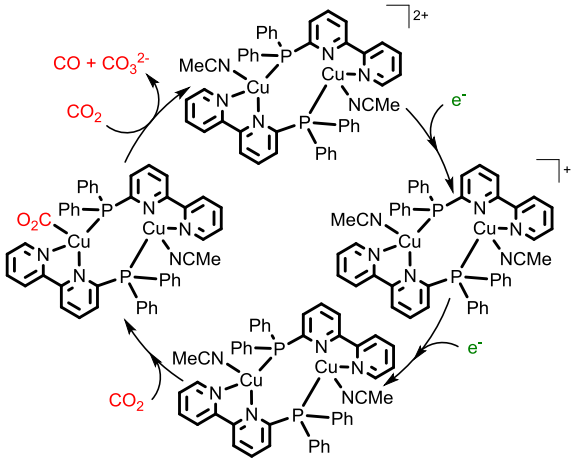

Scheme 11. Mechanism proposed for the catalytic reduction of CO_2 to CO catalysed by the copper complexes reported by Kubiak and Haines.

Durand and collaborators mentioned in their 1988 report that cyclic voltammograms of $[Cu(phen)_3]^{2+}$ in DMSO exhibit cathodic current enhancement under CO_2 within the two electrochemical features assigned to ligand-based reductions at –1.96 V and –2.12 V *vs*. Fc^+/Fc respectively.[117] They generally define the process as catalytic CO_2 reduction induced by ligand reduction.[117] Building on this work, Costamagna reported a similar behaviour of Cu complexes of hexaaza-macrocylic ligands derived from the condensation of bipyridines ($[Cu(hamc\text{-}bpy)]^{2+}$) and phenanthrolines ($[Cu(hamc\text{-}phen)]^{2+}$), but, while qualitatively similar, no product detection is provided.[129,130,138] The activity of $[Cu(tpy)_2]^{2+}$ for electrocatlytic CO_2 reduction was similarly assessed and current increase were reported under CO_2, along with deposition on carbon electrodes.[122] This observation echoes the rich literature of electocatalytic formate production from CO_2 reduction by copper-based electrodeposited materials and copper electrodes.[139–143]

5. Towards Applications: catalyst immobilization and devices

The development of molecular catalysts for CO_2 reduction was closely followed by efforts to immobilize these catalysts onto solid supports. The immediate interest in immobilizing molecular catalyst for CO_2 reduction is exemplified in the mere two-year gap between the initial publication of the ubiquitous Re(bpy)$(CO)_3$Cl catalyst by Lehn in 1983 and the first attempts to immobilize a variant of that species by Meyer in 1985.[144] Polypyridyl ligands in general are robust and can be easily synthetically modified which makes them amenable to facile immobilization. In this section a non-exhaustive survey of important advancements will be presented, highlighting the various approaches to heterogenization investigated over the years. The discussion will be organized through the type of surface that is supporting the molecular species and we will focus on three main classes of solid supports: electrodes, coordination polymers and membranes. An additional class, semiconductors, will not be presented as comprehensive reviews have recently been published. For more information on these supports, we direct the reader to recent reviews and references in this rapidly evolving area.[24,145–153]

5.1. Modified Electrodes

There had been several reports of the electropolymerization of modified bpy ligands on various electrode surfaces making a logical extension to CO_2 reduction catalysis.[154–158] The first such publication was by Meyer and co-workers in 1985 in which they reported the electropolymerization of Re(vbpy)$(CO)_3$Cl (vbpy = 4-vinyl-4'-methyl-2,2'-bipyridine) on a platinum electrode to afford poly-[Re(vpbpy)(CO)Cl] films.[144,159] Electrochemically initiated polymerization of complexes bearing a vbpy ligand proceeded through the one-electron reduction of the vinyl functional group followed by fast and indiscriminate radical coupling at the electrode surface. The polymerization could be achieved by CV upon sweeping cathodically at slow scan rates (0.1 V/s) in CH_3CN to afford a green film.[144,159] This colour was attributed to the formation of a dimer via reduction of Re(vbpy)$(CO)_3$Cl followed by the loss of a Cl^- to transiently yield Re(vbpy)$(CO)_3$ which can dimerize via the formation of a Re–Re bond within the film Upon exposure to air, the dimeric species was re-oxidized to a monomeric state within the polymer, thus affording a bright yellow colour. This assignment was supported by the presence of an oxidation feature at –0.54 V *vs* Fc^+/Fc for the green-gold film which is in remarkable agreement for the oxidation of the analogous homogeneous Re–Re bonded species. When the film was generated with an excess of PF_6^- anions present, XPS data showed minimal incorporation of phosphorus or fluorine. This suggested that Cl^- was retained in the film and that polymerization occurred faster than complete loss of Cl^-. Thus the green film is a mixture of polymerized $[Re(vbpy)(CO)_3Cl]^-$ and $[Re(vbpy)(CO)_3]_2$ species. The precise steps leading to polymer formation are a complicated combination of electron transfers and ligands loss events that are discussed in detail within reference.[159]

Table 21. Electrode Immobilized polypyridyl complexes assessed for catalytic CO_2 reduction through CPE

Entry	Molecular Precursor		Immobilisation method	Solvent	Applied potential[a]	Time (h)	Products (faradic yields in %)	Ref.
1	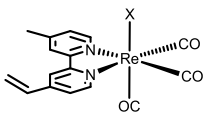	X = Cl	Cathodic cycling on Pt or glassy carbon electrode	CH_3CN	−1.94 V	1.3	CO (92); CO_3^{2-}(—)	144
2		X = Cl		CH_3CN	−1.94 V	0.5	CO (90); $C_2O_4^{2-}$(5)	159
3		X = $NCCH_3$		CH_3CN	−1.94 V	0.5	CO (95); $C_2O_4^{2-}$(—)	159
4		X = Cl	Cathodic cycling with illumination on p-Si and P-WSe_2	CH_3CN	-	-	CO (100)	160
5		X = Cl	Cathodic cycling on TiO_2 in CH_3CN	CH_3CN	-	-	-	161
6	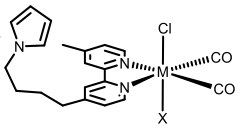	M = Re X = CO	Anodic cycling on Pt electrode	CH_3CN	–1.94 V	2.8	CO (78) CO_3^{2-}(81)	162
7		M = Ru X = Cl	CPE at 0.57 V vs SCE on Pt or carbon electrode in CH_3CN	CH_3CN / H_2O (80:20)	–1.64 V	b	CO (97) $HCOO^-$ (3)	163
8	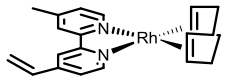		Cathodic cycling on glassy carbon electrode	CH_3CN	–1.99 V	c	H_2 (0-2) CH_3OH (0-38) CH_4 (5-18)	164
9	[Co(4'-vinyl-2,2':6',2"-terpyridine)$_2$]PF_6		Cathodic cycling on Pt or glassy carbon electrode in CH_3CN	DMF	–1.68 V	4	HCOOH (100)	165
10	[Co(4'-vinyl-2,2':6',2"-terpyridine)$_2$]PF_6		Cathodic Cycling on glassy carbon electrode in CH_3CN	H_2O	–1.30 V	d	H_2CO (39)	99
11	[Fe(4'-vinyl-2,2':6',2"-terpyridine)$_2$]PF_6			H_2O	–1.28 V	e	H_2CO (28)	99
12	[Cr(4'-vinyl-2,2':6',2"-terpyridine)$_2$]PF_6			H_2O	–1.30 V	f	H_2CO (87)	99
13	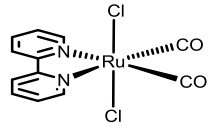		CPE at –2.03 V or Cathodic cycling on Pt or carbon electrode in CH_3CN	CH_3CN / H_2O (95:5)	–1.94 to –1.98 V	b	CO (90-100)	166,167
14				H_2O	–1.36 to – 1.51 V	b	CO (80-97)	166,167
15	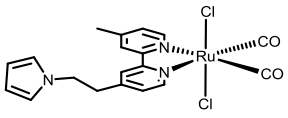		CPE at 0.57 V vs SCE on Pt or carbon felt in CH_3CN	CH_3CN / H_2O (95:5)	–1.88 V	b	CO (90)	166
16				H_2O	–1.52 V	b	CO (80)	166
17	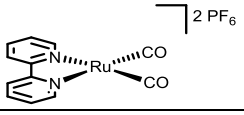		Cathodic cycling on Pt or carbon electrode in CH_3CN	CH_3CN	–1.99 V	b	CO (50) $HCOO^-$ (2)	163
18	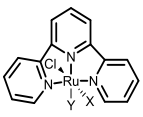	X = Cl Y = CO	Cathodic CPE on carbon electrode in CH_3CN	H_2O	–1.50 V	g	CO (60) $HCOO^-$ (15)	66
19		X = CO Y = Cl	Cathodic CPE on carbon electrode in CH_3CN	H_2O	–1.50 V	g	CO (60) $HCOO^-$ (15)	66

20	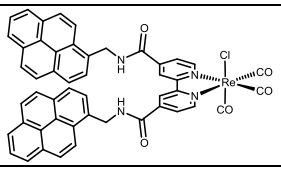	Soaking pyrolytic graphite electrodes in CH_2Cl_2 solutions	CH_3CN	–2.30 V	1.25	CO (70)	[168]
21	$CoCl_2$	[h]	DMF	–2.00 V	0.5	CO	[169]
22	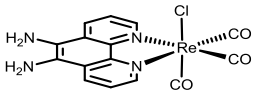	60°C in EtOH mixture with graphitic carbon	CH_3CN	[i]	-	CO (96)	[170]

a: potentials in V *vs.* Fc^+/Fc. b: After 60C are passed. c: After 8 to 16C are passed. d: After 2.3C are passed. e: After 2.9C are passed. f: After 1.1C are passed. g: After 20C are passed. h: Pretreatment of glassy carbon electrode with 4'-para diazonium phenyl-2,2':6',2"-terpyridine followed by soaking in DMF solution. i: 0.5 or 1.0 mA cm^{-2} constant current.

The deposition behaviour of $Re(vbpy)(CO)_3Cl$ was elaborated on a year later by Abruña and co-workers in the context of a broader study involving semiconducting surfaces.[160] The authors reported that direct formation of the bright yellow film occurred using the same system ($Re(vbpy)(CO)_3Cl$, Pt electrode, CH_3CN solvent) but faster scan rates of 0.5 V/s. The green film representative of a polymer with Re–Re bonds was only generated with scan rates slower than 0.2 V/s. This indicated that the nature of the polymerized catalyst can be controlled simply through deposition kinetics. The electrocatalytic activity of the yellow films originating from $Re(vbpy)(CO)_3Cl$ were evaluated by CV under atmospheres of N_2 and CO_2 in an CH_3CN solution.[159] Under N_2, an apparent reversible electrochemical feature is observed on the surface of the electrode at –2.01 V *vs* Fc^+/Fc. Under a CO_2 atmosphere however, that feature is replaced by catalytic current enhancement with an onset potential near –1.79 V *vs* Fc^+/Fc and a pre-feature with a peak current potential at –1.69 V *vs* Fc^+/Fc. When a constant potential of –1.94 V *vs* Fc^+/Fc was applied for 80 minutes (Table 21, Entry 1), the authors report the evolution of CO with a faradaic efficiency of 92.3% with no apparent loss of current density. By estimating the surface coverage of the Re-species, a TON of 516 was calculated. While the evaluation of the activity of the homogeneous analogue also yielded to the detection of high amounts of CO_3^{2-} anions, no carbonates were detected with the heterogeneous polymeric catalyst. The high TONs and the lack of carbonate formation suggests that, upon polymerization of the $Re(vbpy)(CO)_3Cl$ catalyst, a different mechanism is operative. This led to the exciting notion that, beyond any hypothetical practical benefits to motivate the heterogenization of polypyridyl-based catalysts for CO_2 reduction, such strategies might afford the ability to control and alter mechanisms and possibly product selectivity.

A different strategy for electropolymerization of a variant of $Re(bpy)(CO)_3Cl$ was reported by Deronzier and co-workers.[162] The ligand 4-(4-Pyrrol-l-ylbuty1)4'-methyl-2,2'-bipyridine (pyrbpy) was developed and $Re(pyrbpy)(CO)_3Cl$ was synthesized as a deposition precursor. Upon electrochemical oxidation of a solution of $Re(pyrbpy)(CO)_3Cl$ with a Pt electrode in CH_3CN, a feature in the CV with a peak potential of 0.93 V *vs* Fc^+/Fc was attributed to an irreversible pyrrole oxidation leading to the formation of a polymer film on the electrode. Subsequent cathodic sweeps indicated another irreversible feature attributed to reduction of the polymeric species followed by loss of the Cl^- ligand. Repeated

cycling afforded a polymeric film with no noteworthy observations regarding the colour or composition. Since there is no opportunity for the Re-complex to dimerize prior to polymerization, it was claimed that the oxidative deposition led cleanly to poly-[Re(pyrbpy)$(CO)_3$Cl]. The film could also be prepared by holding a constant potential at 0.86 V *vs* Fc^+/Fc. Upon evaluating the electrocatalytic behaviour towards CO_2 reduction, the poly-[Re(pyrbpy)$(CO)_3$Cl] film qualitatively behaved as the poly-[Re(vbpy)$(CO)_3$Cl] film.[162] When Re(pyrbpy)$(CO)_3$Cl was polymerized onto a Pt gauze electrode and a potential of –1.94 V *vs* Fc^+/Fc was applied in a CO_2-saturated CH_3CN, the only reduction product detected was CO **(Table 21** Entry 6). However, the polymer derived from pyrbpy was less stable than that derived from vbpy with substantial current losses observed. Furthermore, equimolar formation of carbonate along with CO was observed. Thus, the Re(pyrbpy)$(CO)_3$Cl polymer likely follows a mechanism similar to the homogeneous systems whereas Re(vbpy)$(CO)_3$Cl accessed an alternate pathway.

Meyer and co-workers investigated a Rh-based system making use of polymerized vbpy on carbon and platinum electrodes.[164] Beginning with [Rh(vbpy)(COD)]Br (COD = 1,5-cyclooctadiene) solutions in CH_3CN, a gold-orange film could be deposited by cycling cathodically under inert atmosphere. The film was found to have two reduction features at –1.54 V and –2.19 V *vs* Fc^+/Fc. Under an atmosphere of CO_2, the first cathodic feature became partially reversible but, upon scanning through a second feature, reversibility and electroactivity was lost for the modified electrode. This loss of activity at more negative potentials was explained as Rh(I) dissolving into solution upon the film being further reduced near the second reduction potential. An important consideration of all polymeric films for CO_2 reduction is that reduced metal centres are often more labile and can leach out from the film into solution. For this system, this could be overcome by studying the film in the presence of excess $[Rh(COD)Cl_2]_2$ in solution. The poly-[Rh(vbpy)COD]Br film proved indeed active in the presence of CO_2 and excess $[Rh(COD)_2Cl_2]_2$ in CH_3CN as shown by current enhancements within CV experiments. No catalytic current enhancements were observed for bare electrodes (Pt, carbon or Rh) or for $[Rh(COD)Cl]_2$ in the absence of the deposited film. Surprisingly, while very little formate, oxalate or CO was observed, the reaction produced significant amounts of CH_4 and CH_3OH, with faradaic yields of up to 18% and 38% respectively, along with H_2. Furthermore, in the presence of acid, ethylene and propylene were also observed. While the exact structure of the active film is unknown, the authors proposed that the activity was due to formation of Rh(0) as shown by XPS data and is in agreement with the observation of a black colour on the film during 1 minute induction period to catalysis. However, ability to obtain highly reduced products of CO_2 reduction and possibly C–C bond formation products is unique to the poly-[Rh(vbpy)COD]Br system as neither metallic Rh nor molecular Rh-polypyridyl complexes have been reported to catalyse such transformations.

The same strategy using vinyl-substituted polypyridyl ligands has also been used to generate Fe-, Ni- and Co-based films.[121,165] Catalytic current enhancement in CO_2-saturated DMF solutions were

observed for poly-[Co(vtpy)$_2$] (vtpy = 4'-vinyl-2,2':6',2"-terpyridine) films under CO_2 at –1.29 V *vs* Fc^+/Fc. This activity is reported at potentials 0.80 V more positive than the homogeneous counterpart, $[Co(tpy)_2]^{2+}$. This remarkable effect, while not well understood, was also observed in the case of poly-[Ni(vtpy)$_2$] films in acetonitrile solution with catalytic currents occurring at potentials 0.8 V more positive than the soluble $Ni(tpy)_2^{2+}$ analogue (–1.61 V and –2.39 V *vs* Fc^+/Fc respectively). While the current enhancement is less apparent for poly-[Fe(vtpy)$_2$], a significant diminution of the overpotential to catalysis is also reported. The quantification and identification of the products of CO_2 reduction were not emphasized but the constant trend of more positive onset potentials is observed upon polymerization. Controlled potential electrolyses of the poly-[Co(vtpy)$_2$] modified electrode revealed efficient production of formate as the primary product of CO_2 reduction (**Table 21** Entry 9). This strategy has also been extended to aqueous systems, where poly-[M(vtpy)$_2$] (M = Co, Fe Cr) were surprisingly found to generate formaldehyde as the major product of CO_2 reduction (**Table 21**, Entries 10-12).[99] Of note, the poly-[Cr(vtpy)$_2$] is the only instance of an immobilized chromium complex for CO_2 reduction and was reported produce formaldehyde with a remarkable faradic efficiency of 87%.

Whereas vinyl-substituted polypyridyl ligands are polymerized via the ligand, Ziessel and co-workers have also demonstrated that CO_2 reduction catalysts can be deposited as polymers onto electrode surfaces via the formation of one-dimensional chains supported by metal-metal bonds.[66,163,166,167] Controlled-potential electrolysis of a solution of Ru(bpy)$(CO)_2Cl_2$ in aqueous acetonitrile at –1.74 V *vs* Fc^+/Fc results in the formation of a dark blue film on the electrode surface (either carbon or Pt). FTIR, UV-visible, mass spectroscopy, and elemental analysis suggested that the film had a polymeric nature with a monomeric unit of [Ru(bpy)$(CO)_2$] containing a network connected via Ru–Ru bonds as depicted in **Figure 6**. Cyclic voltammograms taken in CO_2-saturated CH_3CN in the presence of H_2O showed catalytic current enhancement near –1.39 V *vs* Fc^+/Fc. Bulk electrolysis performed at –1.94 V *vs* Fc^+/Fc resulted in production of CO with 100% faradaic yield **(Table 21** Entry 13) . At longer time points, currents were found to decrease suggesting a degree of instability of the film. Qualitatively identical results were found in unbuffered aqueous solutions. A poly-[Ru(tpy)CO] film could also be prepared using Ru(tpy)$(CO)Cl_2$ as a homogeneous precursor. In that case, CO and formate were produced in water (faradaic yields 60% and 14% respectively) and the film was shown to decompose at a faster rate. This result exemplifies the ability to synthetically control product distribution of the Ru-based film through modifications of the polypyridine ligand. A possible advantage of forming a polymeric network via metal-metal bonds is that the polypyridyl ligand can still be modified to modulate the activity of the electrocatalyst.

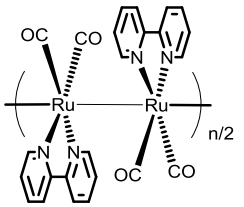

Figure 6. Proposed structure of poly-[Ru(bpy)$(CO)_2$]. Figure adapted from reference [166].

A parallel method to electropolymerization of catalysts onto electrodes is the preparation of polypyridyl copolymers followed by drop casting onto conductive surfaces. The polymerization of pyridyl halides and bipyridyl halides have been shown to afford polymers capable of binding transition metal centres capable of proton reduction.[171–173] Yamamoto and coworkers have demonstrated that such polymeric pyridyl networks can coordinate $NiCl_2$.[174] Upon evaporation of a solution of the copolymer onto a Pt electrode, electrolysis within a CO_2-saturated DMF solution afforded production of CO with 15% faradic efficiency. While reports such as these are limited, the preparation of polymers through chemical means followed by integration onto a conductive surface offers an advantage of direct electropolymerization in that a more diverse set of polymeric materials could be utilized.

An alternate method for immobilizing polypyridyl complexes on electrode surfaces, not as polymeric species but rather as discrete molecular entities more closely resembling the homogeneous precursors, uses non-covalent π-π interactions between pyrene-functionalized ligands and pyrolytic graphite. For example, pyrene-substituted bpy variants can be synthesized,[168] which served to generate Re(pyrene-bpy)$(CO)_3$Cl. Soaking a pyrolytic graphite electrode in a solution of Re(pyrene-bpy)$(CO)_3$Cl in CH_2Cl_2 resulted in a modified electrode surfaces as evidenced by CV and XPS (**Figure 7**). The electrochemical behaviour of such an immobilized Re catalyst was reported to be similar to vbpy-based Re films, with an initial reduction followed by the loss of Cl^- and dimerization to form surface bound $[Re(pyrene\text{-}bpy)(CO)_3]_2^{n+}$. CVs recorded in the presence of CO_2 showed catalytic current enhancement near –1.8 V *vs* Fc^+/Fc. Bulk electrolysis experiments at –2.3 V *vs* Fc^+/Fc for 1.25 hours afforded 58 TON for CO with a faradaic yield of 70% (**Table 21** Entry 20). However, current densities were shown to return to background levels beyond 1 hour of electrolysis. It was proposed that reduction of the pyrenyl moiety occurred and resulted into electrostatic repulsion between the ligand and the electrode.

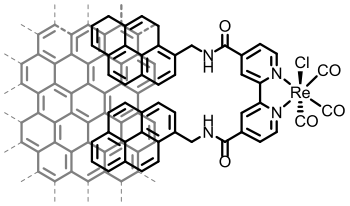

Figure 7. Depiction of noncovalently attached catalyst through π stacking between pyrolytic graphite and pyrene moieties.

Vinyl-polymerization offers poor control over film thickness and film morphology and noncovalent linkages possibly decompose upon reduction. In contrast, aryl-diazonium-substituted polypyridyl ligands can be used to electrochemically generate modified carbon electrode surfaces with a more uniform distribution of catalyst sites with possible covalent linkages to a carbon electrode surface. The reaction proceeds via liberation of an equivalent of N_2 and formation of an aryl radical that is believed to react with the carbon surface (**Scheme 12**). It was recently demonstrated that a glassy carbon electrode can be modified by cycling between 0.30 V and –0.90 V *vs* Fc^+/Fc at 0.05 V/s while immersed in an acetonitrile solution of tpy-Ph-N_2^+ BF_4^- for 10 scans.[169] Soaking this modified electrode in solution of $CoCl_2$ in DMF resulted in a modified electrode with CV features similar to that of $Co(tpy)Cl_2$ (**Scheme 12**). CVs taken in DMF in the presence of CO_2 resulted in catalytic current enhancement with an onset near –1.62 V *vs* Fc^+/Fc. Bulk electrolysis experiments at –2.00 V *vs* Fc^+/Fc resulted in formation of CO, which represented 70 TON per cobalt atom after 30 minutes (**Table 21** Entry 21). Beyond 30 minutes, the current essentially returned to baseline with no detectable CO released. This can be attributed to CO binding to the cobalt centres with rate-limiting release of CO.

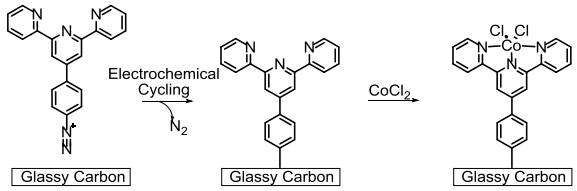

Scheme 12. Preparation of glassy carbon modified electrode via aryl-diazonium modified ligands and with post-modification metalation.

Recently, a different immobilization method with covalent linkages has been reported. As *o*-quinone moieties found on the edge planes of graphite can condense with substituted *o*-phenylenediamines, Re(5,6-diamino-phen)$(CO)_3Cl$ was used to modify graphite electrodes (**Scheme 13**).[170] The increased conjugation between the catalyst and the electrode was proposed to overcome poor conductivity issues in other polymeric films deposited onto electrodes. Catalytic current enhancement using this modified electrode was observed in CO_2-saturated acetonitrile with an onset near –2.0 V *vs* Fc^+/Fc. CO was the primary product of CO_2 reduction with a faradaic yield of 96% (**Table 21** Entry 22). Tafel analysis of the modified electrode indicated that the reaction was limited by a one-electron transfer. This is distinct from the homogeneous Re(phen)$(CO)_3Cl$ analogue which operates with an equilibrium electron transfer followed by a rate limiting chemical event. This system allowed TONs near 12,000, which outperforms all other immobilized Re systems, illustrating the importance in conductivity through the catalyst linkage to the electrode.

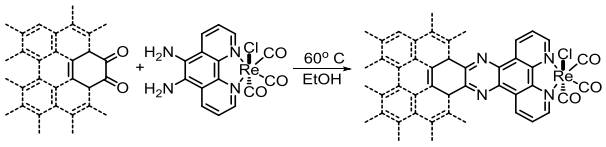

Scheme 13. Preparation of highly conjugated covalently linked immobilized catalyst on a pyrolytic graphite electrode

5.2. Coordination Polymers

Coordination polymers and metal-organic frameworks (MOFs) have emerged as an interesting class of solids that are composed of an extended array of inorganic subunits connected by organic linkers. The latter can also function as ligands for catalysts thus affording the opportunity to immobilize homogeneous catalysts within the coordination polymers and MOFs. One of the most common linker motifs is a dicarboxylate phenyl moiety that is capable of bridging two inorganic clusters. When that linker is biphenyl-4,4'-dicarboxylate (bpdc), substitution with 5,5'-dicarboxylate-2,2'-bipyridine (dcbpy) unit is often convenient. These substitutions open up the possibility of coordinating a polypyridyl catalyst within the polymer directly. One major drawback to the use of coordination polymers and MOFs is that these materials tend to be poorly conductive and not readily amenable to electrocatalysis. Therefore, studies involving immobilized catalysts for CO_2 reduction within these supports have primarily focused on integration within photocatalytic systems.

Table 22. Functionalized Coordination Polymers assessed for photocatalytic CO_2 reduction

Entry	Coordination Polymer	Solvent[a]	Irradiation	Photosensitizer/ Electron donor	Time (h)	Products (TON)	Ref.
1	$Re(CO)_3$@UiO-67	CH_3CN	>300nm	None / TEA	6	CO (5); H_2 (0.5)	175
2	CpRh@UiO-67	CH_3CN	>415nm	$Ru(bpy)_3Cl_2$ / TEOA	10	HCO_2^- (47); H_2 (36)	94
3	$Mn(CO)_3$@UiO-67	DMF	470nm	$Ru(dmb)_3(PF_6)_2$ / BNAH and TEOA	4	HCO_2^- (50) CO (4.5); H_2 (1)	107
4	$Re(CO)_3$@MOF-1	CH_3CN	410nm	None / TEA	6	CO (6.44); H_2 (0.4)	176
5		THF	410nm	None /TEA	6	CO (0.32); H_2 (4.15)	176
6	$[Ir(ppy)_2(dcbpy)]_2Y(OH)_3$	CH_3CN	>500nm	TEOA	6	HCO_2^- (1.5)	177

The first example came from Lin and co-workers in 2011.[175] UiO-67 has the chemical formula $Zr_6O_4(OH)_4(bpdc)_6$, with zirconium oxide/hydroxide nodes connected by bpdc linkers (structures depicted in **Figure 8**). The photocatalyst Re(dcbpy)(CO)Cl was successfully incorporated into UiO-67 synthetically by treating $ZrCl_4$ with a mixture of H_2dpdc and $Re(dcbpy)(CO)_3Cl$ during the preparation of the UiO-67 framework. The nanocrystalline powder obtained after the synthesis was confirmed by powder XRD to be isostructural to UiO-67 and was found to contain 2.7 mole percent of $Re(dcpy)(CO)_3Cl$. Catalytic assays with a suspension of this new MOF **$Re(CO)_3$@UiO-67** were performed in a CO_2 saturated acetonitrile with 5% volume triethylamine included as a sacrificial electron donor. Irradiation with a 300 nm long pass filter for 6 hours resulted in the formation of CO and H_2 (10:1 ratio) with a turnover number of 5 (**Table 22** Entry1). Control reactions in which the samples were

photolysed in the absence of CO_2 or left in the dark yielded no detectable CO, confirming the photocatalytic generation of CO from CO_2. A major benefit of catalyst immobilization is the ease of catalyst reclamation and reuse.

Lin and co-workers demonstrated that **$Re(CO)_3$@UiO-67** could be re-isolated via centrifugation and drying in 75% yield. When reintroduced into a catalytic run, the activity of the material was fully retained. However, activity was lost when the procedure was reproduced for a third catalytic run. In total, after 20 hours of irradiation, a TON of 10.9 was estimated. The deactivation of the material was attributed to slow leaching of Re into the solution upon reduction. As a homogeneous catalyst under identical conditions and after 6 hours of irradiation, Re(dcbpy)(CO)Cl was found to produce 2.5 TONs for CO and 0.5 TONs for H_2. Irradiation beyond 6 hours did not afford more products. Thus, upon heterogenization within a MOF, the Re catalyst becomes more selective for CO and has about a 2-fold increase in stability.

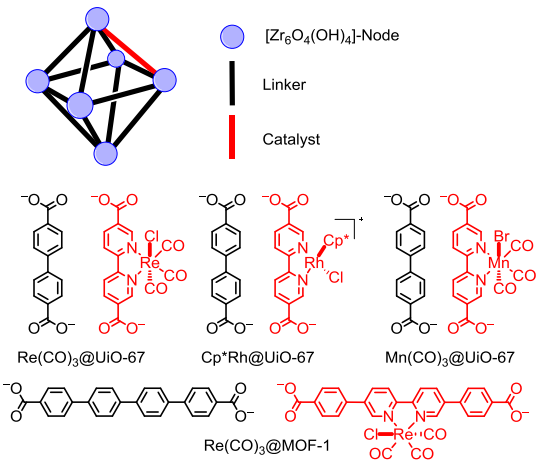

Figure 8. Schematic representation of UiO-67 framework and organic linkages and catalysts found within modified MOFs for photocataytic reduction of CO_2.

The parent UiO-67 framework has been shown be a versatile MOF capable of supporting other polypyridyl CO_2 reduction catalysts with alternate synthetic strategies. The incorporation of Cp*Rh(dcbpy)Cl_2 within UiO-67 was also reported through post-synthetic exchange procedures to afford **Cp*Rh@UiO-67**.[94] Soaking UiO-67 nanocrystals in an aqueous solution of Cp*Rh(dcbpy)Cl_2 resulted in substitution of the catalyst for the dpdc linker. The length of time during which the nanocrystals were allowed to soak in the solution of the Rh catalyst provided a variable amount of catalyst substitution ranging from 5 to 35% mole percent. This synthetic strategy resulted in much higher catalyst loadings within the UiO-67 crystals than observed for the earlier **$Re(CO)_3$@UiO-67** system. Photocatalysis was evaluated in a CO_2-saturated acetonitrile/triethanolamine mixture (5:1 volumetric ratio) with 10mM Ru(bpy)$_3Cl_2$ as a photosensitizer. Upon irradiation (>415 nm) the **Cp*Rh@UiO-67** produced only two products, formate and H_2 (**Table 22** Entry 2). Catalysis continued steadily for 6 hours

before deactivation, due to decomposition of the photosensitizer. Use of $^{13}CO_2$ as a substrate resulted in production of $H^{13}CO_2^-$ as identified by ^{13}C NMR. **Cp*Rh@UiO-67** could be re-isolated with 90% yield and reused 6 times. Over the course of 6 catalytic runs (representing a total photolysis time of over 4 days) 80% of the activity of the material was retained, which demonstrated the remarkable stability of the heterogenized catalyst.

As previously mentioned in **Section 3.4**, the homogeneous catalyst Cp*Rh(dcbpy)Cl_2, at low concentrations (below 0.1 mM) gave similar TONs and product distributions after 6 hours of irradiation under similar conditions. However, at higher catalyst loadings, significant decomposition of catalyst was observed. In contrast, higher catalyst loadings within **Cp*Rh@UiO-67** did not result in any loss of activity. This suggests a possible bimetallic decomposition pathway that is operative in solution but not upon heterogenization due to the site isolation of the catalytic centres. For **Cp*Rh@UiO-67**, there was increased production of H_2 relative to formate when the catalyst was incorporated beyond 10 mol%. This is attributed to thermal decomposition of formate into H_2 and CO_2 known to be catalysed by $[Cp^*Rh(bpy)]^{2+}$ systems.

The groups of Kubiak and Cohen have reported the immobilization of the Mn(dcbpy)$(CO)_3$Br catalyst within UiO-67 as well.[107] In that case, UiO-67 was first prepared with a 1:1 ratio of dcbpy and dpdc. Using a post-synthetic modification procedure, soaking the crystalline solid in a solution of $Mn(CO)_5Br$ in Et_2O, 76% of the available dcbpy linkers coordinated the Mn to afford an immobilized Mn(dcbpy)$(CO)_3$Br within UiO-67, **Mn$(CO)_3$@UiO-67**, with 38% mole catalyst loading. Photocatalysis experiments were performed in CO_2-saturated DMF/TEOA (4:1 volumetric ratio) containing 0.5 mM (Ru(dimethyl-bpy)$_3$]$(PF_6)_2$ as a photosensitizer and 0.2 M BNAH as a sacrificial electron donor. Irradiation with a 470 nm LED light source led to the formation of formate (with 96% selectivity and 50 TONs after 4 hours and 110 TONs after 18 hours (**Table 22** Entry 3). The catalyst could be recovered and reused with a slight decrease in TONs over the course of 4 experimental runs (from 50 TONs for the first 4-hour photolysis to 17 TONs for the fourth 4-hour photolysis). The heterogeneous **Mn$(CO)_3$@UiO-67** catalyst was found to outperform the homogeneous analogue Mn(dcbpy)(CO)Br, in terms of both activity and stability. The framework was proposed to contribute to the stabilization of reduced intermediates and in inhibiting bimetallic decomposition pathways that are known to be operative in the Mn(bpy)$(CO)_3$Br system.

With this report, UiO-67 has been shown to support three different catalysts and to replicate the homogenous system activities while consistently affording increased catalyst stability. Despite the success in using UiO-67 as a MOF solid support, one important consideration is that activity could be limited by diffusion of photosensitizers, substrates, electron donors, and products through the pores. Lin and co-workers sought to demonstrate that larger pore sizes could result in enhanced activity.[176] An analogous structure of UiO-67 using a tetraphenyl-dicarboxylate linker (dctp) was prepared, referred to

as MOF-1 within the manuscript. Returning to the $Re(bpy)(CO)_3Cl$ parent system, a related biphenylcarboxylate-bipyridyl ligand (bpcbpy) could be prepared and used to synthesize $Re(bpdcbpy)(CO)_3Cl$. Treatment of $ZrCl_4$ with a mixture of dctp and $Re(bpcbpy)(CO)_3Cl$ afforded the MOF-1 structure with an immobilized Re catalyst, **$Re(CO)_3$@MOF-1**. In CO_2-saturated organic solvents containing TEA as a sacrificial donor irradiation with a 410 nm LED led to CO and H_2 (**Table 22** Entries 4 and 5), in solvent-dependent ratios (1:13 and 16:1 in THF and CH_3CN, respectively) and TONs (TON_{CO} = 0.32 in THF and 6.44 CH_3CN). However, catalyst deactivation occurred and was proposed to arise from desorption of the Re centre from the MOF along with partial hydrogenation of the pyridine rings. Again the catalytic MOF proved more stable than the soluble $Re(bpyde)(CO)_3Cl$ analogue. While not claimed to be definitive proof of enhanced activity with larger pore size, these results clearly suggest a benefit to tuning the pore sizes of MOFs to facilitate diffusion.

Luo and co-workers have synthesized a one-dimension coordination polymer comprised of yttrium-hydroxide nodes linked together by dcbpy.[177] The bipyridyl moiety can coordinate an "$Ir(ppy)_2$" fragment resulting in a coordination polymer with the monomeric unit having the chemical formula $[Y(OH)_2((dcbpy)Ir(ppy))_2]$. Photocatalytic assays were performed in CO_2-saturated acetonitrile with 5% triethanolamine as a sacrificial electron donor. Irradiation was performed using 420-800 nm light. Upon irradiation of 40 mg of the coordination polymer for 6 hours, 38 μmol of formate were detected as the only product. Whereas the exact nature of the catalytic centre is unknown, the quantity of formate represents just over 1.5 TON per Ir centre (**Table 22** Entry 6). Compared to the homogeneous analogue $Ir(ppy)_2(dcbpy)$, the coordination polymer had identical selectivity with a slight enhancement in activity. However, after 6 hours of irradiation, the homogeneous system was completely inactive. In contrast, the coordination polymer could be easily recollected and retained full activity over 5 successive catalytic runs with only slight leaching of Ir into solution.

The use of MOFs and coordination polymers as solid supports for CO_2 reduction catalysts is still an emerging field. With the ubiquitous nature of biphenylene linkers used within these structures, substitutions with functionalized polypyridyl catalysts have been shown to be a convenient strategy to integrate catalysts with these polymers. To date, catalytic activity has generally been conserved upon immobilization with substantial increases in overall stability and recyclability of the catalysts. While primarily limited to photocatalytic applications so far, as advances are being made in conductive MOFs and coordination polymers, integration into electrocatalytic systems should become more feasible moving forward.

5.3. Membranes

The use of porous membranes as solid supports for catalyst immobilization offers several practical advantages over other strategies. Membranes are often conductive and interface easily with electrode surfaces, thereby affording direct integration with electrode materials. They also can be tuned

to have hydrophobic properties, which should assist in inhibiting proton reduction. Membranes are versatile and have good stability in various solvents and at various pHs in aqueous media. Furthermore, immobilization of catalysts can often occur simply via adsorption from a solvent in which the catalysts are soluble. The modified membrane can then operate in solvents where the catalyst is typically insoluble and in which homogeneous catalysis would be impossible.

The most important membrane for immobilizing CO_2 reduction catalysts is the Nafion© membrane which consists of a poly-tetrafluoroethane backbone with perfluorovinyl substituents that terminate in sulfonate functionalities. Kaneko and co-workers first reported the immobilization of $Re(bpy)(CO)_3Br$ and $Re(tpy)(CO)_3Br$ within a Nafion© membrane in 1993.[178] The electrochemical behaviour of the immobilized Re catalysts in aqueous media closely mimics that of the homogeneous analogues previously described, with reduction followed by loss of Br^- and then by the formation of a dimeric species. CO_2 electroreduction produced formic acid, CO and H_2. The selectivity for CO_2 vs H^+ reduction and for formic acid vs CO was shown to be dependent on the applied potential (**Table 23** Entries 1-6). For both the $Re(bpy)(CO)_3Br$ and $Re(tpy)(CO)_3Br$ systems, applying more negative potentials resulted in greater H^+ reduction. When more positive potentials are used with the $Re(bpy)(CO)_3Br$ system, the reaction favours formic acid over CO as a product of CO_2 reduction. It thus appears as if CO was produced at a relatively constant faradaic efficiency regardless of applied potential. However, more positive potentials favour the formation of formic acid, while more negative potentials favour the formation of H_2. Thus, it is likely that productive cycles affording formic acid and H_2 share a common intermediate with a potential-dependent selectivity determining step.

Table 23. Membrane immobilized catalysts assessed for electrocatalytic CO_2 reduction tested in H_2O at pH 7

Entry	Molecular Precursor		Immobilisation method	Applied potential[a]	Time (h)	Products (faradic yields in %)	Ref.
1	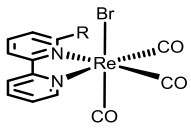	R = H	DMF/alcohol solution mixed with Nafion© and drop-cast onto basal-plane pyrolytic graphite	−1.46 V	4.30	HCOOH (48); CO (17); H_2 (39)	178
2		R = H		−1.56 V	4.27	HCOOH (12.4); CO (29); H_2 (53)	178
3		R = H		−1.66 V	2.08	HCOOH (12); CO (17); H_2(78)	178
4		R = H		−1.76 V	2.38	HCOOH (7); CO (8); H_2 (68)	178
5		R = Py		−1.66 V	3.04	HCOOH (15); H_2 (51)	178
6		R = Py		−1.76 V	3.19	HCOOH (8); H_2 (82)	178
7	$Co(tpy)_2(PF_6)_2$		Soaking Nafion©/basal plan pyrolytic graphite electrode in aqueous solution of catalyst	−1.26 V	4.84	HCOOH (51); H_2 (13)	179
8				–1.51 V	3.89	HCOOH (10); H_2 (68)	179
9				–1.71 V	3.06	HCOOH (5); H_2 (87)	179
10	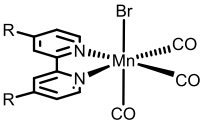	R = H	CH_3CN/alcohol solution mixed with Nafion© drop-cast onto glassy carbon electrode	–1.50 V	4	CO (26); H_2 (17)	180
11		R = H		–1.60 V	4	CO (22); H_2 (24)	180
12		R = H		–1.70 V	4	CO (51); H_2 (24)	180
13		R = H		–1.80 V	4	CO (7); H_2 (81)	180
14		R = H	CH_3CN/alcohol solution mixed with Nafion© and CNT	–1.45 V	4	CO (11); H_2 (52)	180
15		R = H		–1.65 V	4	CO (22); H_2 (47)	180

			drop-cast onto glassy carbon electrode				
16		R = H	CH_3CN/alcohol solution mixed with Nafion© and MWCNT drop-cast onto glassy carbon electrode	–1.60 V	4	CO (50); H_2 (14)	[181]
17		R = H		–1.70 V	4	CO (52); H_2 (11)	[181]
18		R = ^{t}Bu		–1.60 V	4	CO (44); H_2 (46)	[181]
19		R = ^{t}Bu		–1.70 V	4	CO (75); H_2 (24)	[181]
20		R = OH		–1.60 V	4	CO (40); H_2 (1)	[181]

a: potentials in V *vs.* Fc^+/Fc.

Kaneko and co-workers quickly extended this strategy of immobilization to the $[Co(tpy)_2]^{2+}$ catalytic system (**Table 23** Entries 7-9).[179] Using analogous procedures as was reported with the Re systems, they prepared glassy carbon electrodes coated with Nafion© containing $[Co(tpy)_2](PF_6)_2$. Qualitatively similar results could be found in which CO_2 electroreduction is favoured at more positive potentials. Of note, the major CO_2 reduction product was formic acid and not CO, with faradaic efficiencies as high as 51.4% at –1.26 V *vs* Fc^+/Fc applied potential.

Cowen and co-workers have revisited Nafion© as a solid support. Using similar methods as Kaneko and co-workers, $Mn(bpy)(CO)_3Br$ could be immobilized within Nafion© by soaking the membrane in an acetonitrile/propanol solution of $Mn(bpy)(CO)_3Br$.[180] The modified Nafion© was then drop cast onto glassy carbon electrodes or mixed with carbon nanotubes (CNTs) as high surface area electrodes. Cyclic voltammograms in aqueous solutions at pH 7 were qualitatively similar to those of the homogeneous system, with evidence for dimerization occurring upon reduction. This suggests that the Mn catalysts either freely diffuse within the membrane or are immobilized in localized clusters allowing them to interact with each other. Controlled potential electrolyses of the films on glassy carbon electrodes between –1.5 and –1.8 V *vs* Fc^+/Fc in a CO_2 saturated aqueous solution at pH 7 led to the production of CO along with H_2 (**Table 23** Entries 10-13). Total faradic efficiencies were found to be as high as 51% with as much as 471 TONs for CO production.[180] When the modified Nafion© is supported on multi-walled carbon nanotubes (MWCNTs), a 10-fold current density enhancement was observed by CV at slow scan rates.[181] However, controlled potential electrolyses determined that the current enhancement was primarily due to formation of H_2, now the major product in a 2:1 ratio (**Table 23** Entries 16-17).

An attractive feature of catalyst immobilization within Nafion© is that most synthetic variants of a catalyst should be amenable to heterogenization. There should be a high degree of functional group tolerance to immobilization so activity could be synthetically tuned similarly to homogeneous systems. To demonstrate this, Cowen and co-workers further reported the immobilization of three variants of $Mn(bpy)(CO)_3Br$: $Mn(bpy\text{-}^tBu)(CO)_3Br$, $Mn(bpy\text{-}COOH)(CO)_3Br$ and $Mn(bpy\text{-}OH)(CO)_3Br$.[181] All three complexes were homogeneous catalysts for CO_2 reduction to CO in acetonitrile. However, upon immobilization of $Mn(bpy\text{-}COOH)(CO)_3Br$ within Nafion© and then on MWCNTs, no CO_2 reduction

could be observed in aqueous solution at pH 7. In contrast, the immobilized Mn(bpy-^{t}Bu)(CO)$_3$Br demonstrated high activity for CO_2 reduction under similar conditions with the formation of H_2 and CO in a 3:1 ratio, with 46.1 TONs of CO in 4 hours (**Table 23** Entries 19-20). These observations indicate that catalyst performance within Nafion© cannot be assumed to directly relate to solution behaviour. However, it also shows that there is a possibility to tune activity through substitution. Replacing bpy with bpy-^{t}Bu resulted in an increase in TONs for CO over 4 hours from 35.9 to 46.1, representing an activity enhancement of over 28%.[181]

6. Conclusions and Perspectives

Polypyridine-metal complexes make the largest class of molecular catalysts for CO_2 electro- and photo-reduction. This journey through this family of catalysts provides a clear view of their potential for applications. This is in particular due to a quite broad and quick development of electrode materials based on such complexes, taking advantage of the modern methodologies available for immobilizing ligands or complexes within solids or at the surface of electrodes. Indeed there is no doubt that future technological devices for CO_2 reduction will use solid materials, thus challenging molecular chemists positively with regard to the contribution of their science to the development of new energy technologies.

On the other hand, despite these interesting conclusions, it is striking to observe a number of limitations and challenges that need to be addressed.

First, while there is a general consensus that efforts should focus on non-noble metals, the greatest majority of studies still concern catalysts based on 4d and 5d metals, with Re and Ru complexes continuing to enjoy broad investigations. In contrast, probably because the initial observations on Fe-, Cu-complexes were disappointing, these metals have been essentially ignored. This is not true for Co-, and to a lesser extent for Ni-complexes. However, so far, the performances of this subclass of catalysts, in terms of faradic yields, stability and turnover numbers, have not reached the appropriate level for further developments. Probably the most novel and interesting system is the Mn-based one discovered by Deronzier and coll. Nevertheless, there is an urgent need to explore the polypyridine platform more extensively for discovering new catalysts based on Fe, Co, Ni, Mn and Cu.

Second, while polypyridines can potentially be modified synthetically to afford a variety of ligands with various electronic and steric (important to control critical monomer/dimer) effects, it is surprising to see so little variation in the structure of the most studied ligands, such as bipyridine, phenanthroline and terpyridine for example. The substituents are generally limited to methyl, tert-butyl and carboxyl groups. This is due to the fact that only few such derivatives are commercially available and little effort has been made in developing synthetic strategies for producing original derivatives of bpy, phen and tpy ligands. It is even more surprising when one considers the importance of such ligands in general inorganic, coordination and organometallic chemistry. These efforts should be engaged now, in order to further understand basic aspects of the reactivity and selectivity of the best catalysts and further improve their performances.

Third, with the exception of the Re-based catalysts, so far the number of deep mechanistic investigations is very limited. Still, catalytic intermediates are incompletely characterized and sometimes contradictory mechanisms have been proposed for similar systems. While indeed there is no relevance spending excessive efforts to mechanistically characterize weakly active systems, some of the catalysts described in this review article clearly deserve more in-depth mechanistic investigations. Here again, this knowledge will obviously inspire the chemists towards new and more efficient, selective and stable systems.

Even though the advent of a new world based on renewable energies and storage technologies is urgent enough time and support should be given to the chemists to address some of these very fundamental questions.

ACKNOWLEDGMENT

We acknowledge financial support from the French National Research Agency (Labex program: DYNAMO, ANR-11-LABX-0011; ANR project: Carbiored ANR-12-BS07-0024-03) and from Fondation de l'Orangerie for individual Philanthropy and its donors.

7. References

1 N. S. Lewis and D. G. Nocera, *Bridge*, 2015, **45**, 41–47.
2 N. S. Lewis and D. G. Nocera, *Proc. Natl. Acad. Sci. U. S. A.*, 2006, **103**, 15729–15735.
3 T. R. Cook, D. K. Dogutan, S. Y. Reece, Y. Surendranath, T. S. Teets and D. G. Nocera, *Chem. Rev.*, 2010, **110**, 6474–6502.
4 J. Qiao, Y. Liu, F. Hong and J. Zhang, *Chem. Soc. Rev.*, 2014, **43**, 631–75.
5 C. Costentin, M. Robert and J.-M. Savéant, *Chem. Soc. Rev.*, 2013, **42**, 2423–36.
6 J. England, E. Bill, T. Weyhermüller, F. Neese, M. Atanasov and K. Wieghardt, *Inorg. Chem.*, 2015, **54**, 12002–12018.
7 M. Wang, T. Weyhermüller, E. Bill, S. Ye and K. Wieghardt, *Inorg. Chem.*, 2016, acs.inorgchem.6b00609.
8 M. Wang, J. England, T. Weyhermu and K. Wieghardt, *Inorg. Chem.*, 2014, **53**, 2276–2287.
9 C. C. Scarborough, K. M. Lancaster, S. DeBeer, T. Weyhermueller, S. Sproules and K. Wieghardt, *Inorg. Chem.*, 2012, **51**, 3718–3732.
10 A. Winter, G. R. Newkome and U. S. Schubert, *ChemCatChem*, 2011, **3**, 1384–1406.
11 C. Kaes, A. Katz and M. W. Hosseini, *Chem. Rev.*, 2000, **100**, 3553–3590.
12 J. Hawecker, J.-M. Lehn and R. Ziessel, *Chem. Commun.*, 1983, 536–538.
13 N. Elgrishi, Pierre et Marie Curie - Paris VI, 2015.
14 J. R. Aranzaes, M.-C. Daniel and D. Astruc, *Can. J. Chem.*, 2006, **84**, 288–299.
15 C. G. Zoski, *Handbook of Electrochemustry*, Elsevier, Oxford, 2007.
16 M. L. Pegis, J. A. S. Roberts, D. J. Wasylenko, E. A. Mader, A. M. Appel and J. M. Mayer, *Inorg. Chem.*, 2015, **54**, 11883–8.
17 M. L. Clark, K. A. Grice, C. E. Moore, A. L. Rheingold and C. P. Kubiak, *Chem. Sci.*, 2014, **5**, 1894–1900.
18 F. Franco, C. Cometto, F. Sordello, C. Minero, L. Nencini, J. Fiedler, R. Gobetto and C. Nervi, *ChemElectroChem*, 2015, **2**, 1372–1379.
19 J. Tory, G. Gobaille-Shaw, A. M. Chippindale and F. Hartl, *J. Organomet. Chem.*, 2014, **760**, 30–41.
20 J. Tory, B. Setterfield-Price, R. A. W. Dryfe and F. Hartl, *ChemElectroChem*, 2015, **2**, 213–217.
21 J. Hawecker, J. M. Lehn and R. Ziessel, *Helv. Chim. Acta*, 1986, **69**, 1990–2012.
22 J. Hawecker, J.-M. Lehn and R. Ziessel, *J. Chem. Soc. Chem. Commun.*, 1984, **984**, 328–330.
23 J.-M. Savéant, *Chem. Rev.*, 2008, **108**, 2348–2378.
24 G. Sahara and O. Ishitani, *Inorg. Chem.*, 2015, **54**, 5096–5104.
25 B. P. Sullivan, C. M. Bolinger, D. Conrad, W. J. Vining and T. J. Meyer, *J. Chem. Soc. Chem. Commun.*, 1985, 1414–1416.
26 F. P. A. Johnson, M. W. George, F. Hartl and J. J. Turner, *Organometallics*, 1996, **15**, 3374–3387.
27 J. M. Smieja and C. P. Kubiak, *Inorg. Chem.*, 2010, **49**, 9283–9289.
28 S. A. Chabolla, E. A. Dellamary, C. W. Machan, F. A. Tezcan and C. P. Kubiak, *Inorganica Chim. Acta*, 2014, **422**, 109–113.
29 K. Wong, W. Chung and C. Lau, *Jounal Electroanal. Chem.*, 1998, **453**, 161–170.
30 J. M. Smieja, E. E. Benson, B. Kumar, K. A. Grice, C. S. Seu, A. J. M. Miller, J. M. Mayer and C. P. Kubiak, *Proc. Natl. Acad. Sci. U. S. A.*, 2012, **109**, 15646–15650.
31 E. E. Benson and C. P. Kubiak, *Chem. Commun.*, 2012, **48**, 7374–7376.
32 S. Meister, R. O. Reithmeier, M. Tschurl, U. Heiz and B. Rieger, *ChemCatChem*, 2015, **7**, 690–697.
33 J. A. Keith, K. A. Grice, C. P. Kubiak and E. A. Carter, *J. Am. Chem. Soc.*, 2013, **135**, 15823–15829.
34 C. Riplinger and E. A. Carter, *ACS Catal.*, 2015, **5**, 900–908.
35 C. Riplinger, M. D. Sampson, A. M. Ritzmann, C. P. Kubiak and E. A. Carter, *J. Am. Chem. Soc.*, 2014, **136**, 16285–16298.
36 E. E. Benson, M. D. Sampson, K. A. Grice, J. M. Smieja, J. D. Froehlich, D. Friebel, J. A. Keith, E. A. Carter, A. Nilsson and C. P. Kubiak, *Angew. Chemie - Int. Ed.*, 2013, **52**, 4841–4844.
37 E. E. Benson, K. A. Grice, J. M. Smieja and C. P. Kubiak, *Polyhedron*, 2013, **58**, 229–234.

38 M. D. Sampson, J. D. Froehlich, J. M. Smieja, E. E. Benson, I. D. Sharp and C. P. Kubiak, *Energy Environ. Sci.*, 2013, **6**, 3748–3755.
39 K. A. Grice, N. X. Gu, M. D. Sampson and C. P. Kubiak, *Dalton Trans.*, 2013, **42**, 8498–503.
40 Y. Hayashi, S. Kita, B. S. Brunschwig and E. Fujita, *J. Am. Chem. Soc.*, 2003, **125**, 11976–11987.
41 J. Agarwal, E. Fujita, H. F. Schaefer and J. T. Muckerman, *J. Am. Chem. Soc.*, 2012, **134**, 5180–5186.
42 C. W. Machan, S. A. Chabolla, J. Yin, M. K. Gilson, F. A. Tezcan and C. P. Kubiak, *J. Am. Chem. Soc.*, 2014, **136**, 14598–14607.
43 H. Hori, O. Ishitani, K. Koike, F. P. A. Johnson and T. Ibusuki, *Energy Convers. Manag.*, 1995, **36**, 621–624.
44 K. Koike, H. Hori, M. Ishizuka, J. R. Westwell, K. Takeuchi, T. Ibusuki, K. Enjouji, H. Konno, K. Sakamoto and O. Ishitani, *Organometallics*, 1997, **16**, 5724–5729.
45 H. Takeda, K. Koike, H. Inoue and O. Ishitani, *J. Am. Chem. Soc.*, 2008, **130**, 2023–2031.
46 T. Morimoto, T. Nakajima, S. Sawa, R. Nakanishi, D. Imori and O. Ishitani, *J. Am. Chem. Soc.*, 2013, **135**, 16825–16828.
47 A. Kobayashi, H. Konno, K. Sakamoto, A. Sekine, Y. Ohashi, M. Iida and O. Ishitani, *Chemistry*, 2005, **11**, 4219–26.
48 Y. Tamaki, K. Koike, T. Morimoto and O. Ishitani, *J. Catal.*, 2013, **304**, 22–28.
49 Y. Tamaki, K. Koike and O. Ishitani, *Chem. Sci.*, 2015, **6**, 7213–7221.
50 B. Gholamkhass, H. Mametsuka, K. Koike, T. Tanabe, M. Furue and O. Ishitani, *Inorg. Chem.*, 2005, **44**, 2326–2336.
51 H. Hori, F. P. A. Johnson, K. Koike, O. Ishitani and T. Ibusuki, *J. Photochem. Photobiol. A Chem.*, 1996, **96**, 171–174.
52 H. Hori, J. Ishihara, K. Koike, K. Takeuchi, T. Ibusuki and O. Ishitani, *J. Photochem. Photobiol. A Chem.*, 1999, **120**, 119–124.
53 S. Sato, K. Koike, H. Inoue and O. Ishitani, *Photochem. Photobiol. Sci.*, 2007, **6**, 454–461.
54 Y. Tamaki, K. Watanabe, K. Koike, H. Inoue, T. Morimoto and O. Ishitani, *Faraday Discuss.*, 2012, **155**, 115–127.
55 E. Kato, H. Takeda, K. Koike, K. Ohkubo and O. Ishitani, *Chem. Sci.*, 2015, **6**, 3003–3012.
56 Z.-Y. Bian, K. Sumi, M. Furue, S. Sato, K. Koike and O. Ishitani, *Dalton Trans.*, 2009, 983–993.
57 C. D. Windle, M. V Câmpian, A.-K. Duhme-Klair, E. A. Gibson, R. N. Perutz and J. Schneider, *Chem. Commun.*, 2012, **48**, 8189–8191.
58 C. Matlachowski, B. Braun, S. Tschierlei and M. Schwalbe, *Inorg. Chem.*, 2015, **54**, 10351–10360.
59 J. Schneider, K. Q. Vuong, J. A. Calladine, X.-Z. Sun, A. C. Whitwood, M. W. George and R. N. Perutz, *Inorg. Chem.*, 2011, **50**, 11877–11889.
60 A. Nakada, K. Koike, T. Nakashima, T. Morimoto and O. Ishitani, *Inorg. Chem.*, 2015, **54**, 1800–1807.
61 Y. Tamaki, K. Koike, T. Morimoto, Y. Yamazaki and O. Ishitani, *Inorg. Chem.*, 2013, **52**, 11902–11909.
62 H. Ishida, H. Tanaka, K. Tanaka and T. Tanaka, *J. Chem. Soc., Chem. Commun*, 1987, **197**, 131–132.
63 H. Ishida, K. Tanaka and T. Tanaka, *Organometallics*, 1987, 181–186.
64 J. R. Pugh, M. R. M. Bruce, B. P. Sullivan and T. J. Meyer, *Inorg. Chem.*, 1991, **30**, 86–91.
65 C. W. Machan, M. D. Sampson and C. P. Kubiak, *J. Am. Chem. Soc.*, 2015, **137**, 8564–8571.
66 S. Chardon-Noblat, P. Da Costa, A. Deronzier, S. Maniguet and R. Ziessel, *J. Electroanal. Chem.*, 2002, **529**, 135–144.
67 B. A. Johnson, S. Maji, H. Agarwala, T. A. White, E. Mijangos and S. Ott, *Angew. Chemie - Int. Ed.*, 2015, **55**, 1825–1829.
68 L. Duan, G. F. Manbeck, M. Kowalczyk, D. J. Szalda, J. T. Muckerman, Y. Himeda and E. Fujita, *Inorg. Chem.*, 2016, **55**, 4582–4594.
69 H. Nagao, T. Mizukawa and K. Tanaka, *Inorg. Chem.*, 1994, **33**, 3415–3420.
70 Z. Chen, C. Chen, D. R. Weinberg, P. Kang, J. J. Concepcion, D. P. Harrison, M. S. Brookhart and T. J. Meyer, *Chem. Commun.*, 2011, **47**, 12607–12609.

71 Z. Chen, P. Kang, M.-T. Zhang and T. J. Meyer, *Chem. Commun.*, 2014, **50**, 335–337.
72 Z. Chen, J. J. Concepcion, M. K. Brennaman, P. Kang, M. R. Norris, P. G. Hoertz and T. J. Meyer, *Pnas*, 2012, **109**, 15606–15611.
73 M. M. Ali, H. Sato, M. M. Ali, H. Sato, T. Mizukawa, K. Tsuge, M. Haga and K. Tanaka, *Chem. Commun.*, 1998, **2**, 249–250.
74 J. M. Lehn and R. Ziessel, *J. Organomet. Chem.*, 1990, **382**, 157–173.
75 P. Voyame, K. E. Toghill, M. A. Méndez and H. H. Girault, *Inorg. Chem.*, 2013, **52**, 10949–10957.
76 H. Ishida, T. Terada, K. Tanaka and T. Tanaka, *Inorg. Chem.*, 1990, **29**, 905–911.
77 A. Rosas-Hernández, H. Junge and M. Beller, *ChemCatChem*, 2015, **7**, 3316–3321.
78 Y. Kuramochi, M. Kamiya and H. Ishida, *Inorg. Chem.*, 2014, **53**, 3326–3332.
79 A. Paul, D. Connolly, M. Schulz, M. T. Pryce and J. G. Vos, *Inorg. Chem.*, 2012, **51**, 1977–1979.
80 Y. Kuramochi, J. Itabashi, K. Fukaya, A. Enomoto, M. Yoshida and H. Ishida, *Chem. Sci.*, 2015, **6**, 3063–3074.
81 S. Chardon-noblat, A. Deronzier, R. Ziessel and D. Zsoldos, *Inorg. Chem.*, 1997, **36**, 5384–5389.
82 K. Toyohara, H. Nagao, T. Mizukawa and K. Tanaka, *Inorg. Chem.*, 1995, **34**, 5399–5400.
83 D. H. Gibson, J. G. Andino and M. S. Mashuta, *Organometallics*, 2006, **25**, 563–565.
84 T. A. White, S. Maji and S. Ott, *Dalton Trans.*, 2014, **43**, 15028–15037.
85 A. Begum and P. G. Pickup, *Electrochem. commun.*, 2007, **9**, 2525–2528.
86 M. R. M. . Bruce, E. Megehee, B. P. Sullivan, H. Thorp, T. R. . O'Toole, A. Downard and T. J. Meyer, *Organometallics*, 1988, **7**, 238–240.
87 M. R. M. Bruce, E. Megehee, B. P. Sullivan, H. H. Thorp, T. R. Otooie, A. Downard, J. R. Pug and T. J. Meyer, *Inorg. Chem.*, 1992, **31**, 4864–4873.
88 S. Chardon-Noblat, A. Deronzier, F. Hart, J. Van Slageren and T. Mahabiersing, *Eur. J. Inorg. Chem.*, 2001, 613–617.
89 J. Chauvin, F. Lafolet, S. Chardon-Noblat, A. Deronzier, M. Jakonen and M. Haukka, *Chem. - A Eur. J.*, 2011, **17**, 4313–4322.
90 C. M. Bolinger, B. P. Sullivan, D. Conrad, J. A. Gilbert, N. Story and T. J. Meyer, *J. Chem. Soc., Chem. Commun*, 1985, 796–797.
91 C. M. Bolinger, N. Story, B. P. Sullivan and T. J. Meyer, *Inorg. Chem.*, 1988, **27**, 4582–4587.
92 C. Caix, S. Chardon-noblat and A. Deronzier, *J. Electroanal. Chem.*, 1997, **434**, 163–170.
93 P. Paul, B. Tyagi, A. K. Bilakhiya and M. M. Bhadbhade, *Inorg. Chem.*, 1998, **37**, 5733–5742.
94 M. B. Chambers, X. Wang, N. Elgrishi, C. H. Hendon, A. Walsh, J. Bonnefoy, J. Canivet, E. Alessandra Quadrelli, D. Farrusseng, C. Mellot-Draznieks and M. Fontecave, *ChemSusChem*, 2015, **8**, 603–608.
95 R. O. Reithmeier, S. Meister, B. Rieger, A. Siebel, M. Tschurl, U. Heiz and E. Herdtweck, *Dalton Trans.*, 2014, **43**, 13259–13269.
96 S. Sato, T. Morikawa, T. Kajino and O. Ishitani, *Angew. Chemie - Int. Ed.*, 2013, **52**, 988–992.
97 P. Paul, *J. Chem. Sci.*, 2002, **114**, 269–276.
98 A. G. M. M. Hossain, T. Nagaoka and K. Ogura, *Electrochim. Acta*, 1997, **42**, 2577–2585.
99 J. A. Ramos Sende, C. R. Arana, L. Hernandez, K. T. Potts, M. Keshevarz-K and H. D. Abruna, *Inorg. Chem.*, 1995, **34**, 3339–3348.
100 M. Bourrez, F. Molton, S. Chardon-Noblat and A. Deronzier, *Angew. Chemie - Int. Ed.*, 2011, **50**, 9903–9906.
101 J. M. Smieja, M. D. Sampson, K. A. Grice, E. E. Benson, J. D. Froehlich and C. P. Kubiak, *Inorg. Chem.*, 2013, **52**, 2484–2491.
102 C. W. Machan, C. J. Stanton, J. E. Vandezande, G. F. Majetich, H. F. Schaefer, C. P. Kubiak and J. Agarwal, *Inorg. Chem.*, 2015, **54**, 8849–8856.
103 M. D. Sampson, A. D. Nguyen, K. A. Grice, C. E. Moore, A. L. Rheingold and C. P. Kubiak, *J. Am. Chem. Soc.*, 2014, **136**, 5460–5471.
104 M. D. Sampson and C. P. Kubiak, *J. Am. Chem. Soc.*, 2016, **138**, 1386–1393.
105 F. Franco, C. Cometto, F. Ferrero Vallana, F. Sordello, E. Priola, C. Minero, C. Nervi and R. Gobetto, *Chem. Commun.*, 2014, **50**, 14670–14673.
106 J. Agarwal, T. W. Shaw, H. F. Schaefer and A. B. Bocarsly, *Inorg. Chem.*, 2015, **54**, 5285–5294.
107 H. Fei, M. D. Sampson, Y. Lee, C. P. Kubiak and S. M. Cohen, *Inorg. Chem.*, 2015, **54**, 6821–

6828.
108 M. Bourrez, M. Orio, F. Molton, H. Vezin, C. Duboc, A. Deronzier and S. Chardon-Noblat, *Angew. Chemie - Int. Ed.*, 2014, **53**, 240–243.
109 D. C. Grills, J. Farrington, B. H. Layne, S. V. Lymar, B. A. Mello, J. M. Preses and J. F. Wishart, *J. Am. Chem. Soc.*, 2014, **136**, 5563–5566.
110 M. Hammouche, D. Lexa, M. Momenteau and J. M. Saveant, *J. Am. Chem. Soc.*, 1991, **113**, 8455–8466.
111 L. Gamier, Y. Rollin and J. Périchon, *J. Organomet. Chem.*, 1989, **367**, 347–358.
112 H. Takeda, H. Koizumi, K. Okamoto and O. Ishitani, *Chem. Commun.*, 2014, **50**, 1491–1493.
113 P. L. Cheung, C. W. Machan, A. Y. S. Malkhasian, J. Agarwal and C. P. Kubiak, *Inorg. Chem.*, 2016, **55**, 3192–3198.
114 C. Costentin, S. Drouet, M. Robert and J.-M. Savéant, *Science (80-.).*, 2012, **338**, 90–94.
115 C. Costentin, G. Passard, M. Robert and J.-M. Savéant, *Proc. Natl. Acad. Sci.*, 2014, **111**, 14990–14994.
116 C. Costentin, M. Robert and J. M. Savéant, *Acc. Chem. Res.*, 2015, **48**, 2996–3006.
117 T. C. Simpson and R. R. Durand, *Electrochim. Acta*, 1988, **33**, 581–583.
118 S.-N. Pun, W.-H. Chung, K.-M. Lam, P. Guo, P.-H. Chan, K.-Y. Wong, C.-M. Che, T.-Y. Chen and S.-M. Peng, *J. Chem. Soc. Dalt. Trans.*, 2002, 575–583.
119 J. Chen, D. J. Szalda, E. Fujita and C. Creutz, *Inorg. Chem.*, 2010, **49**, 9380–9391.
120 C. Arana, S. Yan, M. Keshavarz-K, K. T. Potts and H. D. Abruña, *Inorg. Chem.*, 1992, **31**, 3680–3682.
121 C. Arana, M. Keshavarz, K. T. Potts and H. D. Abruña, *Inorganica Chim. Acta*, 1994, **225**, 285–295.
122 N. Elgrishi, M. B. Chambers, V. Artero and M. Fontecave, *Phys. Chem. Chem. Phys.*, 2014, **16**, 13635–13644.
123 H. Takeda, K. Ohashi, A. Sekine and O. Ishitani, *J. Am. Chem. Soc.*, 2016, **138**, 4354–4357.
124 J. M. Lehn and R. Ziessel, *Proc. Natl. Acad. Sci. U. S. A.*, 1982, **79**, 701–704.
125 R. Ziessel, J. Hawecker and J.-M. Lehn, *Helv. Chim. Acta*, 1986, **69**, 1065–1084.
126 T. Hirose, S. Shigaki, M. Hirose and A. Fushimi, *J. Fluor. Chem.*, 2010, **131**, 915–921.
127 F. R. Keene, C. Creutz and N. Sutin, *Coord. Chem. Rev.*, 1985, **64**, 247–260.
128 N. Elgrishi, M. B. Chambers and M. Fontecave, *Chem. Sci.*, 2015, **6**, 2522–2531.
129 J. Costamagna and J. Canales, *Pure Appl. Chem.*, 1995, **67**, 1045–1052.
130 M. Isaacs, J. C. Canales, M. J. Aguirre, G. Estiú, F. Caruso, G. Ferraudi and J. Costamagna, *Inorganica Chim. Acta*, 2002, **339**, 224–232.
131 S. Daniele, P. Ugo, G. Bontempelli and M. Fiorani, *J. Electroanal. Chem.*, 1987, **219**, 259–271.
132 K. Lam, K. Wong, S.-M. Yang and C.-M. Che, *J. Chem. Soc. Dalt. Trans.*, 1995, 1103–1107.
133 P. A. Christensen, A. Hamnett, S. J. Higgins and J. A. Timney, *J. Electroanal. Chem.*, 1995, **395**, 195–209.
134 J. Canales, J. Ramirez, G. Estiu and J. Costamagna, *Polyhedron*, 2000, **19**, 2373–2381.
135 Y. Mori, D. J. Szalda, B. S. Brunschwig, H. A. Schwarz and E. Fujita, *Mol. Photochem.*, 1998, **254**, 279–292.
136 J. S. Field, R. J. Haines, C. J. Parry and S. H. Sookraj, *Polyhedron*, 1993, **12**, 2425–2428.
137 R. J. Haines, R. E. Wittrig and C. P. Kubiak, *Inorg. Chem.*, 1994, **33**, 4723–4728.
138 J. P. Muena, M. Villagrán, J. Costamagna and M. J. Aguirre, *J. Coord. Chem.*, 2008, **61**, 479–489.
139 A. S. Varela, M. Kroschel, T. Reier and P. Strasser, *Catal. Today*, 2016, **260**, 8–13.
140 R. Kas, R. Kortlever, A. Milbrat, M. T. M. Koper, G. Mul and J. Baltrusaitis, *Phys. Chem. Chem. Phys.*, 2014, **16**, 12194–12201.
141 T. N. Huan, E. S. Andreiadis, J. Heidkamp, P. Simon, E. Derat, S. Cobo, G. Royal, A. Bergmann, P. Strasser, H. Dau, V. Artero and M. Fontecave, *J. Mater. Chem. A*, 2015, **3**, 3901–3907.
142 D. Ren, Y. Deng, A. D. Handoko, C. S. Chen, S. Malkhandi and B. S. Yeo, *ACS Catal.*, 2015, **5**, 2814–2821.
143 J. H. Montoya, A. A. Peterson and J. K. Nørskov, *ChemCatChem*, 2013, **5**, 737–742.
144 T. R. O'Toole, L. D. Margerum, T. D. Westmoreland, W. J. Vining, R. W. Murray and T. J. Meyer, *J. Chem. Soc. Chem. Commun.*, 1985, 1416–1417.

145 R. L. House, N. Y. M. Iha, R. L. Coppo, L. Alibabaei, B. D. Sherman, P. Kang, M. K. Brennaman, P. G. Hoertz and T. J. Meyer, *J. Photochem. Photobiol. C Photochem. Rev.*, 2015, **25**, 32–45.
146 Y. Yamazaki, H. Takeda and O. Ishitani, *J. Photochem. Photobiol. C Photochem. Rev.*, 2015, **25**, 106–137.
147 P. D. Tran, L. H. Wong, J. Barber and J. S. C. Loo, *Energy Environ. Sci.*, 2012, **5**, 5902–5918.
148 C. D. Windle and E. Reisner, *Chim. Int. J. Chem.*, 2015, **69**, 435–441.
149 M. K. Brennaman, R. J. Dillon, L. Alibabaei, M. K. Gish, C. J. Dares, D. L. Ashford, R. L. House, G. J. Meyer, J. M. Papanikolas and T. J. Meyer, *J. Am. Chem. Soc.*, 2016, **138**, 13085–13102.
150 J. J. Walsh, C. Jiang, J. Tang, A. J. Cowan, S. J. A. Moniz, S. A. Shevlin, D. J. Martin, Z.-X. Guo, J. Tang, X. Wang, K. Maeda, A. Thomas, K. Takanabe, G. Xin, J. M. Carlsson, K. Domen, M. Antonietti, J. Liu, Y. Liu, N. Liu, Y. Han, X. Zhang, H. Huang, Y. Lifshitz, S. Lee, J. Zhong, Z. Kang, J. Hong, S. Yin, Y. Pan, J. Han, T. Zhou, R. Xu, L. Shi, L. Liang, F. Wang, M. Liu, K. Chen, K. Sun, N. Zhang, J. Sun, S. Min, G. Lu, X. Zhang, L. Yu, C. Zhuang, T. Peng, R. Li, X. Li, Y. Shiraishi, Y. Kofuji, S. Kanazawa, H. Sakamoto, S. Ichikawa, S. Tanaka, T. Hirai, C. A. Caputo, M. A. Gross, V. W. Lau, C. Cavazza, B. V. Lotsch, E. Reisner, X. Wang, G. Zhang, S. Zang, Z. Lan, C. Huang, G. Li, G. Dong, Y. Zhang, Q. Pan, J. Qiu, A. Thomas, A. Fischer, F. Goettmann, M. Antonietti, J.-O. Müller, R. Schlögl, J. M. Carlsson, S. W. Hu, L. W. Yang, Y. Tian, X. L. Wei, J. W. Ding, J. X. Zhong, P. K. Chu, K. Takanabe, K. Kamata, X. Wang, M. Antonietti, J. Kubota, K. Domen, D. J. Martin, P. J. T. Reardon, S. J. A. Moniz, J. Tang, D. J. Martin, K. Qiu, S. A. Shevlin, A. D. Handoko, X. Chen, Z. Guo, J. Tang, Y. Zheng, L. Lin, X. Ye, F. Guo, X. Wang, J. Lin, Z. Pan, X. Wang, J. Lin, Y. Hou, Y. Zheng, X. Wang, K. Maeda, K. Sekizawa, O. Ishitani, R. Kuriki, K. Sekizawa, O. Ishitani, K. Maeda, R. Kuriki, H. Matsunaga, T. Nakashima, K. Wada, A. Yamakata, O. Ishitani, K. Maeda, J.-M. Lehn, R. Ziessel, R. Ziessel, J. Hawecker, J.-M. Lehn, J. Grodkowski, P. Neta, H. Kisch, D. Bahnemann, S. Sato, T. Morikawa, S. Saeki, T. Kajino, T. Motohiro, E. Pastor, F. M. Pesci, A. Reynal, A. D. Handoko, M. Guo, X. An, A. J. Cowan, D. R. Klug, J. R. Durrant, J. Tang, A. J. Cowan, W. Leng, P. R. F. Barnes, D. R. Klug, J. R. Durrant, C. Ye, J. X. Li, Z. J. Li, X. B. Li, X. B. Fan, L. P. Zhang, B. Chen, C. H. Tung, L. Z. Wu, H. Zhang, Y. Chen, R. Lu, R. Li, A. Yu, H. Kasap, C. A. Caputo, B. C. M. Martindale, R. Godin, V. W.-H. Lau, B. V. Lotsch, J. R. Durrant, E. Reisner, A. J. Cowan, J. Tang, W. Leng, J. R. Durrant, D. R. Klug, A. J. Cowan, J. R. Durrant, W. Wei and T. Jacob, *Phys. Chem. Chem. Phys.*, 2016, **18**, 24825–24829.
151 C. D. Windle, E. Pastor, A. Reynal, A. C. Whitwood, Y. Vaynzof, J. R. Durrant, R. N. Perutz and E. Reisner, *Chem. - A Eur. J.*, 2015, **21**, 3746–3754.
152 R. Kuriki, K. Sekizawa, O. Ishitani and K. Maeda, *Angew. Chemie Int. Ed.*, 2015, **54**, 2406–2409.
153 K. Sekizawa, K. Maeda, K. Domen, K. Koike and O. Ishitani, *J. Am. Chem. Soc.*, 2013, **135**, 4596–4599.
154 K. Pool and R. P. Buck, *J. Electroanal. Chem. Interfacial Electrochem.*, 1979, **95**, 241–246.
155 S. Anderson, E. C. Constable, M. P. Dare-Edwards, J. B. Goodenough, A. Hamnett, K. R. Seddon and R. D. Wright, *Nature*, 1979, 280, 571–573.
156 P. Ghosh and T. G. Spiro, *J. Am. Chem. Soc.*, 1980, **102**, 5543–5549.
157 H. D. Abruna, P. Denisevich, M. Umana, T. J. Meyer and R. W. Murray, *J. Am. Chem. Soc.*, 1981, **103**, 1–5.
158 H. D. Abruna, T. J. Meyer and R. W. Murray, *Inorg. Chem.*, 1979, **18**, 3233–3240.
159 T. R. O'Toole, B. P. Sullivan, M. R.-M. Bruce, L. D. Margerum, R. W. Murray and T. J. Meyer, *J. Electroanal. Chem. Interfacial Electrochem.*, 1989, **259**, 217–239.
160 C. R. Cabrera and H. D. Abruña, *J. Electroanal. Chem. Interfacial Electrochem.*, 1986, **209**, 101–107.
161 F. Cecchet, M. Alebbi, C. A. Bignozzi and F. Paolucci, *Inorganica Chim. Acta*, 2006, **359**, 3871–3874.
162 S. Cosnier, A. Deronzier and J.-C. Moutet, *J. Electroanal. Chem. Interfacial Electrochem.*, 1986, **207**, 315–321.
163 S. Chardon-Noblat, M.-N. Collomb-Dunand-Sauthier, A. Deronzier, R. Ziessel and D. Zsoldos,

Inorg. Chem., 1994, **33**, 4410–4412.
164 T. R. O'Toole, T. J. Meyer and B. P. Sullivan, *Chem. Mater.*, 1989, **1**, 574–576.
165 H. C. Hurrell, a. L. Mogstad, D. a. Usifer, K. T. Potts and H. D. Abruna, *Inorg. Chem.*, 1989, **28**, 1080–1084.
166 M.-N. Collomb-Dunand-Sauthier, A. Deronzier and R. Ziessel, *Inorg. Chem.*, 1994, **33**, 2961–2967.
167 M.-N. Collomb-Dunand-Sauthier, A. Deronzier and R. Ziessel, *J. Chem. Soc., Chem. Commun.*, 1994, 189–191.
168 J. D. Blakemore, A. Gupta, J. J. Warren, B. S. Brunschwig and H. B. Gray, *J. Am. Chem. Soc.*, 2013, **135**, 18288–18291.
169 N. Elgrishi, S. Griveau, M. B. Chambers, F. Bedioui and M. Fontecave, *Chem. Commun.*, 2015, **51**, 2995–2998.
170 S. Oh, J. R. Gallagher, J. T. Miller and Y. Surendranath, *J. Am. Chem. Soc.*, 2016, **138**, 1820–1823.
171 T. Yamamoto, Y. Yoneda, T. Maruyama, R. Ramaraj, P. Natarajan, T. Yamamoto, Z.-H. Zhou, T. Maruyama, T. Kanbara, T. Yamamoto, T. Maruyama, T. Ikeda, M. Sisido, M. A. Hayes, C. Mekel, E. Schiz, M. D. Ward, J. M. Calvert, T. J. Meyer, B. Durham, J. L. Walsh, C. L. Carter, T. J. Meyer, G. J. Samuels, T. J. Meyer, N. E. Tokei-Takvoryam, R. E. Hemingway, A. J. Bard, N. Oyama, Y. Takimura, H. Matsuda, T. Yamamoto, K. Sanechika, S. Masuoka, T. Kohzuki, A. Nakamura, C. Pac, S. Yanagida, M. C. Cooke, J. Homer, A. W. P. Jarvie, J. D. Miller, N. W. Alcock, P. N. Bartlett, V. M. Eastwick-Field, G. A. Pike, P. G. Prigle, S. Dérien, E. Duñach and J. Périchon, *J. Chem. Soc., Chem. Commun.*, 1992, **0**, 1652–1654.
172 L. Li, R. G. Hadt, S. Yao, W.-Y. Lo, Z. Cai, Q. Wu, B. Pandit, L. X. Chen and L. Yu, *Chem. Mater.*, 2016, **28**, 5394–5399.
173 T. Maruyama and T. Yamamoto, *J. Phys. Chem. B*, 1997, **101**, 3806–3810.
174 T. Yamamoto, T. Maruyama, Z.-H. Zhou, T. Ito, T. Fukuda, Y. Yoneda, F. Begum, T. Ikeda and S. Sasaki, *J. Am. Chem. Soc.*, 1994, **116**, 4832–4845.
175 C. Wang, Z. Xie, K. E. DeKrafft and W. Lin, *J. Am. Chem. Soc.*, 2011, **133**, 13445–13454.
176 R. Huang, Y. Peng, C. Wang, Z. Shi and W. Lin, *Eur. J. Inorg. Chem.*, 2016, DOI: 10.1002/ejic.201600064.
177 L. Li, S. Zhang, L. Xu, J. Wang, L.-X. Shi, Z.-N. Chen, M. Hong and J. Luo, *Chem. Sci.*, 2014, **5**, 3808–3813.
178 T. Yoshida, K. Tsutsumida, S. Teratani, K. Yasufuku and M. Kaneko, *J. Chem. Soc., Chem. Commun.*, 1993, 631–633.
179 T. Yoshida, T. Iida, T. Shirasagi, R.-J. Lin and M. Kaneko, *J. Electroanal. Chem.*, 1993, **344**, 355–362.
180 J. J. Walsh, G. Neri, C. L. Smith and A. J. Cowan, *Chem. Commun.*, 2014, **50**, 12698–12701.
181 J. J. Walsh, C. L. Smith, G. Neri, G. F. S. Whitehead, C. M. Robertson and A. J. Cowan, *Faraday Discuss.*, 2015, **183**, 147–160.